

**DEVELOPMENT & CHARACTERIZATION OF IN-SITU
ALUMINUM ALLOY COMPOSITES FOR
TRIBOLOGICAL APPLICATIONS**

By

AMNEESH SINGLA

(SAP ID- 500024421)

**SCHOOL OF ENGINEERING
(DEPARTMENT OF MECHANICAL ENGINEERING)**

SUBMITTED

**IN PARTIAL FULFILLMENT OF THE REQUIREMENT OF
THE DEGREE OF**

DOCTOR OF PHILOSOPHY

TO



UNIVERSITY WITH A PURPOSE

**UNIVERSITY OF PETROLEUM AND ENERGY STUDIES
DEHRADUN
June, 2019**

UNDER THE GUIDANCE OF

DR. RAJNISH GARG

Professor

Mechanical Engineering Department
UPES, Dehradun

ACKNOWLEDGMENTS

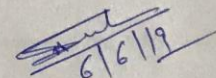
I would like to take this opportunity to express my deepest gratitude to my supervisor **Dr. Rajnish Garg, Professor, Mechanical Engineering, UPES, Dehradun** for their encouragements, direction, and advice in all the way throughout the research. I also would like to acknowledge them for their kind attitude, optimistic approach, and trust throughout the entire journey to carry out the research work in positive direction.

Moreover, I am thankful to our honorable **Chancellor Dr. S. J. Chopra, Vice Chancellor Dr. Deependra Kumar Jha, Associate Dean Research Dr. Jitendra Kumar Pandey and Dean, School of Engineering, Dr. Kamal Bansal** for motivating me with space and environment in the serene campus of University of Petroleum & Energy Studies, Dehradun, India to carry out the work.

Finally, I am indebted to my family members, my parents Mr. Sushil Gupta and Ms. Sunita Gupta for their love, blessing and support throughout my life. This work could have been an inaccessible dream without the moral encouragement and assistance from my better half, Shikhi and my son Ansh. This work is also the outcome of the blessing guidance and support of my adoring siblings Mr. Naveen Singla, Amita Gupta & Mr. Abhay Gupta.

DECLARATION

I hereby declare that this submission is my own work and that, to the best of my knowledge and belief, it contains no material previously published or written by another person nor material which has been accepted for the award of any other degree or diploma of the university or other institute of higher learning, except where due acknowledgment has been made in the text.


6/6/19

Amneesh Singla

Enrollment No. 500024421

CERTIFICATE FROM SUPERVISOR

This is to certify that the thesis on “**Development & Characterization of In-Situ Aluminum Alloy Composites for Tribological Applications**” by **Amneesh Singla** in the Partial completion of the requirements for the award of the Degree of Doctor of Philosophy (Engineering) is an original work carried out by him under my supervision and guidance.

It is certified that the work has not been submitted anywhere else for the award of any other diploma or degree of this or any other University.

Supervisor

Dr. Rajnish Garg
Professor
Department of Mechanical Engineering
UPES, Dehradun

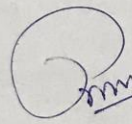

06/06/2019

TABLE OF CONTENTS

Acknowledgements	ii
Declaration	iii
Certificate from supervisor	iv
Abstract	v
List of symbols	
List of abbreviations	
List of figures	
List of tables	
CHAPTER 1 INTRODUCTION	1
1.1 Motivation for Research work	1
1.2 Problem statement	5
CHAPTER 2 LITERATURE REVIEW	7
2.1 Introduction	7
2.2 Processing routes of AMC's	8
2.2.1 The reaction between solid and liquid	9
2.2.1.1 Self- Propagating High-Temperature Synthesis	9
2.2.1.2 Exothermic Dispersion	10
2.2.1.3 Direct Reaction Synthesis (DRS)	10
2.2.1.4 Flux assisted synthesis	10
2.2.1.5 Directed melt oxidation (DIMOX)	11
2.2.1.6 Reactive Squeeze casting	12
2.2.2 The reaction between Solid –Solid	13
2.2.2.1 Powder metallurgy	13
2.2.2.2 Diffusion Bonding	14
2.2.3 The reaction between liquid-liquid	14
2.2.3.1 Stir Casting Method	15

2.2.3.2 Infiltration process	16
2.2.3.3 Spray deposition.....	16
2.2.3.4 In situ Process	16
2.3 Parameters for Stir casting	18
2.3.1 Stirrer position and shape.....	18
2.4 Reinforcement particles distribution into the molten metal alloy matrix.....	20
2.5 Effect of porosity in cast composites	22
2.6 Wetting of particles.....	23
2.7 Processing parameters.....	24
2.7.1 Stirring speed	24
2.7.2 Stirring temperature	25
2.7.3 Preheating of the particles.....	25
2.7.4 Holding time	25
2.7.5 Adding/feeding rate of the particles.....	26
2.8 Mechanical Properties of the composites.....	26
2.8.1 Properties of particulate composite.....	27
2.8.2 Tensile properties of in-situ composites	28
2.8.3 Effect of oxide reinforcement	30
2.9 Tribological Aspects in Al MMC.....	32
2.9.1 Abrasive wear	33
2.9.2 Adhesive wear.....	35
2.10 Comparison of Insitu, Exsitu & other processing techniques.....	41
2.11 Formulation of the problem.....	42
2.12 Research Gaps.....	43
2.13 Objectives.....	43

CHAPTER 3 RESEARCH METHODOLOGY	44
3.1 Material Selection	45
3.1.1 Al and Al-Si as Matrices	45
3.1.2 Vanadium Pentoxide as oxide particles	47
3.2 Processing	48
3.2.1 Development of Al-Si and Al-based Composites	48
3.3 Particles content estimation	52
3.4 Volume fraction determination	53
3.5 Porosity measurement	54
3.6 Characterization	55
3.6.1 Thermal Analysis	55
3.6.2 Microstructure	55
3.6.2.1 Sample preparation`	56
3.6.2.2 Etchants Used.....	60
3.6.3 XRD Analysis	60
3.7 Mechanical Behavior	61
3.7.1 Microhardness	61
3.7.2 Tensile testing	62
3.7.3 Wear testing	63
CHAPTER 4 RESULT & DISCUSSION PURE AL & V2O5	65
4.1 Al-V2O5 Characterization	65
4.1.1 Thermodynamics characteristics of the in-situ reaction	65
4.1.2 XRD Analysis	66
4.1.3 Microstructural evaluation	67
4.1.4 Scanning Electron Microscopy	70
4.2 Mechanical Properties	73
4.2.1 Microhardness and tensile strength.....	73

4.3 Tribological Behavior	77
4.3.1 Coefficient of friction	77
4.3.2 Volume loss	80
4.3.3 Wear rate	81
4.3.4 Worn surface morphology	83
4.4 Discussion.....	84
CHAPTER 5 RESULT & DISCUSSION AL-SI & V2O5	88
5.1 Al-7Si Characterization.....	88
5.1.1 Designation of the developed composite	88
5.1.2 XRD Analysis	89
5.1.3 Microstructural characterization	90
5.1.4 SEM Analysis	92
5.2 Mechanical Properties	94
5.2.1 Microhardness and Tensile Testing	94
5.3 Heat treatment	96
5.3.1 Effect of heat treatment on microstructure	97
5.4 Comparison of Mechanical Properties of as cast & heat treated composites.....	100
5.4.1 Effect of heat treatment on the hardness.....	100
5.4.2 Effect of heat treatment on Tensile Properties.....	101
5.5 Comparison of result with literature.....	103
5.5.1 Effect of Volume fraction of reinforcement on porosity	105
5.5.2 Effect on Tensile strength	106
5.6 Tribological Behavior	107
5.6.1 Coefficient of friction	107
5.6.2 Volume loss	111
5.6.3 Wear	112
5.6.4 Worn surfaces	114

5.7 Effect of reinforcement.....	115
5.8 Effect of parameters on wear.....	116
5.9 Discussion.....	116
CHAPTER 6 CONCLUSION.....	120
6.1 Future Scope.....	125
6.2 Publications obtained from this work.....	125
6.2.1 Peer reviewed journal	125
REFERENCES.....	126

ABSTRACT

The journey for enhanced performance prompts proceeding with search for new materials; metallic, nonmetallic and composites. The easiest method for the development of the composite is the casting method in which various types of reinforcement; continuous or discontinuous are added to a continuous matrix; metallic or nonmetallic to produce the improved material. In this context, the betterment can be achieved either by the external addition of fine reinforcement particles or by the generation of such reinforcement particles within the matrix. For the advancement of aluminum-based composites, the in-situ method provides better dispersion of fine particle of alumina as well as valuable alloying elements in the matrix. In in-situ method, the reduction reaction is responsible for the improved properties, accomplished by adding the oxides in the liquid aluminum. In ex-situ, it is challenging to distribute uniformly the externally added particles in the matrix and to produce composite with sufficient ductility. Using in-situ method it is possible to develop ductile Al-based metal matrix composite with the addition of metal oxides to generate alumina particles as reinforcement. Thereafter, examinations in assorted systems of aluminum and the oxides accept connected and the present analysis has been agitated out in this context.

Chapter1 describes the necessity and motivation for the tribological study of aluminum based in-situ composite developed by stir casting method. This chapter covers the basic introduction part of various aluminum based composite; their classification, application in various industries and setting the problem statement.

Chapter 2 contains a very exhaustive review of the existing literature on in-situ development of aluminum/aluminum alloy and other matrices based composites. There are various parameters, which influence the composite fabrication, and all the associated parameters are discussed in this chapter. This review of literature aims at knowing the different processing techniques, which are currently in use for the development of the composites and the effect of different processing parameters such as stirring speed, the shape of the blade, the temperature of the melt and preheating of oxide particles on the properties of the developed composites.

This chapter describes the effectiveness of different compounds used so far to produce different types of oxide and other particles in different matrices through in-situ reduction reaction. The effect of metal oxide addition to generate reinforcement and heat treatment on mechanical and tribological properties of different in-situ metal matrix composites is critically reviewed. Different standards used for characterization, determination of mechanical properties and evaluation of tribological characteristics of composites are thoroughly described. Finally, research gap are identified to formulate the objective of present study, which are included in this chapter.

Chapter 3 describes the experimental procedures and test methods followed in the present study for the fabrication, microstructural characterization, mechanical testing and tribological testing of pure aluminum/aluminium alloy based in-situ composites. Composites having two different matrices (pure Al & Al-Si alloy) reinforced with different volume fraction of Al_2O_3 have been fabricated under similar processing condition (stirring speed, shape of stirrer, pouring temperature, etc.) using bottom-pouring stir casting furnace. As received commercially pure aluminum and aluminum silicon alloy have been examined under optical emission spectrometer for elemental composition. Composite specimens for different tests have been prepared as per the testing standards. Microstructural characterization of the as cast & heat treated composites has been carried out according to ASTM standards using optical microscope, Scanning Electron Microscope, Energy Dispersive Spectroscopy. Microhardness measurement and tensile testing of base alloy and fabricated composites have been carried out according to ASTM standards using Vicker's microhardness tester and computerized Universal Testing Machine. Dry sliding wear behavior and friction properties of base matrices and fabricated composites have been determined at different loads and sliding distance under constant sliding speed using pin on disc tribotester.

As mentioned earlier, two different composites; commercially pure aluminum based and Al-Si alloy based both reinforced with varying amount of Al_2O_3 particles have been fabricated and tested. The test results and discussion on the test results for two different types of composites have been divided in two

chapters: Chapter 4 and chapter 5. Chapter 4 covers the test results of commercially pure aluminum based metal matrix composites followed by discussion on these results. Chapter 5 covers the test results of Al-Si alloy based metal matrix composites followed by discussion on these results.

Chapter 4 presents the results of various tests conducted on commercially pure aluminum based composites. Pure Al-Al₂O₃ composites with varying amount of Al₂O₃ particles have been successfully fabricated by adding 1 wt.%, 2 wt.%, 3 wt.%...V₂O₅ particles to the aluminum melt for in-situ reaction. As received commercially pure aluminum has traces of Si, Zn, and Mg as revealed by optical emission spectroscopy. The volume fraction of Al₂O₃ particles has been found to be 0.72, 2.1 and 3.4 against 1%, 3% and 5% weight percentage addition of V₂O₅ particle respectively. Volume fraction of Al₂O₃ particles increases with increasing V₂O₅ addition as the rate of in-situ reaction depends upon the amount of V₂O₅ particle addition to the melt. The microstructure of the composites reveals the uniform distribution of fine Al₂O₃ particles and other phases along the boundaries and within the grains of α -Al. Smaller grain size of the composite matrix as compared to pure Al indicates the grain refinement caused by vanadium, which is released during in-situ reaction between the molten aluminum and the vanadium pentoxide. XRD analysis of the composites confirms the presence of primary Al₂O₃ particles and intermetallic Al₃V phase together with mixed oxides in the microstructure. EDX analysis reveals the formation of Al₂O₃ particles of almost stoichiometric composition. Despite of employing degassing using inert gas during casting, porosity could not be eliminated. Porosity content has been found to increase with the increasing volume fraction of Al₂O₃ particles in the composites.

Mechanical properties of commercially pure aluminum increase with the addition of Al₂O₃ reinforcement as the properties of all aluminum based in-situ composites are found to be higher than commercially pure aluminum. However, properties increase up to a certain fraction of Al₂O₃ reinforcement in the composites and decreases afterwards. Maximum improvement in mechanical properties is achieved with 5 wt. % addition of V₂O₅ particles. Coefficient of friction of Al-based in-situ composites is found to be less than

that of pure aluminum. It varies randomly with sliding distance but increases with increasing load and decreases with the increasing volume fraction of Al_2O_3 particles for all values of sliding distance. Wear volume follows the same trend as the coefficient of friction as it increases with increasing load and decreases with increasing volume fraction of reinforcement. There are many factors responsible for the observed improvement in mechanical and tribological properties of Al based composites to a certain extent of V_2O_5 addition and deterioration afterwards. Role of each of these factors is discussed thoroughly in the context of the observed behavior and included in the discussion part of this chapter.

Chapter 5 presents the results of the tests conducted on Al-Si based in-situ composite followed by discussion. In addition to Al_2O_3 and Al_3V phase, primary Si is also found to present in the microstructure as confirmed by XRD analysis. Test results of Al-Si based composites follow similar trends as observed for pure Al-based in-situ composites. However, for Al-Si based as cast composites, maximum hardness, maximum strength, and best wear performance have been achieved with 3 wt. % V_2O_5 addition. Same factors mentioned in the previous chapter are majorly responsible for improvement in mechanical and tribological properties of Al-Si based composites. Role of each factor is discussed thoroughly and included in the discussion part of this chapter.

This chapter also presents the results of mechanical tests conducted on the heat treated composites. Mechanical properties of as cast Al-Si based in-situ composites are improved to a great extent after the heat treatment. Dissolution of alloying elements in the solution of α -aluminum during homogenization process and subsequent trapping during rapid cooling is responsible for the observed improvements. Precipitation of fine Mg_2Si phase during ageing process also contributes to the observed improvement in mechanical properties of the composites.

Chapter 6 consists the conclusion drawn from the present work and future scope of this work. This study indicates that it is possible to modify the

mechanical and tribological properties of aluminum and aluminum alloy by the addition of oxides. Further improvement in properties of the composites with heat treatable matrices can be achieved by suitable heat treatment.

LIST OF SYMBOLS

A_r	Real contact area	m^2
F	Friction force	N

<i>H</i>	Indentation hardness	N/m^2
<i>K</i>	Wear coefficient	-
<i>N</i>	Normal load	N
<i>p, P</i>	Contact pressure	N/m^2
<i>q</i>	Heat generated per unit area	W/m^2
<i>r</i>	Ball radius	M
<i>S</i>	Shearing strength	N/m^2
<i>SWR</i>	Specific wear rate	mm^3/Nm
<i>V</i>	Velocity	m^2/s
<i>V_w</i>	Total wear volume	m^3
<i>WSD</i>	Wear scar diameter	mm
<i>μ</i>	Coefficient of friction	-
<i>ρ</i>	Density	Kg/m^3

LIST OF ABBREVIATIONS

PDN	Particulate dispersion number
ASTM	American Society for Testing and Materials

COF	Coefficient of friction
OES	Optical Emission Spectrometer
POD	Pin on disc
XRD	X ray Diffraction
SEM	Scanning electron microscope
SAE	Society of automotive engineers
DTA	Differential Thermal Analysis
SDAS	Secondary dendrite arm spacing

LIST OF FIGURES

Figure No	Caption	Page No.
Figure 1.1	Classification of Composite	2
Figure 2.1	Powder metallurgy Production process	13

Figure 2.2	Types of Mechanical Stirrer	20
Figure 3.1	Optical Emission Spectrometer	46
Figure 3.2	Bottom Pouring Stir Casting furnace	50
Figure 3.3	DTA Curve for Al-7Si-V ₂ O ₅	51
Figure 3.4	Cross section of the composite (a) H1 and H4 are the upper and lower horizontal section. Whereas H2 and H3 are the middle ones (b) V1 and V2 denote the vertical surfaces.	54
Figure 3.5	Inverted Metallurgical Microscope	56
Figure 3.6	FE SEM	56
Figure 3.7	Precision Saw for sample cutting	57
Figure 3.8	Hydraulic Specimen Mounting Press	58
Figure 3.9	Belt Grinder	59
Figure 3.10	Double disc Variable speed grinder-polisher	59
Figure 3.11	Automatic Polishing Machine	60
Figure 3.12	X-Ray Diffractometer	61
Figure 3.13	Vickers Microhardness tester	62
Figure 3.14	Pin On Disc Tester	64
Figure 4.1	XRD Pattern of Al-V Composite	67
Figure 4.2	XRD pattern of the filtered residue obtained from composite AV5	67
Figure 4.3	Micrographs of (a) pure aluminum (b) AV3 (c) AV5 (d & e) AV7 at low & high magnification respectively	69
Figure 4.4	Back Scattered Image of AV5 composite	70
Figure 4.5	SEM images of (a) AV3 (b) AV5 (c) AV7	71
Figure 4.6	EDAX Analysis of particle present in Al-V composite	72
Figure 4.7	SEM Image of Extracted Al ₂ O ₃ Particles	73
Figure 4.8	Variation of Microhardness with the amount of V ₂ O ₅	74
Figure 4.9	Tensile Strength Variation with the addition of V ₂ O ₅	75
Figure 4.10	SEM images of tensile fractured surfaces of (a) AV5 (b) AV7	77
Figure 4.11	Coefficient of friction as a function of sliding distance at (a) 10 N (b) 20 N & (c) 30 N Load	79
Figure 4.12	Cumulative Coefficient of friction as a function of load	80
Figure 4.13	Volume loss vs Load of cast in-situ composites	81
Figure 4.14	Specific wear Rate as a function of the applied load	82
Figure 4.15	Micrographs of worn surface (a) & (b) AV% at 20N & 30 N load (c) & (d) AV& at 20N & 30N load respectively.	84
Figure 5.1	XRD analysis of Al-7Si composites	89
Figure 5.2	Microstructure of AS alloy & its composites (a) Al-Si (b) ASV1 (c) ASV3 (d) ASV5	92
Figure 5.3	SEM images of (a) ASV1 (b) ASV3 (c) ASV5	93
Figure 5.4	EDAX of Al-7Si Composite	94

Figure 5.5	Hardness variation with the addition of V_2O_5 addition	95
Figure 5.6	Tensile strength variation with the V_2O_5 addition	96
Figure 5.7	Heat Treatment Diagram	97
Figure 5.8	Optical micrographs of Al-Si base alloy and its composites after heat treatment (a) Al-Si (b) ASV1 (c) ASV3 (d) ASV5	99
Figure 5.9	Hardness of AS alloy as cast & its heat-treated composites	101
Figure 5.10	Comparison of UTS of Al-Si alloy as cast & its heat-treated composites	102
Figure 5.11	Variation of porosity with vol. % of the Al_2O_3 content	106
Figure 5.12	Coefficient of Friction with sliding distance (a) 10N load (b) 20N load (c) 30N load	109
Figure 5.13	Variation of Coefficient of friction with load	111
Figure 5.14	Variation of volume loss with load at a 1000m sliding distance	111
Figure 5.15	Variation of wear with load for Al-Si based composites	113
Figure 5.16	Wear rate of the different composite at different loads	113
Figure 5.17	SEM image of the composite with 5% V_2O_5	114

LIST OF TABLES

No.	Title	Page No.
Table 2-1	Thermodynamics Data for Al_3V , Al_2O_3 , Al, V_2O_5 , and V	13
Table 2-2	Usage of AMCs Processing Routes	17

Table 2-3	Tensile Properties comparison of Insitu & exsitu TiB ₂ /Al composite	28
Table 3-1	Composition of as received Aluminum Ingot (wt. %)	46
Table 3-2	Composition of as received Al-7Si alloy (wt.%)	46
Table 3-3	Properties of Vanadium Pentoxide (V ₂ O ₅)	47
Table 3-4	Parameters used for Aluminum composite Fabrication	48
Table 3-5	Designation of Aluminum composite	49
Table 3-6	Process Parameters Used for Al-7Si composites	51
Table 4-1	Mechanical Properties of Al-Al ₂ O ₃ Composite with Various Percentage of V ₂ O ₅	74
Table 5-1	Designation of Al-Si alloy & its composite	88
Table 5-2	Mechanical properties of AS and its composites	95
Table 5-3	Heat treatment Parameters	97
Table 5-4	Mechanical properties of Al-Si and its composites before and after heat treatment	100
Table 5-5	Comparison of Al-Al ₂ O ₃ composite properties	104
Table 5-6	Formation Enthalpy of intermetallic in Al-V system (V less than 25 at.%).	118

CHAPTER 1 INTRODUCTION

1.1 Motivation for Research work

The idea of blending numerous constituents to yield a novel material with unique and hitherto unavailable properties is quite old. Humans have been producing stronger composites and lightweight materials since 1500 B.C. to construct durable structures. Later, in 1200 A.D., Mongols created composite based bows using a combination of wood, bones, and animal glue. The composite bows were very powerful and accurate weapons on earth until the discovery of gunpowder. Since then, composite materials have been identified in several forms throughout the history of mankind.

The development of modern composites probably began in 1940 when the graphite/polyamide composites utilized in space transport orbiter. An ever-increasing call for newer, lightweight, stronger and stiffer materials in various sectors such as automobile, aerospace, transportation, and construction has led the advancement of composite fabrication techniques. In 1960, mechanical properties and fracture mechanics of composites were of prime interest for researchers and manufacturers.

Composites are broadly categorized by matrix (polymer, metal, or ceramic) and reinforcement (fiber, particle, flake, etc.). The broad classification is shown in Figure 1.1. The metallic, polymeric, and ceramic matrices lead to metal-matrix composites (MMCs) [1], polymer-matrix composites (PMCs) [2]–[4] and ceramic matrix composites (CMCs) [5], [6] respectively. Generally, the reinforcement embedded in a matrix improves the overall properties of the composites. The improvement in properties largely depends on the size, shape, and volume of the reinforcement. The Matrix

holds the reinforcement, and usually, the developed composite material shows better properties over the individual materials. The composites exhibit a higher strength to weight ratio, lower specific gravity, and better physical and mechanical properties than numerous conventional materials. Consistent developments have prompted the utilization of composite materials in advanced applications. The significance of composite materials in industry is revealed by the fact that out of more than 1800 materials utilized presently in the business sector, more than 200 are composites[7].

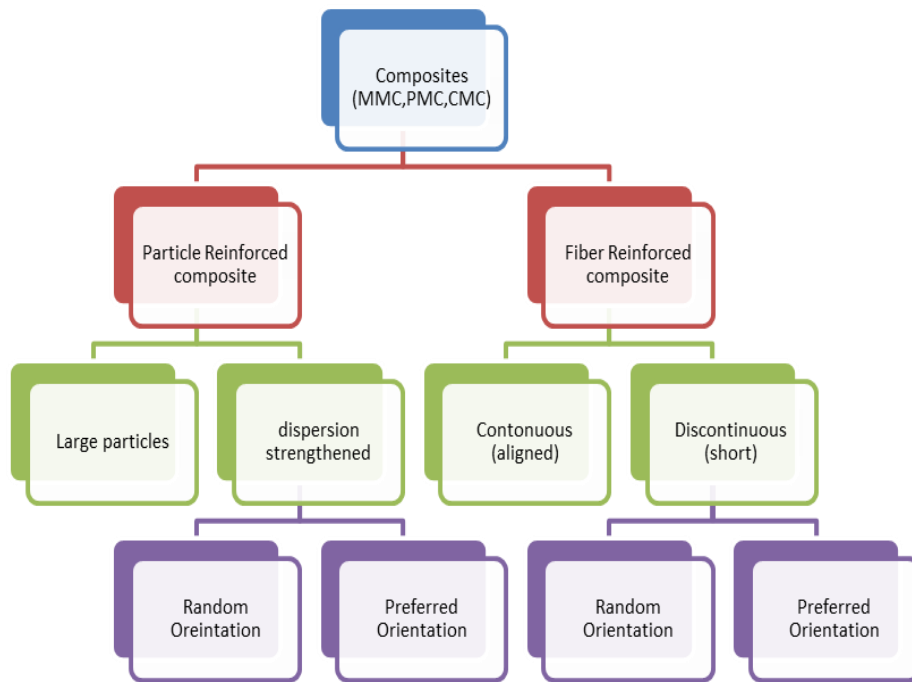


Figure 1.1 Classification of Composite

The properties of a composite material mainly depend on types of constituent materials, their individual properties, their distribution and the possible interaction among them. The reinforcements used for fabricating the composites have different size and shape that can significantly influence the overall properties [8]–[10]. The volume fraction of the reinforcement in a composite determines its degree of interaction with matrix and is responsible for the extent of improvement in properties over that of the individual constituent material.

To cover across-the-board applications, it is essential for modern engineering to produce such a kind of material, which can provide a good

combination of various properties. This requires the optimization of various parameters (such as type, size, shape, volume fraction, and distribution) of reinforcement to combine with a different type of matrices. In recent years, out of the three categories of the composites, i.e. (1) Metal Matrix (2) Polymer Matrix and (3) Ceramic Matrix composite, the metal matrix composites (MMCs) have gained the most attention because of their increasing demand in civil, military, aerospace, aeronautics, defense and security sectors.

The MMCs consists of a metallic matrix (Al, Ti, Cu, Zn, and their alloys) which is generally soft & ductile and a ceramic reinforcement (oxides, carbides, nitrides, borides, etc.) which is relatively hard and brittle. These reinforcement materials for metal matrix composites are easily available commercially. The metallic matrix offers various properties like toughness, formability, ductility, electrical and thermal conductivity. On the other hand, ceramic reinforcement provides good strength, hardness, high modulus and low thermal expansion at ambient and elevated temperatures.

Worldwide, Engineers and researchers are working on the development of MMCs with enhanced mechanical and physical properties. MMCs can be developed with continuous or discontinuous reinforcements. The selection of the reinforcement depends upon its availability, cost, and properties required for a specific application of the composite. The MMCs with continuous reinforcement offer extraordinary improvements in properties and therefore can be used for highly specific applications. However, continuously reinforced MMCs are limited to a few applications because of inadequate availability, high cost, the involvement of complex fabrication technique and directional properties.

A fiber is portrayed by its length, which is more prominent as compared to its cross-sectional dimensions. The shape, size, and orientation of the fibers decide their ability to contribute to the properties of the composite. Fibers are exceptionally promising in enhancing the crack resistance of the composite since a reinforcement with high aspect ratio suppresses the development of early cracks within a weak matrix. In the case of fiber

reinforced MMCs, the matrix holds the fibers and protects them from the environment. On applying the load or stress on such composites, the load or stress is uniformly transferred to the fibers from the matrix. The common problems associated with fiber reinforced MMCs are poor wetting of fibers by metal matrix, the great possibility of fiber mismatch, fiber damage, especially during the processing of the composite at high temperatures, heterogeneity in the microstructure, and difficulty in processing the composite.

On the other hand, the discontinuously reinforced composites are relatively cheap as their manufacturing process is quite simple and economical. Therefore, the discontinuous reinforcements in the form of particulates are commonly used to fabricate MMCs. Nowadays almost double the volumes of MMCs are fabricated by casting and liquid processing route instead of solid-state processing route. In particulate metal matrix composites (PMMCs) or the particle-reinforced composites, as the name itself demonstrates, particles act as reinforcements. The shape and size of the particle play a vital role in governing the material properties. The size of the particles may be of the order of micrometer or nanometer with a narrow variation or wide variation. The shape of particles may be round, cubic, tetragonal, platelet, other customary shapes or unpredictable. Particles as fillers can significantly improve various properties of the resulting composites such as strength, stiffness, high wear resistance, great resistance to friction, hardness, and shrinkage reduction especially, at elevated or high temperatures.

Aluminum and its alloys are among the most popular matrices for the PMMCs composite development. Aluminum and its alloys are very ductile, excellent corrosion resistant and exhibits good specific strength. Aluminum alloys are more cost effective than most of the other comparable matrix materials. Aluminum alloys are broadly classified as the casting alloys and wrought alloys. Aluminum Alloys are designated by a series comprised of 4 digits like 1xxx, 2xxx, and 3xxx ... up to 9xxx where the first digit represents the major alloying elements of the alloy like Cu, Zn, Mn, Mg, Si, etc. and remaining three digits represents the other alloying elements in the alloy. These alloys offer an extra choice for selection of matrix material because of

their low weight and interesting combination of mechanical and tribological properties. Pure aluminum is corrosion resistant but lacks in strength and wear resistance. On the other hand, aluminum alloys do not resist corrosion to such an extent but exhibit good strength and wear resistance. The shortcomings of pure aluminum and its alloys can be minimized/avoided by reinforcing them with ceramic particles. Researchers reported significant enhancements in mechanical properties and wear behavior by adding nonmetallic phases such as oxides, carbides, borides, and nitrides, etc.

The present study attempts to fabricate the Al-Al₂O₃ metal matrix composites using in-situ approach for structural and tribological applications. In addition, this work explore the effects of processing parameters on mechanical and tribological properties and on microstructure of developed composite.

1.2 Problem statement

The introduction of ceramic and oxide particles in an aluminum and aluminum alloy based matrix can be obtained by well-known approaches called ex-situ and in-situ. In the *ex-situ* method, the reinforcement is externally added in the matrix by stir casting or powder processing route. However, in the case of the *in-situ* method, the reinforcing phase is generally produced during the fabrication process within the matrix itself. For *ex-situ*, it is quite easy to control the reinforcement size and shape in the embedded matrix but in *in-situ*, the knowledge of chemical reaction and the resulting product of the reaction is highly desired. The shape, size, of the reinforcement and their uniform distribution primarily control the properties; mechanical and tribological in PMMCs. The *in-situ* composites have potential advantages over *ex-situ* composites like higher interfacial strength, better wettability, better particle size & distribution, improved mechanical properties at a economic cost of production. The major challenge of fabrication of *in-situ* composites includes a limited choice of reinforcements. The reinforcements should be thermodynamically feasible as the nucleation and growth processes govern their size & shape. In case of cast aluminum composites in which the

reinforcement particles are introduced externally, it is very difficult to introduce particles of size less than 20 μm due to significant clustering, resulting in the composite being very brittle [11].

The existing literature revealed that *in-situ* approach together with a stir casting has not been used so far for the production of Al-Al₂O₃ metal matrix composites using V₂O₅ as reducing agent for the in-situ reaction. Therefore, an effort has been made to fabricate Al-Al₂O₃ composites through *in-situ* approach together with stir casting technique. Commercially available pure aluminum (99.65%), hypoeutectic Al-Si alloy with 7% Si (approx.) and V₂O₅ particles of 10-15 μ size have been used. The present study also investigates the effect of V₂O₅ particle concentration and various process parameters of stir casting such as shape of the blade, casting and pouring temperature, stirring speed, etc. on the size and dispersion of Al₂O₃ particles in the composites. Effect of these parameters on mechanical and tribological properties for as cast and heat-treated samples have also been investigated. The properties considered, for the investigation are tensile strength, elongations, ductility, hardness, coefficient of friction, specific and bulk wear etc.

CHAPTER 2 LITERATURE REVIEW

This chapter covers the various fabrication techniques of aluminum alloy based metal matrix composites used by early researchers. Special importance is given to the particulate aluminum metal matrix composites developed by stir casting method with and without in-situ approach. The review is mostly focused on the mechanical and tribological properties of the composites. Identified research gaps have been summarized to formulate the problem statement and setting the objectives of this study as presented in the last section of this chapter.

2.1 Introduction

The intensive research in the arena of materials has given a creative approach to produce superior materials at low cost and with enhanced properties to accomplish the demands of the various engineering sector. Aluminum alloys have a wide range of applications Worldwide, due to their excellent properties [12]–[14]. Aluminum alloys exhibit higher specific strength, higher ductility and are more economical as compared to other nonferrous materials [15]. Yet, the applications are restricted because of less resistance to wear. To overcome this problem, numerous hard ceramic particles like SiC, TiB₂, MoO₃, ZnO, ZrB₂, TiO₂, etc. are incorporated in aluminum alloys to enhance their mechanical and tribological properties. Great improvements have been reported in the properties by the addition of non-metallic phases (like borides, nitrides, oxides, and carbides, etc.) to aluminum alloys [16], [17]. Numerous methods have been reported for the addition of particles in the aluminum matrix, the two most common methods are *ex-situ*, and *in-situ*. In the *ex-situ* method, reinforcement particles are added externally whereas, in the *in-situ* method, reinforcement particles are generated within the matrix. In-situ composites have superior adhesion between the matrix and reinforcement than the *ex-situ* [18], [19]. In-situ method is very cost effective and provides superior mechanical and tribological properties. The *in-situ* method facilitates

the uniform dispersion of the thermodynamically stable reinforcement particles formed by the in-situ reaction [20].

Wear is treated as a serious problem in all the mating parts having relative motion regardless of its domain of occurrence. With the advancement of technology, the demand for the materials having good tribological properties is increasing [21].

Al-Si alloys have attracted considerable attention among all the existing aluminum alloys due to their exceptional properties [22]. Al-Si alloys contribute to more than 80% of aluminum castings because of their very good castability [23]. Al-Si alloys have comprehensive usage in automobile and aerospace sector due to lightweight, low density, great fluidity and low coefficient of thermal expansion[24]. The wear behavior of the Al-Si alloys can be further enhanced with the addition of reinforcement particles.

Generally, the composite consists of the matrix and reinforcement. Matrix can be metallic, nonmetallic, polymer or ceramics, etc. Reinforcement are flakes, particles, whiskers, or fibers. In any composite, if the matrix is metallic, then it is termed as metal matrix composites. Similarly, polymeric and ceramic matrices lead to polymer-matrix composites (PMC), and ceramic matrix composites (CMC). Generally, the reinforcement is embedded in the matrix and it improves the overall properties. Matrix holds the reinforcement, and, if designed properly, the newly developed composite shows better properties over its constituents. There are many ways to add the reinforcement into the matrix.

2.2 Processing routes of AMC's

The primary issues associated with the fabrication of a composite for a given application are selection and distribution of constituent phases, the interfaces, and their possible tailoring. To enhance the properties, researchers for the development of aluminum-based composites have used several processing techniques. Researchers have reported the classification of in-situ fabrication techniques for the metal matrix composites. Tjong et. al. identified a

processing techniques for commercial production of the in-situ composites in agreement with the temperature and reactants of the metal matrix [25]. The processing routes are classified on the basis of their reaction in different states.

2.2.1 The reaction between solid and liquid

In this technique, reactants react inside the melt to make in situ fortifying stages or may react with a few constituents of the melt to make in situ ceramic reinforcement. In this procedure, the strengthening particles are created inside the dissolvable medium (the grid) by means of dispersion of the reacting components. This technique has been accepted broadly for the synthesis of metal matrix composites. The solid-liquid reaction process is further classified as follows;

2.2.1.1 Self- Propagating High-Temperature Synthesis

The SHS process was developed by Merzhov and coworkers in 1992. In this technique, a combustion wave is used to handle the high amount of heat generated by the material, which suddenly proliferates through the reactants and transforms them into the products. Self-supporting response front is a critical element of the SHS responses where three fundamental prerequisites are satisfied keeping in mind the end goal to complete self-maintaining response. This process yields high purity products as at high temperature the volatilization of impurity occurs. The SHS has been utilized for the handling of melt and intermetallic grid composites (IMCs).

Literature reveals that the SHS process is extensively used for the intermetallic composites as well as for the production of ceramics [26]–[32]. Less work has been reported by this method for in-situ metal matrix composite because of high exothermic reactions. Fabrication of Al-based composite by SHS reaction was first reported by Choi et al. with TiC [33].

2.2.1.2 Exothermic Dispersion

Martin Marietta Laboratories, USA, developed exothermic dispersion (XD) methodology in 1980's. In this process, powders of ceramics are heated at a very high temperature in the presence of metallic phase. The ceramic elements eventually formulate the hard particles within the solvent phase due to the exothermic reaction between the elements.

TiB₂ strengthened Al based in situ composites have been synthesized by Kuruvilla et al (1990) by utilizing XD procedure. They have pressed the powders of Al, Ti, and B at high temperatures in the presence of inert gas, resulting in the formation of in-situ TiB₂ particles with a size of nearly 1 μm [34].

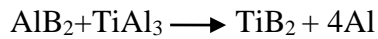
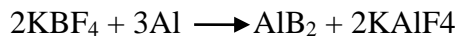
2.2.1.3 Direct Reaction Synthesis (DRS)

In this case, in-situ ceramic reinforcing particles are generated due to the exothermic reaction between reactant powder and molten metal. Maity et al. (1993) have used DRS process to developed Al₂O₃ reinforced composite by adding TiO₂ to the melt at 973 K. Uniformly dispersed fine Al₂O₃ particles of 3 microns are formed in the composite due to the reaction between TiO₂ and molten aluminum [35]. Researchers have developed TiC reinforced Al matrix composites by melting aluminum and a carbide-forming element in a MgO crucible under an inert atmosphere and adding SiC particles as a source of solid Carbon. The work reports that the size of SiC particle has great influence on the dispersion of TiC particles and on rate of reaction [36].

2.2.1.4 Flux assisted synthesis

The process is also termed as a mixed salt reaction. The process was developed and patented by London Scandinavian Metallurgical Company (LSM). This technique was based on their prevailing technology of producing fine grained aluminum alloys and used further for the fabrication of aluminum matrix composites. It requires the addition of a mixture of potassium

hexafluoro titanate (K_2TiF_6) and potassium tetrafluoroborate (KBF_4) to the stirred aluminum melt. The atomic ratio of the salts is the atomic ratio required for TiB_2 particles. Following reactions take place between the salts and aluminum melt.



Kellie and wood have reported the successful fabrication of the TiB_2 reinforced aluminum metal matrix composite with TiB_2 Concentration up to 12 volume % [37]–[40].

Chen and Chung have used a similar approach for the fabrication of in-situ formed TiB_2 particles in 2024 Al composite. They have used TiO_2 , KBF_4 and Na_3AlF_6 powders to form the Al alloy composites. This technique was well established for the viable production of the composites[41]. However, the particle matrix interface was not clear as stated by Davies et al. He has reported an undesirable coating on TiB_2 particles due to the existence of salt in the reaction [38]. Chen et al. concluded that the composites formed by the mixed oxide system exhibit better mechanical properties in TiB_2/Al -4wt. % Cu composites than the composite made-up by the mixed salt reaction system [42].

2.2.1.5 Directed melt oxidation (DIMOX)

The DIMOX method has been developed by Lanxide Enterprise, USA to acquire adaptable metal-ceramic composites. Its central advantage is its capacity to produce intricately shaped thick composites with appropriate properties to address the issues of a diverse scope of utilization. In this process, Al- alloy-containing Mg is oxidized at a temperature range of 1263 to 1680K. The product formed due to the reaction usually grows in the outward direction from the metal surface. Growth takes places either into voids or into filler material and continues until the reaction is stopped due to insufficient

supply of molten metal. The end product is an interrelated oxide network with filled molten metal in the interstitial sites. The reaction kinetics is further expedited by adding the filler material like whiskers, fibers, and particles. This procedure is broadly used to harvest ceramics and metal reinforced composites [6], [43]–[45].

2.2.1.6 Reactive Squeeze casting

Howlett made the main endeavor for Squeeze casting in 1976. He attempted to make carbon fiber reinforced aluminum composites. Later on, this procedure was connected to the creation of metal matrix composites.

Japanese researchers found that aluminum responds promptly with various reinforcements. The idea of Reactive Squeeze casting was conceived at Hiroshima University in 1990 and Fukunaga was the first to use it for the development of Al-Al₂O₃ in-situ composites. He used TiO₂ in powder or whisker form to prepare a preform and then it was kept in a preheated die. The liquid aluminum was then transferred and pressed at a moderately low speed to fill the preform. Phases like α -Al₂O₃, Al₃Ti, and TiAl were formed due to the reaction between TiO₂ and molten aluminum. Through this experiment, they concluded that the fabrication of intermetallic composites with uniform structure is very difficult through RSC technique [46].

As of late, Pan and Pan et al. announced RSC technique for the creation of Al-based composites. They observed that the reaction, which takes place during reactive squeeze casting, is very difficult to control. In addition, they found the heterogeneous structure of the formed composite [47], [48]. It is also reported that heat treatment at 1073 K is required to achieve uniform microstructure & In situ formation of alumina and Al₃Ti and the composite fabricated by RSC technique using TiO₂-Al combinations [49], [50].

2.2.2 The reaction between Solid –Solid

2.2.2.1 Powder metallurgy

Powder metallurgy is one of the well-known technique utilized for the fabrication of MMCs. It is also termed as Powder blending and consolidation process. The procedure for the production of the MMC by this route is shown in Figure 2.1



Figure 2.1 Powder metallurgy Production process

Chianeh et al. have utilized the powder metallurgy technique for the fabrication of in-situ Al-Al₃Ti composite. In this procedure, Ti and pure Al powders were blended and were sintered at 600⁰C for 5 hours. After the sintering, Al₃Ti intermetallic particles were formed [51]. The fine intermetallic particles of the reinforcement works as a strengthening agent and improves the properties of the composites.

Al₃V-39 wt. % Al₂O₃ nanocomposites were synthesized by mechano-chemical reaction. A stoichiometric mixture of Al and V₂O₅ (6.7 g V₂O₅ and 9.3 g Al) was ball milled according to the following reaction:

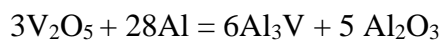


Table 2-1 Thermodynamics Data for Al₃V, Al₂O₃, Al, V₂O₅, and V

Phase	Temp. Range(K)	ΔH^{0}_{298} (KJ/mol)	ΔH^{0}_m (KJ/mol)	C_p (J/molK)
-------	----------------	-------------------------------	---------------------------	----------------

Al ₃ V	298-1607	-20	-	119.54-(43.01x10 ⁻³ T)- (12.18x10 ⁵ T ⁻²)+(6154x10 ⁻⁶ T ²)
Al ₂ O ₃	298-2327 2327-3900	-1657.7	107.58	117.49+(10.38x10 ⁻³ T)- (37.11x10 ⁵ T ⁻²) 184.1
Al	-	0	-	-
V ₂ O ₅	-	-1550.2	-	-
V	-	0	-	-

Table 2-3 shows the free energy and enthalpy at various temperature ranges. The phases formed were Al₃V, Al₂O₃, Al, V₂O₅, and V [52].

2.2.2.2 Diffusion Bonding

It is also termed as foil-fiber-foil technique. The process is commonly used for the fabrication of monofilament-reinforced composites. The Ti-based composite is generally produced by this method. The main problem with this process is heterogeneous distribution and the large volume fraction of fibers. This is not a suitable process for producing the composites of complex shapes.

2.2.3 The reaction between liquid-liquid

Liquid-liquid reaction process uses the response between two streams of liquid metal to produce strengthening refractory particles. In this strategy, at least two fast, turbulent, liquids of metal streams having fragments of a ceramic stage (high temperature) are made to mix with each other in a blending chamber, bringing about intimate blending and reaction to deliver the second stage. The liquid particle blend is then cast in a mold or quickly solidified through melt spinning or by means of atomization. The technique has been extremely successful in fabricating copper-based composites fortified with

TiB₂ particulates of Nano size (50 nm). Lee et al. produced the copper matrix composite for the electrical applications using this method [53].

2.2.3.1 Stir Casting Method

In Stir casting, technique hard or soft ceramic particles are added to the molten or semi-molten metal and stirred with a mechanical stirrer in a crucible. Reinforcing powders are incorporated during stirring of the melt to get uniform dissemination of the particles throughout the melt. The uniformity of dispersion depends on the stirring speed, temperature as well as the time of stirring. Some matrices may require the addition of a wetting agent to improve mixing. The incorporation of high strength refractory particles in a soft matrix provides intermediate mechanical properties that of constituents involved. Generally, metals have a beneficial spectrum of properties with a blend of high strength and high ductility, but low stiffness. Stiffness can be improved by adding stiff and strong brittle ceramic particles to these metals. For instance, aluminum and SiC are very different materials and have different mechanical properties with a Young's Moduli of 70 and 400 GPa respectively, yield strengths of 35 and 600 MPa respectively. When these two materials are combined to form a composite of Al6061/SiC/17p (T6 condition), new material of 96.6 GPa Young's modulus and 510 MPa yield strength is obtained [54]. The blend of materials could be such that one of the constituents gives the continuous phase called matrix while the other is dispersed as a discontinuous phase in the matrix. If any particle/fiber of the distributed phase is not reachable from any other particle/fiber inside the composite without crossing the matrix, this composite is called discontinuously reinforced composite. For these composites, mechanical properties can be further enhanced by optimizing the geometry, size, relative quantity, distribution of the reinforcing phases and by varying the processing conditions.

Generally, for bulk production of discontinuously reinforced composites, stir casting is preferred among the various other existing techniques. The

particular advantages of this process lie in its ease of processing, cost, flexibility, and applicability for larger size components with mass production.

2.2.3.2 Infiltration process

In this process, AMC is produced by the injection of molten aluminum alloy into the spaces of the permeable preforms of fiber (continuous/short), whisker and particles. The infiltration of the preform depends on size and shape of the reinforcement. The infiltration can be achieved with or without the use of vacuum or pressure. It is important to use the mixture of alumina and silica as a binder so that the shape and integrity of the preform could be maintained. This process is quite suitable for the manufacturing of aluminum alloy based composite with reinforcement of particles, whiskers, and fibers. At some level, porosity is observed in this process. The process is applicable to produce aluminum composites with the reinforcement range of 10-70%.

2.2.3.3 Spray deposition

As the name suggests, in this technique, ceramic particles or whiskers/fibers are injected into the spray for the production of aluminum matrix composites. This process often exhibits a porosity of about 5-10% and inhomogeneous particle distribution. Spray process is applicable for both continuous and discontinuous fiber reinforced composites. The production cost of aluminum composites by this method is relatively less and lies in between that of stir casting and powder metallurgy processes.

2.2.3.4 In situ Process

The process in which reinforcement is generated within the matrix due to the reaction is termed as in situ process. Most of the different process like solid-liquid, liquid-liquid, and liquid-gas fall under the in situ process category. This process normally occurs in the presence of the inert environment. Composites can be cast either by direct oxidation process or by the substitution reaction.

In DIMOX, the metal is heated at a very high temperature in order to expose it to an oxidizing atmosphere. For aluminum, this temperature is 900°C. In this case, the molten metals oxidize and form the in situ alumina phase. For the wetting purpose, magnesium and zinc are added in very small quantities. This process is suitable for the fabrication of metal-ceramic composites.

In in-situ method, substitution reaction occurs between the metal oxide and the molten aluminum to form a thermodynamically stable phase. The oxides which are generally used for in situ process are TiO₂ [55], MnO₂ [56], SiO₂ [57], CuO [58], [59], ZnO [60], MoO₃ [61] etc. The resultant product of the reaction is in-situ Al- Al₂O₃ composite because of the reduction of oxide particles by molten aluminum.

Table 2-1 list the practicality of various available processing routes for the development of Al based metal matrix composites [62].

Table 2-2 Usage of AMCs Processing Routes

Types of AMC	Blending & consolidation	Diffusion Bonding	Vapor deposition & consolidation	Stir casting	Infiltration Process	Spray deposition	In-situ reactive process
Continuous fiber-reinforced	Not in Use	Not in Use	In Practice	Not in Use	In Practice	Not in Use	
Mono filament-reinforced	Not in Use	In Practice	In Practice	Not in Use	Generally not used	In Practice	Not in Use
Particle reinforced AMCs	In Practice	Not in Use	In Practice	In Practice	In Practice	In Practice	In Practice
Whisker-reinforced AMCs	In Practice	Not in Use	In Practice	Generally not used	Generally not used	In Practice	Not in Use

The continuity in the distribution of ceramic particulate in the slurry prepared by mixing the various components depends on the type of mixing process used. During processing by agitation in a reactive environment, the reaction products & surface oxides floating on the liquid surface move into the melt and expose a fresh surface for oxidation and gas absorption. Thus, there will be enhanced the formation of the porous surface in the cast product along with the presence of other surface oxides.

2.3 Parameters for Stir casting

2.3.1 Stirrer position and shape

Combining of particles with the molten metal depends on many parameters such as holding temperature, amount & type of particles and their behavior. Comprehensive distribution of reinforcement particles in a melt can take place when a stirrer applies high shear rate in the radial direction. Due to the radial direction of the stirrer, the settling of the particles remains limited. Particle lift is related to flow parameters quantified by particulate dispersion number (PDN).

PDN for a coaxial rotating cylinder is given by the following equation [63]

$$\text{PDN} = [H_0 (\mu \Omega)^{1/2}] / [r^{1/4} d^{3/4} V_t]$$

Where H_0 denotes the height of molten metal,

μ is the viscosity of the slurry

Ω is the angular velocity

r is the radius of the inner cylinder,

d is the gap between the inner and outer cylinders,

V_t is the particle settling velocity

$\text{PDN} > 1$, indicates that the secondary flow velocity is higher than the settling velocity and the particles with a density higher than the liquid will not settle at the bottom and will be lifted up. On the contrary, when PDN is less than 1, it indicates that the particles will settle down. In order to get a homogeneous dispersion, PDN value should be more than 4, is the required condition [64]. The shear action also facilitates the washing of the contaminants and oxides from the surface of the particles and due to this action, the liquid near the particles is continuously refreshed.

The change in viscosity with shear at different temperatures has been studied, viscosity decreases when the shear rate increases. This is attributed to the non-

Newtonian pseudo-plastic nature of the slurry [65]. Increase in viscosity is directly proportional to the volume fraction of the reinforcing particles. The crucible must have a dished or flat bottom. Conical bottoms with angles greater than 150 degrees with the horizontal are not advantageous, as it will trap a pocket of liquid at the bottom of the cone.

According to Ray (1995), some important ratios that require attention when mixing is done using turbine stirrer are; Z/T , D/T , C/D and $(Z-C)/D$ where Z , D , C , and T are depth of alloy in the crucible, diameter of the turbine stirrer, the height of the stirrer and the diameter of the crucible respectively. It is required that the turbine stirrer is kept with 35% fluid beneath it and 65% fluid above it. If a stirrer is to be placed so as to exceed 65% or 35% liquid above or below the stirrer respectively, multiple turbine stirrers must be employed. For bottom pouring, two turbines stirrers are more beneficial than one. Two turbines stirrers are generally required if the ratio of liquid depth to crucible diameter, Z/T , exceeds 1.3. One turbine is placed at 0.5 to 1.0 D below the top surface of the liquid and the other may be placed in the bottom part of the crucible. Ghosh and Ray have carried out an extensive investigation on particle employment through the vortex and have suggested an optimum stirring condition of $D/T = 0.6$ and $C/T = 0.8$ for particle incorporation [66][67].

Harnby et al. have given a rational base for selection of the type of stirrers in terms of increase in viscosity and decrease in speed amongst propeller, turbine paddle anchor, helical ribbon, and helical screw type of stirrers. Turbine type stirrers are widely used for dispersing of particles in the molten alloys. Depending on the direction of discharge, turbine stirrers may be of two types - radial and axial. In flat blade type radial turbine stirrers, the discharge is perpendicular to the centerline of the crucible but in pitched blade type axial stirrers, a secondary flow is generated in the axial direction due to the transfer of momentum from high to low regions causing rise of particles[68]. The stirrers of different designs are shown in Figure 2.2.

		
Straight Blade Stirrer	Three Blade Propeller	Four Blade
		
Anchor stirrer	Turbine Stirrer	Helical Ribbons

Figure 2.2 Types of Mechanical Stirrer

Al-Jarrah et al. have shown solidification of Al/Al₂O₃ composite with the use of turbine type stirrer. Stirring contributes to the transfer of particles into the molten alloy and helps to disperse and suspend the particles in the melt [69], [70] It has been concluded that particle incorporation in case of turbine type stirrer is more as compare to other flat blade type stirrers. In the stir-casting method, high porosity is also reported in the developed composites.

2.4 Reinforcement particles distribution into the molten metal alloy matrix

Among the difficulties faced in synthesizing composites, settling and flotation of the particles in crucible or in the mold is very common. In stir casting, this problem occurs due to density difference of molten alloy and the reinforcement. Dispersion of reinforcing particle in molten alloy depends largely on the viscosity of the slurry, which in turn depends on the particle incorporation extent in the melt. The viscosity facilitates effective mixing by

parting up agglomerates, minimizing gas entraps, aids settling rate and making the distribution of particles more uniform [64], [65], [71].

Distribution of reinforcement particles depends on the various factors as follows;

- Type, size and amount of reinforcement
- Processing temperature
- Holding time
- Design of stirrer and stirring speed
- Preheating of mould and reinforcement particles
- Pouring temperature

In the case of in-situ technique, it is very important to understand how the reinforcement particles are incorporated into the melt. Many techniques have been used so far for the introduction of particles into the melt, and few of them are mentioned below:

- Addition of particles into the mould filled with the molten alloy.
- Incorporation of reinforcement particles by using injection gun in the presence of an inert environment.
- Squeezing of particles with the help of reciprocating bars into the melt.
- Dispersion of particles by means of centrifugal action.
- Mixing of particles in the melt by high ultrasound intensity.
- Gravity casting with high vacuum and at high temperature for a long period.

Another method, termed as the vortex method, has been found as one of the utmost appropriate method for the development of composite. As the name

suggests, in this method, the formation of vortex takes place due to the continuous stirring of the molten alloy.

The development of the vortex creates the pressure difference between the outer and the inner surfaces of the molten alloy, which eventually sucks the particles into the melt. This method gives a better & uniform distribution of the reinforcement particles [65], [71].

2.5 Effect of porosity in cast composites

Porosity effect the mechanical properties of composites up to a large extent. Generally, mechanical properties decrease with increasing porosity. It is undesirable and therefore it is very necessary to decrease the level of porosity.

There are many reasons due to which level of porosity increases. The main reason by which porosity arises is the gas entrapment. At the time of the casting, during particle addition in the molten alloy, air bubbles are also sucked along with the particles by molten metal. This entrapment of air in melt occurs due to the vortex formation.

Ray et. al. has shown that the porosity is related to holding time, holding temperature and the position of the stirrer. They have reported that the porosity decreases when holding temperature increases and vice-versa [72]. According to Lloyd, the volume fraction of the particles is responsible for the porosity level. Higher porosity level has been reported with a large amount of volume fraction. Porosity increases linearly with particle content [70], [73].

Another important source of porosity is moisture and the size of the particles. Miwa has proved that the moisture absorption by the particle increases the porosity in the composite. The moisture absorption depends on the temperature used for heating the particles. The moisture can be removed by heating the particles above 220⁰ C. The temperature range for heating the particle is 220-600⁰C [74]. The use of inert gas also gives good results in terms of porosity level. While using the inert gas, it is highly recommended

that the distance of the mould from the furnace should be as short as possible [75].

2.6 Wetting of particles

Wettability is described as the capability of a liquid to wet a surface. It is also defined in terms of the angle between the drop of the fluid and the solid surface. The angle formation depends upon the surface tension. If the surface tension of a liquid is high, then it will form a droplet. Whereas, if surface tension is low, the liquid will be spread over the surface.

In terms of energy, if a surface has high surface energy, the drop will spread over it, and a droplet will be formed in case of low surface energy. This is an after effect of interfacial energy minimization. For the minimization of energy, the surface with high energy always tends to be covered with the liquid of lower energy.

The wetting is represented by contact angle θ , which depends on the interfacial tension of the surfaces. There are three cases of wetting with respect to the angle.

$\theta=0$ represents perfect wetting

$0^\circ < \theta < 90^\circ$ represents a high degree of wetting.

$90^\circ < \theta < 180^\circ$ represents poor wetting

A sound casting requires wetting of ceramics particles by molten alloy, which in turn needs to have an interfacial reaction between them. According to Murthy and Rao, for the achievement of superior mechanical properties, an interfacial bond of good strength is required. The bond strength rely on the chemical reaction and the wettability between nonmetallic reinforcement & the molten state matrix [45].

The wetting can be enhanced either by improving the surface energies or by reducing the surface tension of the liquid [76]. Wetting can also be promoted by

- 1) Coating the solid particles by Ni and Cu. The coating is done in order to increase the surface energy. The coating of Cu and Ni have been reported on the graphite particles for the development of Al composites by Surappa and Rohtagi [77]–[79].
- 2) By adding wetting agents like Magnesium, Silicon, Titanium, and Scandium, etc. in the molten alloy. Mg has been used as a wetting agent by many researchers in the development of Aluminum matrix composites. Abdulhaqq has examined the influence of Mg addition on wetting and the microstructure of Al-MnO₂ composites. He has observed no major changes in the microstructure of cast In situ composite when Mg content increased from 0 to 8% at 670⁰C processing temperature [80].
- 3) By the heat treatment of the particles.

To promote wettability, an attempt has been made by Yilmaz. He has observed that the bond strength can be maximized by keeping the solid particle for a longer period in the molten metal.

The chemical reaction and the addition of various chemicals also promote wettability. Sodium tetraborate [81], [82], Nitrogen [83], solid Mg Nitride [84], Organic solvents and Alcohol [85], etc. have been used by researchers for the wettability improvement of alumina particles.

2.7 Processing parameters

There are various parameters, which affect the processing of AMCs. If we control these parameters, a defect-free composite can be produced.

2.7.1 Stirring speed

Optimum stirring speed is very essential for mixing the particles in the melt. It is observed that a proper stirring speed by keeping the right position of the stirrer (65% liquid above the stirrer and remaining down the stirrer) promotes wettability. Stirring would give better results if the slurry is in the stage of

solidifying rather than in fully liquid condition. In the complete liquid condition, the particles mostly tend to float on the surface and they won't mix irrespective of the speed of the stirrer. It is advised that the stirring should be done when the slurry is in solidifying stage and once the stirring is completed, the slurry should be heated again to bring in a liquid condition before pouring.

2.7.2 Stirring temperature

Stirring temperature has a substantial role in the fabrication of metal matrix composite. Stirring temperature initiates and accelerates the chemical reaction among the reinforcement and the base alloy. The viscosity decreases by increasing the stirring temperature, which in turn affects the particle distribution within the matrix. As discussed earlier, the mixing of particles is bit difficult if the viscosity of the slurry is less.

2.7.3 Preheating of the particles

Most of the researchers have advised the preheating of the particles before adding into the melt. Preheating decreases, the temperature difference between the molten metal alloy, the reinforcement, and gives better mixing. Any kind of impurity and moisture is also removed by preheating which eventually promotes wettability. In the case of SiC particles, preheating prevents any kind of alteration in the surface composition and it prevents the oxide layer formation on the surface of particles.

2.7.4 Holding time

It is also termed as a stirring time. Better mixing will take place if holding time is less. This is applicable to the temperature where the slurry has sufficient viscosity. In this situation, the velocity of the particles added is very small and they get distributed uniformly in molten state matrix.

For large holding time, there is uniform distribution but agglomeration is also present. The reason behind this cluster formation is the vortex phenomena of

mixing. The air bubbles along with particles sucked by molten alloy form the cluster and increase the porosity. Generally, at high temperature and large holding time, cluster formation and non-uniform distribution of particles take place.

2.7.5 Adding/feeding rate of the particles

The particles should be added with a uniform rate to achieve a defect-free composite. If the addition of particles to the melt is non-uniform, inclusion defects and porosity defects arise. Researchers have used various setups for making the flow uniform and to control the flow rate.

The processing parameters are very important and should be always considered at the time of the composite development since they have the great influence on different mechanical and tribological properties. By controlling these parameters, porosity and the inclusion defect can be minimized. Preheating the mould before pouring the molten alloy into it also prevents the porosity and increases the soundness of the composite. Preheating of the particles before addition promotes the wettability and removes the moisture, which is present due to the atmospheric condition. Stirring speed should not be very high and the distance between the mould and the furnace should be the shortest.

2.8 Mechanical Properties of the composites

The main purpose of combining two or more different homogenous materials to form a composite is to enhance and alter the mechanical properties according to the use and application. The mechanical properties of composite largely depends on the following:

1. Geometrical parameters (amount, size, and shape of dispersed phase)
2. Mechanical properties of constituents (dispersed phase and matrix material)

3. Nature of Interface

The shape and morphology of the dispersed phase determine the load bearing ability of the composites [86]. Based on the shape and morphology, Composites are divided into three categories:

- a) Continuous fiber/whisker reinforced composites
 - b) Discontinuous fiber /whisker reinforced composites
 - c) Particle reinforced composites
- Continuous – The load is applied directly to both the matrix and fiber and finally transfer to the fiber via matrix.
 - Discontinuous - The load is transferred to the dispersed fibers via matrix.
 - Particle – The load is shared equally between the matrix and the reinforced particle.
 - During load transfer, shear stress develops at the interface due to the mismatch of strain in matrix and dispersed phase across the interface.
 - Mechanical properties of fiber and whisker reinforced composites are almost alike whether continuous or discontinuous but the short/ discontinues fibers reinforced composites show more strength than particle reinforced composites. Ductility decreases in composite reinforced with hard or soft particles because of heterogeneous strain developed in the base material. The reinforcement-matrix interface affects the mechanical properties of composites.

2.8.1 Properties of particulate composite

Mechanical properties of particulate composite are organized by deformation characteristics of the matrix and dispersoids present in the matrix. Particle reinforced composites are divided on the basis of the mechanical properties of their constituents. Possible combinations are as follows:

1. Brittle matrix either with ductile particle or brittle particle
2. Ductile matrix either with ductile particle or brittle particle

The composites with ductile and brittle particles in a soft matrix have gained great attention due to their demand in various applications.

In Particulate metal matrix composites, particles act as reinforcement. The shape of the particle can be regular or irregular. It might be round shape, a platelet shape, cubic, tetragonal or any other unpredictable and customary shape but should be equiaxed.

Particles as fillers are commonly used to improve the wear properties, to reduce friction and hardness, to improve stiffness, to enhance the thermal and electrical characteristics, and to reduce shrinkage. Generally, the addition of particles in PMMCs is quite compelling because of their simplicity of fabrication by conventional techniques at lower costs together with a worthy combination of other mechanical properties (Ray, 1993).

2.8.2 Tensile properties of in-situ composites

Westwood reported the first attempt with improved properties for in-situ TiB₂/Al composite [87]. He has observed a great improvement in tensile strength and wear behavior of the developed composite. Later on, Kuruvilla has done the comparison of ex-situ and Insitu TiB₂/Al composite produced with 20Vol. % of TiB₂ particles shown in Table 2-2. [34]. The comparison shows that the tensile strength and yield strength of the developed in-situ composite is almost double and approx.3.5 times greater than ex-situ and pure Al respectively. The fine dispersion and well bonding of the TiB₂ particles is the main reason for this composite strengthening.

Table 2-3 Tensile Properties comparison of Insitu & exsitu TiB₂/Al composite				
Material	UTS (MPa)	Yield	Elongation	Hardness
Pure Al	90	64	21	37
Exsitu	166	121	16	85
Insitu	334	235	7	110

Another in-situ TiB_2 reinforced AMC was developed by reaction method. In this method, the researchers have incorporated carbon with and without Cu and observed good improvement in ductility, yield & tensile strength and Young's modulus without adding Cu. Formation of TiC due to the addition of carbon & subsequent reduction generates Al_3Ti intermetallic and same was found responsible for the improvement. However, Cu addition reduces the TiC formation and promoted the nucleation of Al_3Ti intermetallic. By increasing the TiC particulates, the ductility was found to increase in the developed composite [88].

The effect of volume fraction of reinforcement and particle size, on fracture toughness of in-situ TiB_2 reinforced Al-Cu-Mg alloy based composites have been investigated. The average particle diameter varies from 0.3-1.3 micron and the volume fraction varies 0 to 15 % in these composites. Fracture toughness remains unaffected with the variation in particle size but decreases with increase in volume fraction. This decrease in fracture toughness is ascribed to the pushing of particles during solidification [89].

Aluminum alloy based composites have been developed by in-situ method. Al_2O_3 particles of high purity were formed by the decomposition of $\text{Al}_2(\text{SO}_4)_3$ during Insitu reaction. The composite was characterized and found free of cast defects such as blow holes, porosity, and particle segregation. [90].

The tensile properties of $\text{Al}_2\text{O}_3+\text{TiB}_2/\text{Al}$ composites fabricated by RHP technique have been examined. Insitu TiB_2 particles are formed by adding boron to reduce the intermetallic Al_3Ti phase. High strength has been reported in the composites with TiB_2 particulates as being more effective reinforcement than Al_2O_3 [91]. TiB_2 particle reinforced composite was fabricated by reaction processing method using three different ternary alloy systems namely Ti-Al-B, $\text{TiO}_2\text{-Al-B}$ & $\text{TiO}_2\text{-Al-B}_2\text{O}_3$ system. Particulates of TiB_2 were formed due to in-situ reaction occurs between Ti & B content. Coarse Al_3Ti phase was formed together with TiB_2 particles in case of Ti-Al-B alloy system; whereas fine equiaxed Al_2O_3 & TiB_2 particles were formed in $\text{TiO}_2\text{-Al-B}$ & $\text{TiO}_2\text{-Al-B}_2\text{O}_3$ alloy system. $\text{Al}_2\text{O}_3+\text{TiB}_2/\text{Al}$ composites fabricated using $\text{TiO}_2\text{-Al-B}$

system reveals exceptional mechanical properties. The composite show the improved yield with TiB_2 content. The yield strength of these composite is increased further, by adding CuO in TiO_2 -Al-B system as Al_2Cu precipitates provides strengthening effect. Moreover, CuO has no effect on Insitu reaction [92].

Stir casting technique was used for the development of in-situ TiB_2 /Al alloy composites. The process variables were optimized to generate TiB_2 particulates of 1 to 3-micron size. The increment in the properties was observed by increasing the volume fraction of TiB_2 particles [93].

Various process parameters (temperature, reaction time and mass fraction of TiB_2 particles) were optimized through Response surface methodology. Five different levels of these parameters were taken for optimization & subsequent development of mathematical models for calculating the hardness and strength of in-situ composites at 95% confidence level. The models were validated using ANOVA [94].

Al alloy- TiB_2 and Al-alloy TiC composites were fabricated by the in-situ method. Aluminum alloy A356 was used as matrix and, KBF_4 & K_2TiF_6 salts were used for the reaction. The improvement in hardness was detected due to in-situ formed particles. The segregation of reinforcement was controlled by stirring the slurry until pouring of the melt [95].

2.8.3 Effect of oxide reinforcement

Apart from the carbides and nitrides, ceramic oxides are also used for the fabrication of in-situ composites. Many oxides such as MnO_2 , ZnO , MoO_3 , CuO , SO_3 , and CeO_2 have been used to fabricate Insitu Al_2O_3 /Al composites. These metal/nonmetal oxides are added externally and get reduced by liquid aluminum to form Insitu Al_2O_3 /Al composite. Alumina and other useful materials generate within the melt due to the reduction reaction and contribute to the enhancement of properties.

In-situ Al-Mg- Al_2O_3 composite has been fabricated by the addition of MnO_2 particles in an aluminum-magnesium alloy. MgAl_2O_4 and magnesium oxide are generated by the reaction between MnO_2 and the matrix alloy. The enhancement in strength and hardness is observed due to the dispersion of MgAl_2O_4 particles. Porosity and the degradation of the properties are observed with increasing MnO_2 addition due to the depletion of Mg in the matrix [96].

Many researchers used pure aluminum to fabricate Insitu Al_2O_3 /Al composite by adding copper oxide (CuO) particles. 5 wt. % of CuO particles without any wetting agent were added to the pure aluminum matrix. CuO particles were reduced by molten aluminum to form Cu and Al_2O_3 particles. Researchers observed improvement in properties over base metals by addition of CuO and subsequent formation of in-situ Al_2O_3 particles. A small percentage of CuO was found to be enough to complete the reaction between the matrix and particles [97].

The forming behavior and the mechanical properties were investigated for the Insitu composites formed by the reduction of MoO_3 . The particles were added at a processing temperature of 850°C to the liquid aluminum alloy together with a small amount of Mg as a wetting agent. Better mechanical and wear properties were observed in these composites over the pure aluminum [98].

The formation mechanism of in-situ $\text{Al}_3\text{V}/\text{Al}_2\text{O}_3$ nanocomposite has been investigated. The composite was developed through mechano-chemical reactions that occur between aluminum and V_2O_5 powders after 30 min high energy ball milling of the mixtures of these powders. Nanocrystalline Al_3V and Al_2O_3 are formed with continued milling due to the reaction that takes place in combustion mode between the powders. Al_3V finally decompose in Al & V with continued milling for a long duration of 40 hours. Which leads to optimum milling time of 20 hours for the fabrication of the composite. Insignificant growth of Al_3V & Al_2O_3 after isothermal annealing of as-milled powder at 600°C for 2 hours confirmed the thermodynamic stability of the Nanocomposite. Isothermal annealing has in the ordering of partially disordered Al_3V of as milled composite powder [52].

$\text{Al}_2\text{O}_3/\text{Al}$ composite produced by the displacement reaction has been reported. The composite was fabricated by mixing the powders of Al and CuO using ball milling followed by displacement reaction between Al & CuO during sintering at 900°C in the presence of nitrogen atmosphere. Amorphous Al_2O_3 , formed below 700°C gets transformed into crystalline Al_2O_3 at higher temperatures. Fabricated composite responded well to aging treatment and attained maximum hardness after 4h of aging at 200°C [99]. The cast samples of ex-situ $\text{Al}_2\text{O}_3/\text{Al-Si}$ (A356) alloy composite were prepared using Rheocasting technique. The influence of the dispersion of Nano alumina particles in Al-Si hypoeutectic alloy before and after heat treatment has been investigated. The casting samples of A356 alloy were fabricated by the addition of ex-situ Nano Al_2O_3 particles using the Rheocasting technique. Enrichment in mechanical properties was reported due to refined interlamellar spacing and the dendrite arm length [100], [101].

In-situ reinforced A356-3wt% TiB_2 composite was prepared by the re-melting process. The effect of Sr addition as a modifier has been studied. The optimum modification was obtained with the addition of 0.03 wt% of Sr to the composition. The investigation shows that the enhancement in strength and ductility observed due to changes in Si morphology as well as melt cleanliness[102].

A new in-situ fiber reinforced AMC was developed by powder metallurgy route. The powders of Al and Mg have been used. The tensile properties and microstructure of this composite were analyzed. The composite exhibits substantial enhancement in properties due to the existence of Al-Mg intermetallic compound ($\beta\text{-Al}_3\text{Mg}_2$) [103].

2.9 Tribological Aspects in Al MMC

The friction between two mating surfaces generally causes wear and leads to the progressive loss of materials from the surface. Wear is a severe problem in numerous industries where relative motion exists between two contact surfaces e.g. in the automotive sector, material extraction, and processing,

aerospace, etc.[21], [104]. Wear occurs due to different mechanisms such as adhesion, abrasion, corrosion, and fatigue. At any instance, the complex mechanism of wear may be any one or the combination of these. Sometimes, the combination of the effects also gives a favorable result. For instance, the formation of oxide layer acts as a lubricant or a passive protecting layer and improves resistance to adhesive wear or resistance to corrosion.

The wear behavior depends upon the operating conditions along with the mechanical properties of the composites. Sliding velocity applied load and the temperature are very important aspects to be considered for wear [105]–[107]. Apart from the operating conditions, surface roughness, contact geometry, and grain size also influence the wear substantially. Literature reveals that the mechanical properties responsible for wear behavior are directed by the reinforcement (shape, size and quantity), rate of solidification, chemical composition, and grain refinement [108]–[110].

Wear can be classified as:

- a) on the basis of relative motion (sliding, rolling, reciprocating and impacting)
- b) based on particle removal mechanism
- c) Severity

Wear can be further categorized by the mechanism involved for particle removal.

2.9.1 Abrasive wear

This type of wear happens when hard, irregular, and sharp particles rub against soft surfaces. The coefficient of friction is large in abrasive wear as compared to that in adhesive wear. In this case, due to sliding of hard particles on the surfaces grooves are formed. These hard particles may be an integral part of the rubbing surfaces or might be generated between the surfaces due to oxidation[111].

The particle's grit size play a significant role in the abrasion. Wear mechanism changes from cutting to sliding as the grit size of the particles decreases[112]. The value for the particle grit size can be estimated by the ratio w/r , where w stands for groove width and r is the tip radius of the particle.

As grit size increases, wear volume increases. The depth of the plastically strained region depends on the grit size and the applied load [113]. The similar wear mechanism was found in case of 3-body and 2-body abrasive wear. The dependence of wear rate on sliding time, material hardness and abrasive grain size was found to be similar in 3-body and 2-body abrasion, but wear rates in 3-body abrasion were 10 times less than 2-body abrasion. The reason for low wear rate in 3-body abrasion wear is that on an average basis, a loose abrasive grain spends 90% of its time in rolling whereas only 10% time in abrading the sliding surfaces. This is in accordance with the Archard' s theory [114].

Highest wear resistance is observed with microstructures containing fine and highly scattered particles. The rate of wear depends on the hardness & grit size of the abrasive particles. As grain size decreases, hardness increases and consequently wear resistance increases [115]. In contrast to this finding, another researcher observed a higher wear rate for abrasive particles having hardness greater than 1.2 times of the wearing surface [116].

In abrasive wear, due to hard and sharp abrasive particles, groove formation takes place on the wearing surface. In a groove, the number of debris formed and their shape, size can be estimated with the help of microscopic wear model. An equation for the determination of the degree of penetration by abrasive particles and their relation with hardness and shape is given by:

$$D_p = h/a = R (H/2W)^{1/2} - (\pi R^2 H/2W - 1)^{1/2}$$

Where h = penetration depth

a =contact radius

D_p = degree of penetration

H =hardness of the worn surface

W=load applied

R= radius of asperity

The two bodies abrasive wear has been studied for the Al alloy composites reinforced with alumina fiber. SiC particles of different grit size have been used as abrasive media. The wear resistance of the composite is found to increase with a decrease in the abrasive particle size and vice versa. The effect of volume fraction was also examined and it is found that increase in the volume fraction of fiber with fine abrasive particles does not improve the wear resistance, but wear resistance decreases when fiber volume fraction exceeds 20 % with coarse abrasive particles. The increasing volume fraction de-bonds the matrix-fiber interface and increases the interaction between abrasive particles and fiber reinforcement. This leads to fiber fracture and microcracking, which perform a noteworthy role in determining the wear rate. [117]. A new relationship has been derived for the abrasive wear having alumina fiber as reinforcement. The relationship is expressed as follows:

$$D_c = (3\pi/4)^{1/4} K^{1/2} (\sigma_f/\sigma)^{1/4} (H_m/H_s)^{1/4}$$

Where H_s = hardness of the specimen

H_m = Hardness of the matrix

σ_f = Fracture stress

σ = Contact pressure

K = geometrical constant for Al alloys with SiC (0.6) as abrasive media.

2.9.2 Adhesive wear

This type of wear occurs because of dry contact between the surfaces. In this wear, due to relative motion between the mating surfaces, the particles from one surface stuck on the counter surface. These small particles act as load carriers and the surfaces touch each other by means of these small asperities [118], [119].

Therefore, the hardness of asperities is very important. Additionally, applied load, sliding speed, real area of contact, and hardness of material play a vital role in determining the wear rate. Wear rate is expressed by Archard's equation, as

$$W = KSN/3H$$

S= Sliding distance,

H= bulk hardness of the material,

K= wear coefficient, and N= normal applied load

This equation was based on the ideal sliding conditions and the effect of microstructure was not included. To account for this, another mechanism called delamination theory was proposed.

- This theory was based on the behavior of dislocations, voids and crack formation due to the plastic deformation [120].
- Dislocations are created because of the plastic deformation in the material.
- With continuous sliding of the surfaces, dislocations start to heap-up near the surface.
- This leads to the formation of voids and due to the growth of voids, a crack is initiated parallel to the wear surface.
- The crack is then transformed into the surface shear and sheet-like particles are produced out of it.
- This theory is applicable only where low sliding speed is used so that no phase transformation and diffusion take place.

To calculate the wear, it is important to know about friction. There is no surface, which is completely smooth. All surfaces have some irregularities and grooves, which make the surface rough. At the time relative motion between such surfaces, the rough surface tends to lock the other one to generate friction. This is represented by the frictional force given by equation

$$F = \mu \times N$$

Where μ stands for coefficient of friction and N represents the normal applied load. This implies that the frictional force relies on the load applied.

The reasons for the generation of friction are

- Ploughing by hard particles
- Adhesion between the surfaces
- Deformation of asperities.

The contributions of these factors depend on the environment, speed and load applied. It is reported that ploughing and deformation of asperities are the major contributors to the frictional coefficient [104], [121].

Aluminum alloys reveal unfavorable wear properties however, the addition of ceramic or oxide particles significantly supports in eliminating these drawbacks. The particles incorporated by the traditional stir casting approach leads to poor bonding and also separation of reinforcing particles occurs at the interfaces [122]–[125].

For the enhancement of wear properties, researchers have made many attempts. Si presence shows a great improvement in wear properties. Wear properties increases with more Si content in the composite [126]. Rohtagi has reported a significant reduction in wear rate due to the presence of Al_2O_3 and Silica [127]–[130].

Friction and wear performance of Al-Mg alloy and Al-Mg-Cu alloy based composite was examined. The composite was reinforced with SiC particles. Less wear was observed for copper-containing alloy based composite as compared to Al-Mg alloy based composites. The overall volume loss of the composite was found to decrease up to 5% Cu addition as well as with increasing SiC reinforcement. The enhancement in wear resistance is credited to Silicon carbide particles present in the composites [131].

Another Al-Mg-Cu alloy based composite is fabricated by the addition of 20 wt. % SiO_2 particles to the base alloy matrix. This composite was fabricated through powder metallurgy route and the reinforced phases produced by the

reaction between particles and alloy during sintering were MgAl_2O_4 , MgO , and Mg_2Si . The wear study revealed that the composite could sustain the maximum load of 196 N under dry wear condition and 1764N under lubricated wear condition. The maximum volume loss and friction factor under lubricated wear condition were found to be 0.8 mm^3 and 0.14 respectively. In dry wear conditions, the plastic deformation of the inferior layer and the breaking of SiO_2 particles were observed. Therefore the composite was recommended to be suitable for heavy loads under lubricated sliding wear condition[132].

Effect of TiC addition on the friction and wear behavior of Al-4%Cu based composites was investigated. The composites were developed by casting and powder metallurgy route with varying TiC particle size & content. Significant improvement in wear resistance & hardness was perceived in all the composites prepared through both the routes. However, the composite with fine TiC particles ($0.6\text{-}3.5\mu\text{m}$) display high hardness and low wear resistance as compared to the composite containing coarse particles. The lower wear resistance of composites containing fine carbide particle is credited to the detachment of particles due to poor interfacial bonding from wear surfaces of the composites [133].

The frictional wear behavior of Al-18wt% Mg_2Si composite modified by Nd was investigated. The addition of Nd changes the morphology of primary & eutectic Mg_2Si particles from dendritic to polyhedral and flake-like to dot-like respectively. Peak hardness is observed with 0.5% Nd addition. Better wear resistance has been observed in the Nd modified composites as compared to the composite without Nd. The wear mechanism changes from a combination of abrasive, adhesive and the delamination wear to single mild abrasion wear with the addition 0.5 % Nd [134].

The wear properties of Al-4.5 %Cu in-situ composite reinforced with TiC was examined. The result shows great improvement in the developed composite as compared to the matrix. More porosity was observed in composites with higher TiC content however, a decrease in frictional coefficient with

increasing applied load is observed for composites with higher TiC content. SEM images show crack propagation, grooves, and delamination at worn surfaces. The effective depth of penetration, as well as the size of debris, get reduced by varying the TiC content which eventually leads to a reduction in frictional coefficient [135], [136].

The frictional coefficient & wear rate were examined for TiB₂ reinforced aluminum composite. The experiments were executed on a pin on disc for the determination of the wear rate. Uniform distribution & strong bonding with the matrix was found to be responsible for the improvement of wear properties[94], [137].

The influence of size and volume percent of TiB₂ reinforcement on the wear behavior of 2024 T4 Al alloy based composite have been examined. Composite with fine TiB₂ particles (0.3 μm) exhibits a little less wear for the same volume percentage of TiB₂. less wear has been stated for the composite reinforced with relatively coarse TiB₂ particles (1.3μm) during sliding wear, but composite reinforced with fine particles shows 5 times higher weight loss than composite reinforced with coarse particles during rolling wear. The effect of volume percent of reinforcement on wear is insignificant in the case of fine particles. Improvement in sliding wear is due to the strong interfacial bonding between the matrix and reinforcement [138].

The wear and friction behavior of cast in-situ Al- Al₂O₃ composite has been reported. The composite was developed by addition of MnO₂ particles to the melt, which reduced to Al₂O₃ particles. The investigation shows a decrement in wear rate as well as in volume loss over the base matrix. The effect of porosity on the wear rate has been analyzed. Higher wear rate has been reported with growing porosity content [139].

TiO₂ and MoO₃ particles have been used to develop different composites. The oxide particles were added in the melt of Al-5wt%Mg alloy for reduction to form alumina particles. By increasing the particle content, wear rate decreases for the same testing conditions. Wear debris produced during dry sliding wear

forms a transfer layer which helps in improving the wear resistance at low loads but not for high loads [140].

The wear properties of A356 with 10wt% TiB₂ have been investigated. The composites were prepared using K₂TiF₆ and KBF₄ salts. The resultant TiB₂ produced from the reaction between salts was added in A356 alloy melt. Al-2 wt.% Sc alloy was added in A356 alloy and in A356-10wt.% TiB₂ melt. The morphology of Si particles changes from needle-like shape to fine spheroidal shape due to the presence of Sc. Addition of Sc helps in reducing the Secondary dendrite arm spacing (SDAS) by 50%. Both hardness as well as wear resistance increase due to Sc and TiB₂ addition [141]. Another work for the same composite reveals that the wear rate strongly depends upon the amount of TiB₂ content in the composite instead of the overall hardness of the composite [142].

The wear behavior and mechanical properties of Al-7Si/TiB₂ composite were investigated. The enhancement in wear resistance and mechanical properties was reported by the addition of TiB₂. TiB₂ acted as a modifier of Si Particles and refined the grains of primary α -Al. Worn surfaces confirm adhesion and ploughing as the main wear mechanism at lower loads and for higher loads delamination acts as the main wear mechanism [20].

The powder metallurgy has been used for the fabrication of Al-5%Si-Al₂O₃ in-situ composites. The wear tests were conducted on M-2000 wear tester to evaluate the effect of load, sliding distance and sliding speed on friction coefficient and wear loss. Frictional coefficient and wear increase with an increasing load but both decrease with speed due to the increasing rate of formation of the oxide layer. Coefficient of friction increase initially with sliding distance due to the occurrence of adhesive wear but becomes stable with increasing sliding distance due to dynamic equilibrium formation and demolition of the oxide layer. Main contributing wear mechanisms are found to be abrasive, adhesive and oxidation wear [143].

TiO₂ particles were dispersed in molten aluminum for the development of in-situ Al₂O₃ reinforced aluminum based composite. The wear tests were

performed at different speeds and loads to evaluate the effects of porosity and reinforcement on the wear rate & volume loss. The results indicate a decrease in wear rate and volume loss in cast composites as compared to commercial aluminum. The porosity increases as the reinforcement content increases in the composite. Consequently, the wear rate increases slightly with increasing reinforcement as high porosity leads to more real area of contact [12].

2.10 Comparison of Insitu, Exsitu & other processing techniques

Several processing techniques have been used for the development of Al-Al₂O₃ composite. The review of the available literature shows that strength and properties of composites fabricated by powder metallurgy route increase with Al₂O₃ but it is limited to approx. 4-5 Vol% of the reinforcement. Casting route gives better wettability and high interfacial strength but again the enhancement in properties are limited due to the presence of porosity. The reinforcement size also contributes to the strengthening mechanism. For example, in the case of Nano size alumina particle, excellent enhancement in properties are observed but the properties start decreasing as the volume content increases due to agglomeration problem.

In in-situ composite, the reinforcement is generated within the matrix and is usually multi-phase. In contrast, the ex-situ composites were fabricated by the dispersion of externally added reinforcement. There are numerous reinforcements with different morphologies for in-situ composite. The reinforcement could be ductile or brittle in nature. The potential advantages of in-situ composites over ex-situ composites include:

1. Improved mechanical and fatigue resistance properties with very fine reinforcement.
2. Single crystal reinforcements with small size.
3. The clean interface between reinforcement particles and the base matrix improved wettability.

4. High interfacial strength and thermodynamically stable phases with good weldability and castability.
5. Uniform particle distribution for better properties throughout the bulk.
6. Economical with low-cost potential.
7. Easy to fabricate using conventional methods.

2.11 Formulation of the problem

Extensive research has been carried out on In-situ metal matrix composites. This literature review covered the aspects related to the development, processing techniques and the properties associated with them. This review reveals that:

- (a) For the composite development, Al and its alloys are commonly used as the matrices and particle reinforcement increases the properties.
- (b) Liquid metallurgy route, especially the stir casting is a widely preferred technique for the processing. It is simple, cost-effective and the most commercially viable technique at present.
- (c) Among numerous dispersoids, Al_2O_3 particles are most favored for Al-based alloy due to good chemical compatibility and absence of unwanted reaction among the matrix and reinforcing particles.
- (d) The volume fraction varies from 0.1 to 50 % and the size of reinforcement varies from 0.1-0.5 μm in case of the in-situ composite.
- (e) Several oxides are capable of initiating a substitution reaction with Al to generate fine Al_2O_3 particles in the melt. In situ generated fine Al_2O_3 particles imparts better properties due to uniform distribution and intrinsic and extrinsic effect.
- (f) Pre Heating of the ceramic powder or oxide particles before addition to the molten alloy and the addition of some amount of Mg increases the wettability of alumina particles in the melt.
- (g) Ceramic particles addition significantly increase the wear resistance of the developed composites. Wear behavior depends upon the sliding

distance , applied load, sliding speed, and the type of reinforcement of the numerous ceramics like TiO_2 , MnO_2 , SiO_2 , CuO , B_2O_3 , MoO_3 , and ZnO , etc.

2.12 Research Gaps

- 1) Several oxide materials such as MnO_2 , ZnO , CuO , MnO_2 , and MoO_3 are well-known fillers for high-performance $\text{Al-Al}_2\text{O}_3$ composites. However, other alternate oxide materials such as V_2O_5 have not been explored up to full extent.
- 2) Despite being cost-effective, ease of processing and uniform distribution, liquid processing based in-situ method using V_2O_5 has not been used to fabricate $\text{Al-Al}_2\text{O}_3$ composites.
- 3) Influence of V_2O_5 filler on the mechanical and tribological properties of $\text{Al-Al}_2\text{O}_3$ composite has not been investigated.

2.13 Objectives

1. To fabricate low-cost Al-based in-situ metal matrix composite using pure Aluminum and Al-Si alloy as the matrix material and vanadium oxide (V_2O_5) particles as fillers via liquid metallurgy stir casting route.

2. To Characterize cast in-situ composites using an optical microscope, XRD, SEM, etc.
3. To evaluate the effects of various processing parameters on the mechanical and tribological properties of the metal matrix composites.
4. To evaluate the effect of heat treatment on tribological properties of cast composites.

CHAPTER 3 RESEARCH METHODOLOGY

This chapter covers the detail of the equipment and the experimental procedure used in the investigation. The investigation deals with the synthesis and characterization of cast in-situ composites. In characterization, the main emphasis has been given to the mechanical and wear properties of the composite. For the comparison purpose, the composition of the matrix, unreinforced alloys and their properties have also been studied along with the cast in-situ aluminum based composite.

3.1 Material Selection

3.1.1 Al and Al-Si as Matrices

Selection of the material for the matrix is generally based on the parameters like cost, strength, density, ease of fabrication and processing, etc.

In this study, Al and Al-Si alloy have opted for the fabrication of metal matrix composite. The selection has been made on the basis of their properties like low density, low melting point, availability, castability, good thermal conductivity, light weight, high strength, ease of fabrication and low cost.

In the present investigation, commercially available pure aluminum of 99.65% purity is used for the in-situ metal matrix composite. The material was procured in an ingot form. The Optical Emission spectroscope (SPECTROMAXX, TYPE LMXM6F-F.V, Germany) shown in Figure 3.1, available at UPES, Dehradun, was used to find the elemental composition of the as-received material. The composition of as received ingot observed by Spectro is shown in Table 3-1.



Figure 3.1 Optical Emission Spectrometer

Table 3-1 Composition of as received Aluminum Ingot (wt. %)

Material	Si	Fe	Cu	Mg	Zn	Al
Al-Ingot	0.12	0.15	0	0.01	0.07	Bal.

Al-Si is one of the most favored casting alloy, due to their high fluidity and exceptional mechanical properties. These alloys are available commercially, in the hypoeutectic and hypereutectic form. These alloys have excellent castability that's why they contribute around 80% of aluminum casting. At 12.6% of silicon, Al-Si alloy makes the eutectic composition at 578⁰C eutectic temperature. This is the lowest possible melting temperature. Si is very low-priced and its presence decreases the melting temperature, increases the fluidity, and reduces the possible shrinkage at the time of solidification. In this study, Al-7%Si have been chosen another matrix material for the composite fabrication. Table 3-2 represents the elemental composition of Al-7Si alloy

Table 3-2 Composition of as received Al-7Si alloy (wt.%)

Si	Fe	Cu	Mg	Mn	Zn	Ti	Cr	Al
6.98	0.21	0.16	0.42	0.13	0.02	0.01	0.01	Bal.

The 0.5 wt. % pure Mg has been added at the time of casting to improve the wettability. The addition of Magnesium also decreases the surface tension of the melt.

3.1.2 Vanadium Pentoxide as oxide particles

The selection of metal oxide is a brainy decision. Insitu composite offers an extensive range of reinforcement type, its volume fraction, and the size. For the enhancement of the properties, it is required to understand and control the generation and growth mechanism of reinforcement particles. Alumina particles generated by the in-situ reaction are considered as the most favorable reinforcing material because of their compatibility with Al-matrix. The presence of alumina offers high strength and better wear properties.

In the present study, V_2O_5 has been chosen as the oxide particles. The selection is based on the reduction feasibility of the particles by molten aluminum. Cost-effectiveness and the availability have also been considered as a selection criterion.

Laboratory reagent grade vanadium pentoxide (V_2O_5) has been sourced from SRL Chemicals, Mumbai, with 99.5% purity. The properties of vanadium pentoxide are listed in Table 3-3.

Molecular formula	V_2O_5
Molar mass	181.8800 g/mol
Density	3.357 g/cm ³
Melting point	690 °C
Boiling point	1,750 °C (decomposes)

The average size of V_2O_5 particles was measured by particle size analyzer available in Nano Lab UPES.

3.2 Processing

3.2.1 Development of Al-Si and Al-based Composites

For the development of composite commercially available pure aluminum ingot of about 1100gm was taken. Aluminum was melted in stir casting furnace at 850⁰C. The furnace has the bottom pouring facility and procured from Swam Equipment, Chennai as shown in Figure 3.2. For the stirring of melt stainless steel stirrer has been used. To prevent the dissolution of steel in liquid aluminum, the blade was coated with graphite paste. The preheating of V₂O₅ particles is carried out at a temperature of 250⁰ C before mixing with the liquid aluminum. Preheating is useful to remove the moisture content or any other gases present in the particles. It also avoids a substantial reduction in temperature. The varying amount of V₂O₅ (wt.%) has been used to fabricate the different composites. The knob equipped on the setup controlled the addition rate of the particles. The melt temperature was measured by the thermocouple. The parameters used for the fabrication of the composite are lists in Table 3-4.

**Table 3-4 Parameters used for Aluminum composite
Fabrication**

Parameters	Variables used
Furnace temperature	850 ⁰ C
Melt Temperature	850 ⁰ C
Particle Preheating Temperature	250 ⁰ C
Die Temperature	250 ⁰ C
Stirrer RPM	600
Time of Processing	15 minutes
Amount of V₂O₅ reinforcement	3,5,and 7 wt.%

Magnesium in very small quantity (5gm) was added when the temperature of furnace reached at 850⁰C. The main purpose of adding the magnesium was to enhance the wettability and it also helps in retaining the in-situ generated particles in the melt. The position of the stirrer was kept constant for the proper disperse the V₂O₅ particle into the liquid aluminum. The speed of the stirrer blade used was 600rpm to form the vortex. The molten mixture was poured into the preheated mould after 15 minutes of stirring. At the time of pouring degassing was carried out with the vacuum to prevent the air entrapment. The casting was removed from the mould after natural cooling. The same procedure has been used for the fabrication of all composites.

For the ease, all composites have designated by sample name. The designation has done on the basis of the material composition mentioned in Table 3-5.

Table 3-5 Designation of Aluminum composite

Sample Designation	Material
A	Pure Aluminum
AV3	Al-3% V ₂ O ₅
AV5	Al-5% V ₂ O ₅
AV7	Al-7% V ₂ O ₅

Where A represents the Aluminum,

V stands for V₂O₅

The last digit represents the wt.% of oxide added



Figure 3.2 Bottom Pouring Stir Casting furnace

For the preparation of Al-7Si alloy composite, the DTA has been carried out by using EXSTAR TG/DTA 6300. The powder of Al-7Si and Vanadium pentoxide has been used for the experiment. The heating of the sample is carried out in Al_2O_3 Pan at $10^\circ\text{C min}^{-1}$ in the presence of a nitrogen atmosphere.

Figure 3.3 shows an endothermic peak at 583°C which represents the melting of Al-7Si alloy. Another peak at 673°C has been observed shows the melting of vanadium pentoxide. Declined in peak has been observed between 800-850, this might be the formation of another phase. In the current study, the casting has been done considering the parameters according to DTA analysis.

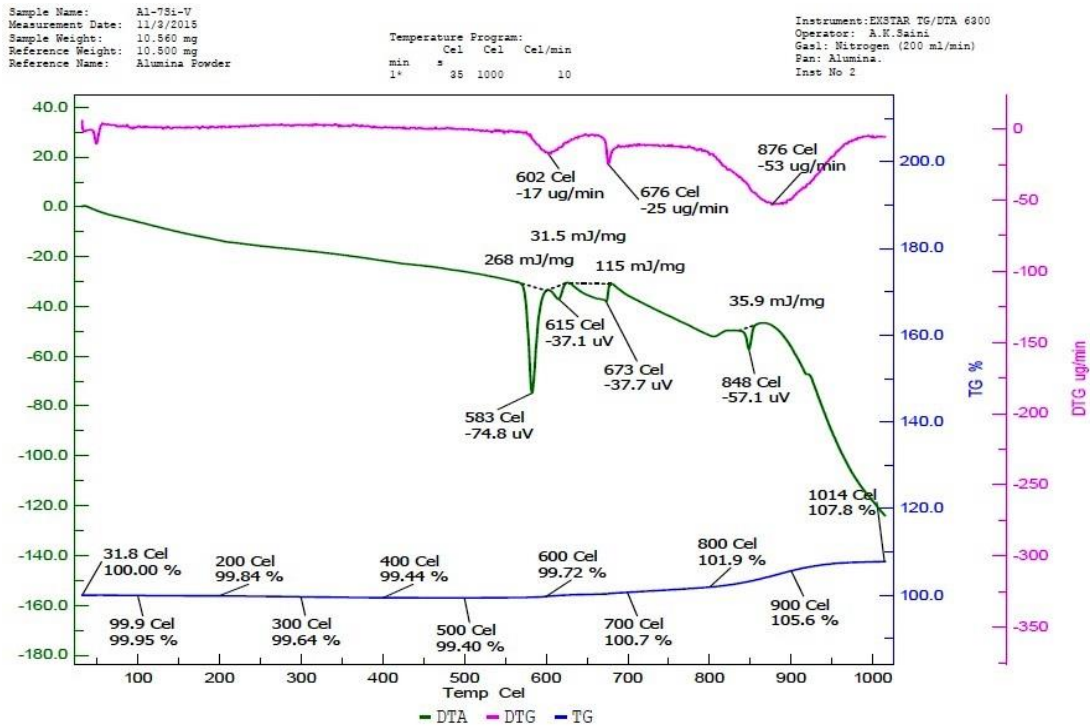


Figure 3.3 DTA Curve for Al-7Si-V₂O₅

In the current study, the casting has been done considering the parameters according to DTA analysis. The length and the diameter of the mould used for the casting were 165mm and 45mm respectively. The same procedure, as used in case of aluminum composite fabrication was used for the fabrication of Al-Si based composites. The composites were made with different wt.% of V₂O₅. The parameters used in the Al-7Si composite fabrication are stated in Table 3-6.

Table 3-6 Process Parameters Used for Al-7Si composites

Parameters	Variables used
Melt Temperature	750 ⁰ C

Particle Preheating Temperature	250 ⁰ C
Die Temperature	250 ⁰ C
Stirrer RPM	700
Time of Processing	15 minutes
Amount of V2O5 added	1,3,5 wt. %

Designation of Al-7Si based Composites is shown in Table 3-7.

Table 3-7 Designation of Al-7Si based Composites

Sample	Material
AS	Aluminum-7% Silicon
ASV1	AS-1% V ₂ O ₅
ASV3	AS-3% V ₂ O ₅
ASV5	AS-5% V ₂ O ₅

AS stands for Al-7Si,

V stands for V2O5

wt.% of oxide particles added is represented by the last digit

3.3 Particles content estimation

The amount of particles present in the composite has been estimated by dissolving the composite in HCL and sodium sulphate. A chemical test has been performed to verify the Al₂O₃ formation. A known mass (3.0 g approx.) of the developed V₂O₅ *in-situ* composite was dissolved in hydrochloric acid (2M) without attacking the unreacted V₂O₅ and Al₂O₃ particles. Sodium sulfate (0.1 M) was used for settling the fine particles. The solution was filtered out with an ashless filter paper(Watman) to obtained insoluble oxide

particles. The filtrate was heated up to 900°C for 1 h and allowed to cool down. The dried filtrate was collected for the mass determination of alumina particles. The mass was measured by an electronic weighing scale (sensitivity 0.1mg). Particle content is estimated by a simple equation:

$$P_{CT} = [(M_c - M_{EP}) / M_c] \times 100\%$$

Where P_{CT} = Particle content

M_c = Mass of the composite

M_{EP} = Mass of extracted particles

3.4 Volume fraction determination

The volume fraction of the composite was determined by using the vertical and horizontal sections of the composite. Firstly, the composites were cut in the vertical and horizontal section as shown in Figure 3.4. H_i and V_i represents the horizontal and vertical sections where $i = 1, 2, 3 \dots n$. The specimens were polished and then examined by the optical Microscope (Material Science lab UPES, Dehradun). For the analysis, the Metallurgy plus Software (Nascent Technology) has been used. The image captured from the Optical microscope was divided into nine discrete elements (pixels). Then the volume fraction of alumina and aluminum alloy composite was calculated.

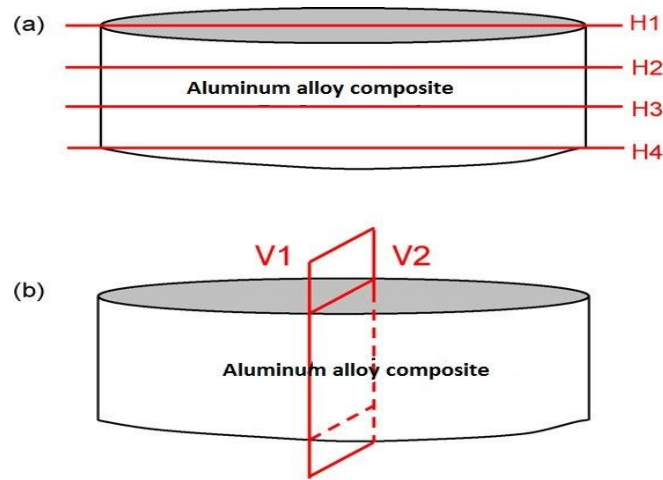


Figure 3.4 Cross section of the composite (a) H1 and H4 are the upper and lower horizontal section. Whereas H2 and H3 are the middle ones (b) V1 and V2 denote the vertical surfaces.

3.5 Porosity measurement

The presence of porosity is very common in the composite made by the stir casting technique. It degrades the property of the composite so it is very essential to measure the porosity present in the composite. Several methods are in use for the porosity measurement like Quantitative metallography and density measurement. The density measurement method is quite simple and generally used. In this method volume fraction of the particles and the porosity has to be calculated. According to ASTM 135-96 standard, the density of the composite and the extracted particles are estimated by the water immersion method.

The volume of the porosity has been estimated by knowing the mass and volume fraction of the composite.

$$M_C = M_M + M_{EP}$$

Where M_C , M_M , and M_{EP} represent the mass of the composite, matrix and the extracted particles respectively.

$$V_C = V_M + V_{EP} + V_P$$

V_P is the volume of the porosity.

$$\text{Now } V_P = V_C - V_M - V_{EP}$$

$$= M_C/\rho_C - M_M/\rho_M - M_{EP}/\rho_{EP}$$

Where ρ_M , ρ_{EP} , and ρ_C , are the density of, matrix, extracted particles and the composite respectively.

3.6 Characterization

3.6.1 Thermal Analysis

For the determination of thermal analysis, the instrument EXSTAR TG/DTA 6300 has been used at Institute Instrumentation Center, IIT Roorkee. The 10.42mg sample weight has been taken for the analysis. The sample was heated in nitrogen (200 ml/min) up to 1000⁰C at the rate of 10⁰C/min. Aluminum powder was taken as reference. The heat flow was recorded in terms of μV . The plot of temperature and heat and the peaks were taken as the basis for selecting the processing temperature.

3.6.2 Microstructure

Microscopic examination has been carried out for the developed in-situ composite and for the unreinforced matrix alloy by using **Inverted Metallurgical Microscope** (Eclipse MA 200, Nikon, Japan) shown in Figure 3.5. The SEM has also been used for the extracted particles and the phase analysis. The **SEM with EDX** facility (IIT Roorkee) has been used for the composition of the phases present shown in Figure 3.6 FE SEM.



Figure 3.5 Inverted Metallurgical Microscope



Figure 3.6 FE SEM

3.6.2.1 Sample preparation`

It is very important that the sample should cut in such a way that it represents the whole specimen. Samples have been taken from more than one orientation

to achieve better results. The sample has been cut with the help of Precision saw (Baincut, Chennai Metco) in order to prevent the mechanical damage and any changes in microstructure shown in Figure 3.7.



Figure 3.7 Precision Saw for sample cutting

After the cutting, it is necessary to mount the sample for proper handling. **Hydraulic Specimen Mounting press** (Bain Mount H MPH007, Chennai Metco, Chennai) has been used for the mounting of specimen Figure 3.8. The mounting was done at 150⁰C by using thermosetting plastic (*e.g.* phenolic resin) with a heating time of 15 Min. and Cooling time 5 Min. Pressure 100bar. The specimen was made of 30mm diameter.



Figure 3.8 Hydraulic Specimen Mounting Press

Various grit size emery paper varying from 220, 320,400,600,800,1000,1200 and 1500 has used for the grinding and polishing. The number indicates SiC grains per square inch i.e. roughness of emery paper. Grinding involves various stages and each stage removes scratches from the previous stage.

The grit size 60 and 80 was used for the initial grinding on Belt Grinder (RADICAL, Ambala) Figure 3.9 and then after the removal of scratches, the specimens were ground and polished on double disc Variable speed grinder-polisher (Bainpol VTD 8”, Chennai Metco) Figure 3.10. After the grinding, the sample has been cleaned in an ultrasonic bath.



Figure 3.9 Belt Grinder



Figure 3.10 Double disc Variable speed grinder-polisher

The polishing carried out on **Automatic Polishing Machine** (Tegramin-25, Struers, Denmark) **Figure 3.11**. A velvet cloth with very fine diamond and alumina paste of grade I and II was used for final polishing. These polished

but un-etched samples have been used for the microscopic examination at various magnification levels.



Figure 3.11 Automatic Polishing Machine

3.6.2.2 Etchants Used

Etchants are used to reveal the microstructure of the metal or composite. Etchant removes the thin layer formed during grinding and polishing. Many etchants can be employed for exposing the grain boundaries of the specimen. Keller's Reagent (1ml HF, 1.5ml HCL in 2.5 ml HNO₃ and 95ml water) is found as the most effective etchant for revealing the grain boundaries of Al and its alloys.

3.6.3 XRD Analysis

It is a nondestructive technique based on Bragg's Law. It is used for estimating the crystal structure of the crystalline material. The cast composite was changed in the powder form for the x-ray diffraction. The extracted particle received from the residue after chemical dissolution has been examined.



Figure 3.12 X-Ray Diffractometer

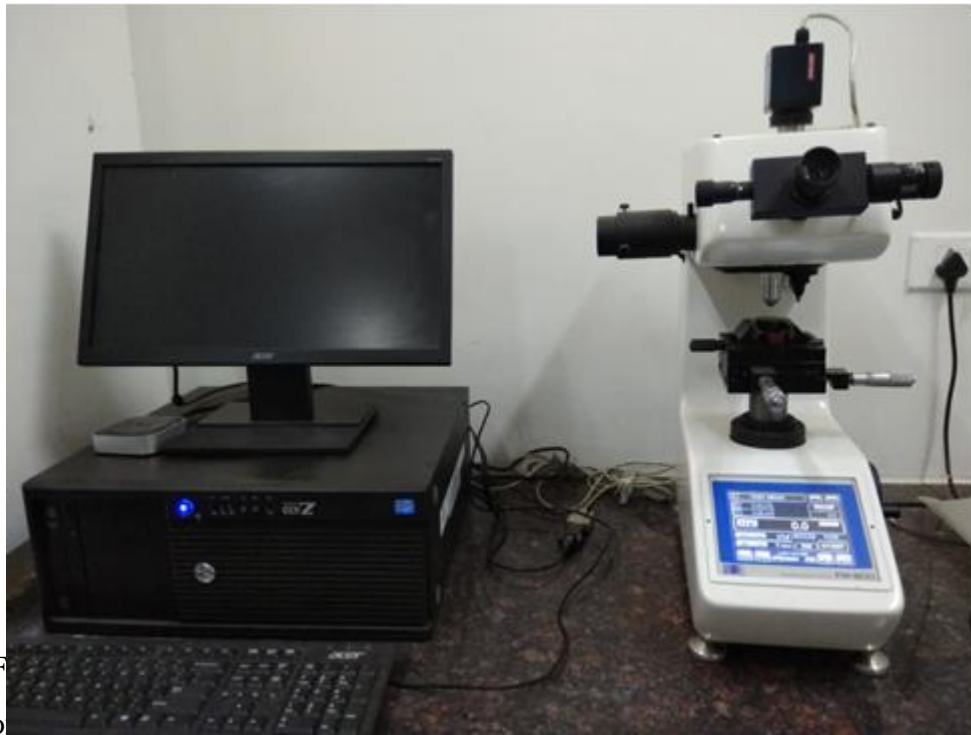
The phases evolved due to the in-situ reaction was identified by XRD (D8 Advanced, Bruker, Germany) Nano Lab, UPES shown in **Figure 3.11**. The investigation was done in a 2θ range between $5-120^\circ$ with a slow scan rate of $1/2^\circ$ per/min using $\text{CuK}\alpha$ radiation. The peaks were matched by X'pert high score software for phase identification.

3.7 Mechanical Behavior

3.7.1 Microhardness

Microhardness of the unreinforced alloy and cast composite specimens were carried out by **Vickers Microhardness tester** (FM-800, Future Tech, Japan) **Figure 3.13**. The effect of reinforcement on the hardness of the matrix and the composite is determined. For better results, the average value of the 10 measurements has been taken. The pyramid shape diamond indenter with

angle 136° at an applied load 100gf, and for a dwell time of 5s was used for the experiment.



was 250Kgf for 10sec.

3.7.2 Tensile testing

For the tensile testing dumbbell shape specimens were prepared. The dimensions of the specimen were considered according to ASTM E8 standard. All the tests were conducted at room temperature. The specimen was gripped properly in jaws to avoid any kind of slippage. Three samples for a given composition has been tested. The average value of the samples with the same composition has been considered. The average values of UTS, yield strength and percentage elongation are reported as the tensile properties of the composite. SEM has been used for finding the surface topology and fracture surface analysis due to the effect of reinforcement.

3.7.3 Wear testing

Wear tests have been carried out according to ASTM G99-95 standard by Pin on Disc (DUCOM, Bangalore, India) Figure 3.14. All tests were conducted under ambient condition. A personal computer was connected with a pin on disc set up for data acquisition. LVDT was employed for the wear determination in micrometers and the mounted sensor sensed the change in terms of frictional forces. For each sample pin weight was measured before and after the test. Weight loss of pin was measured at different applied load and after different sliding distance with highly sensitive weighing balance (Shimadzu AX 200).

Height and the diameter of flat cylindrical pins used for the test were 30 mm & 10 mm respectively. The counterface disc of EN-31 steel (60HRC) of 165mm diameter and 8mm thickness was used with 145 mm as maximum track diameter. The chemical composition of EN31 steel measured with the optical emission spectrometer was found C 1, Si 0.35, Mn 0.5, S 0.05, P 0.05, Cr 1.3, and Fe balanced. To make sure that the surfaces are clean properly ethyl alcohol was used before each experiment. All experiments were conducted at ambient temperature and for each experiment; 40 mm track diameter was used. Sliding distance 1000m and a constant sliding velocity of 0.83 m/s were used for all experiments with applied loads 10 N, 20 N, and 30 N.



Figure 3.14 Pin On Disc Tester

The pin samples were properly cleaned and then polished with different grit size paper 400,600.800 and 1000. The disc was cleaned with A350 Emery paper after each test. The pins were first cleaned with ethyl alcohol and ultrasonicator and then stored in a vacuum oven to prevent it from corrosion. The worn surfaces after the test were examined with trinocular stereo zoom microscope. To obtain the accurate results an average of three readings have been reported.

The difference in the weights of the pin before and after the test was measured for the calculation of bulk wear. Weight loss due to sliding wear has been measured by a weighing scale of accuracy 0.1mg. The volume loss has also been calculated with respect to the reinforcement fraction.

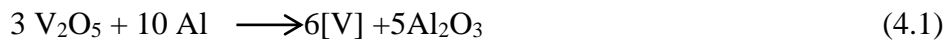
CHAPTER 4 RESULT & DISCUSSION PURE Al & V2O5

The composites with different amount V_2O_5 particles addition in the pure aluminum melt have been developed. It was expected that the reaction will take place between pure aluminum and V_2O_5 particles. Due to high-temperature processing, V_2O_5 particles were reduced and composites reinforced with in-situ generated alumina particles in Al-V alloy matrix have been formed. This chapter covers the results obtained from XRD followed by the microstructural characterization using an optical and scanning electron microscope. Mechanical and tribological properties such as hardness, strength, and wear behavior are determined to study their variations with process parameters. The results are thoroughly discussed to explain the observed variations at the end of this chapter.

4.1 Al-V2O5 Characterization

4.1.1 Thermodynamics characteristics of the in-situ reaction

From the thermodynamic aspect, pure vanadium is formed by the reduction of V_2O_5 according to the reaction as follows.



$$\Delta G_{298}^0 = -3735 \text{ KJ/mol} , \Delta H_{298}^0 = -3727 \text{ KJ/mol}$$

The equation 4.2 shows the formation of Al_3V due to the reaction between the formed vanadium and excess aluminum



$$\Delta G_{298}^0 = -24.5 \text{ KJ/mol} , \Delta H_{298}^0 = -20 \text{ KJ/mol}$$

The negative value ΔG_{298}^0 indicates the thermodynamical feasibility of both reactions. Based on high negative values, it seems that in situ reaction

occurred between Al and V_2O_5 after addition of V_2O_5 particles to pure aluminum melt. Thereby reducing V_2O_5 to form Al_2O_3 as well as Al_3V .

4.1.2 XRD Analysis

The XRD patterns of pure aluminum and different in-situ composites are shown in Figure 4.1. The X-ray diffraction pattern of pure aluminum reveals the presence of Al whereas XRD pattern of composites reveals the presence of Al_2O_3 & Al_3V phases. The height of the peaks corresponding to these phases varies with the amount of V_2O_5 particle addition. There is considerable variation in peak size of pure Al with V_2O_5 addition where maximum peak size is for pure Al matrix and minimum for AV7 composite. The variation in peak size of Al_2O_3 & Al_3V is very less across all the composites but more prominent in case of AV5 composite. The formation of Al_2O_3 due to in-situ reaction has been confirmed by a simple test. About (3.0g) of AV5 in-situ composite sample has been dissolved in hydrochloric acid (2M) without attacking the unreacted V_2O_5 and Al_2O_3 particles[144]. Sodium sulfate (0.1 M) was used for settling the fine particles. The solution was then filtered out with an ashless filter paper (Watman) to obtain insoluble oxide particles. The filtrate was heated up to 900°C for 1 h and allowed to cool down. The dried filtrate was collected for the mass determination of alumina particles. The maximum recovery of the extracted particles was 78.21 %. XRD pattern of the extracted particle from AV5 sample is shown in Figure 4.2 This figure clearly revealed the presence of Al_2O_3 particles formed due to the in-situ reaction between pure Al & V_2O_5 particles. In addition, other phases like Al_3V and $MgAl_2O_4$ and unreacted V_2O_5 are also present as shown in the XRD pattern.

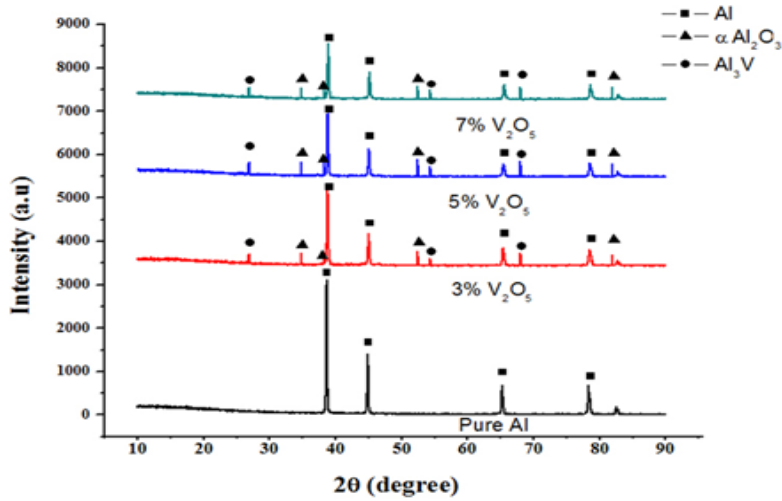


Figure 4.1 XRD Pattern of Al-V Composite

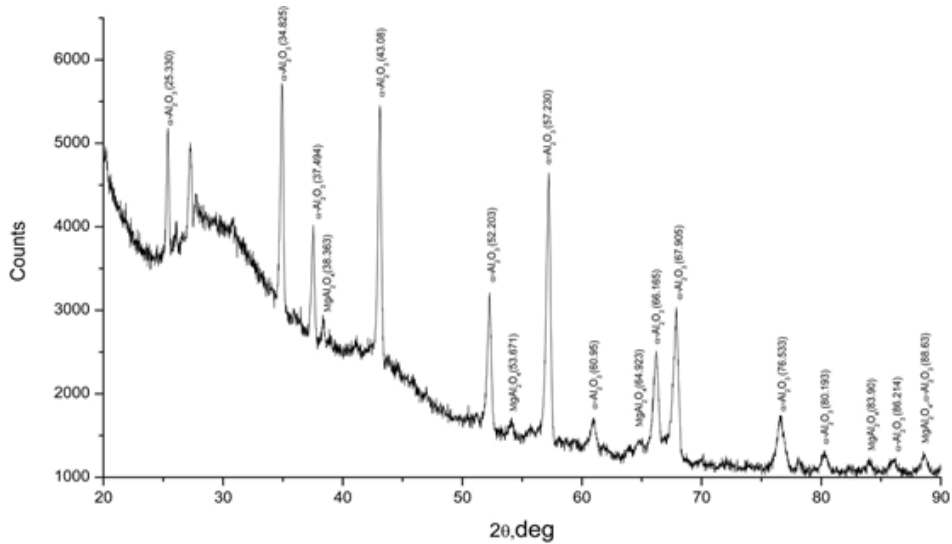


Figure 4.2 XRD pattern of the filtered residue obtained from composite AV5

4.1.3 Microstructural evaluation

Same processing route has been employed to cast Pure Al and different composites. Micrographs of cast Al and the composites are shown in Figure 4.3.

Figure (a) Shows the microstructure of pure aluminum with 5wt. % Mg addition. The dark spots in this microstructure show the presence of porosity and aluminum oxides.

Figure (b) represents the microstructure of the composites produced with 3% addition of Vanadium oxide particles. The microstructure is quite similar to the previous one but the minor changes have observed in terms of grain refinement.

Figure (c) Shows the microstructure of AV5 composite. This Microstructure reveals the presence of oxide particles with substantial grain refinement. The measured grain size of pure Al was found to be $1\mu\text{m}$ whereas for AV5 composite it was found to be slightly less than $1\mu\text{m}$. The observed grain refinement is due to the existence of released vanadium and indicates the uniform distribution of V_2O_5 particles in Al and leading the formation of alumina due to in-situ reaction thus releasing vanadium in the melt causing this refinement.

Figures (d) & (e) show the microstructure of AV7 at two different magnifications. More amount of V_2O_5 addition leads to the formation of more number of Al_2O_3 particles which are agglomerated at the grain boundaries of aluminum crystals which in turn are observed as an elongated cluster in the interdendritic region. Microstructure at higher magnification shows the presence of the intermetallic compound and the same has revealed by XRD.

The release of vanadium is due to the reduction reaction between V_2O_5 particles and molten aluminum. The excess released vanadium reacts with molten aluminum to form Al_3V intermetallic. More addition of V_2O_5 leads to non-uniform distribution as observed in the microstructure.

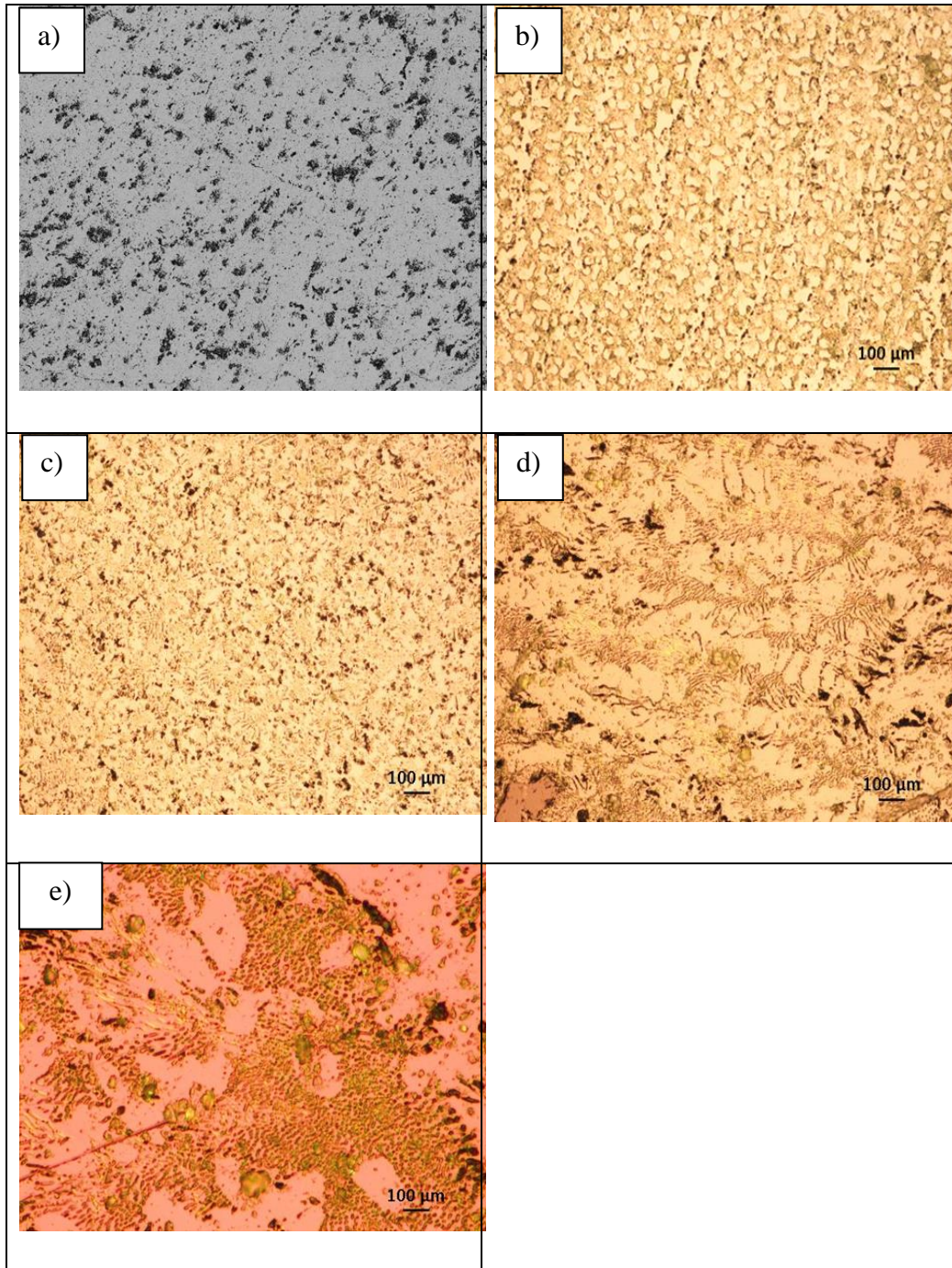


Figure 4.3 Micrographs of (a) pure aluminum (b) AV3 (c) AV5 (d & e) AV7 at low & high magnification respectively

Similar phases have been detected in all the microstructures with the different volume fraction of phases due to the different amount of vanadium oxide addition in the melt. The chemistry of these phases which are formed during the in-situ reaction is very complex leads to the creation of primarily Al_2O_3 ,

MgO, Al₃V, and traces of other phases. The formation of intermetallic Al₃V in in-situ composite confirms other reduction of V₂O₅ by molten aluminum. The distribution of oxide particles in the matrix phase clearly observed in the micrographs.

Figure 4.4 is the backscattered image of AV5 composite shows the dispersion of the particles with in the matrix.

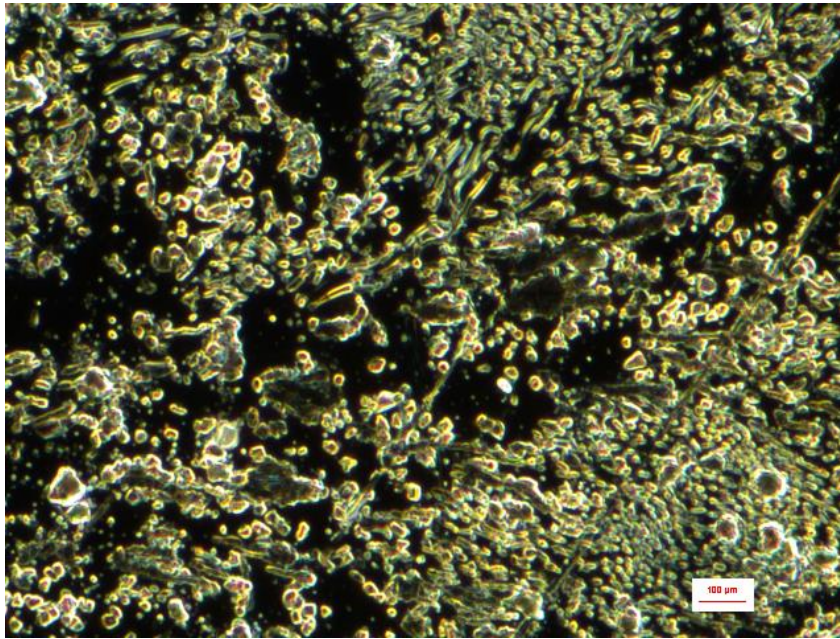
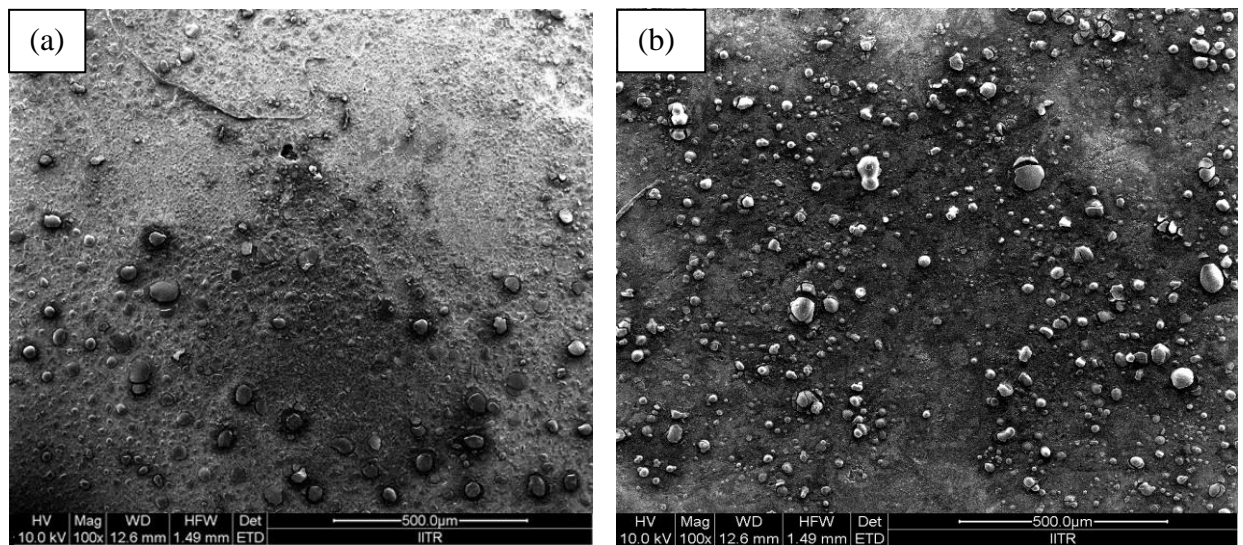


Figure 4.4 Back Scattered Image of AV5 composite

4.1.4 Scanning Electron Microscopy



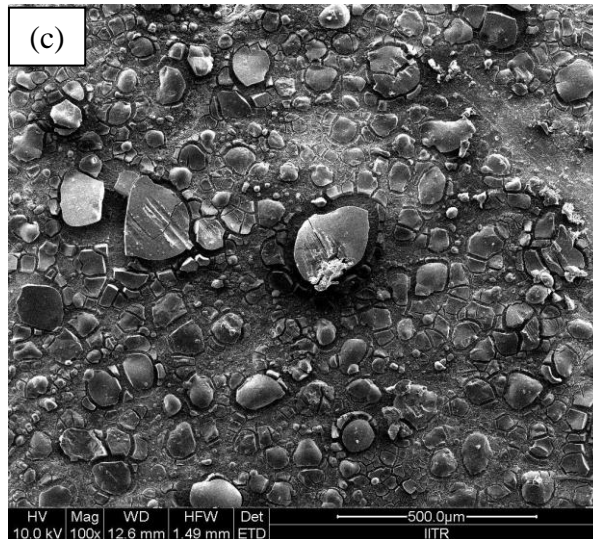
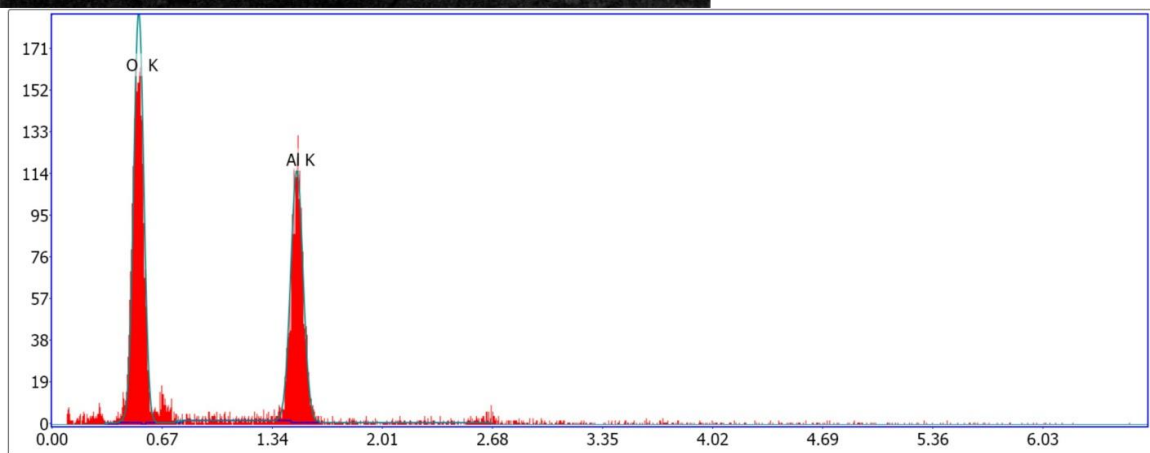
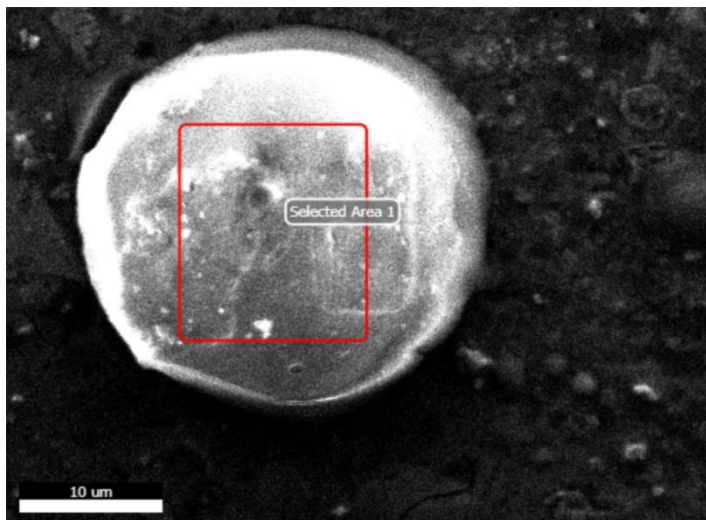


Figure 4.5 SEM images of (a) AV3 (b) AV5 (c) AV7

Scanning electron microscopy of the cast composite was carried out to confirm the formation of Al_2O_3 particles, to see the distribution of Alumina particle as well as to determine the volume fraction of alumina particles in the matrix. Scanning electron microscopy of cast in-situ composite was also carried out to confirm the presence of Al_3V and other phases in the composite. Figure 4.5 (a) to (c) show the SEM image of different as cast in-situ composites. It is clear from the images that distribution of phases is uniform but volume fraction increases with increase in V_2O_5 particle addition to the melt. The EDAX analysis of the particles present in the matrix is shown in Figure 4.6, which confirm the formation of near stoichiometric Al_2O_3 particles during the in-situ reaction between V_2O_5 & Al melt. Distribution is more uniform when 5% V_2O_5 is added, as compared to the higher composition. In the case of 7% addition, the chemical composition of Al_2O_3 is found nonstoichiometric due to unavailability of enough oxygen during the reaction.



Lsec: 30.0 0 Cnts 0.000 keV Det: Octane Pro Det Reso

Element	Weight %	Atomic %	Net Int.
O K	60.88	62.41	94.58
Al K	39.12	37.59	70.21

Figure 4.6 EDAX Analysis of particle present in Al-V composite

The volume fraction of Al_2O_3 particles in different composites determined with the help of image J software using the intercept method. The variation of the volume fraction of Al_2O_3 particles in the matrix is in well agreement with the SEM images of the composites as more particles are observed in the matrix with an increase in V_2O_5 particle addition.

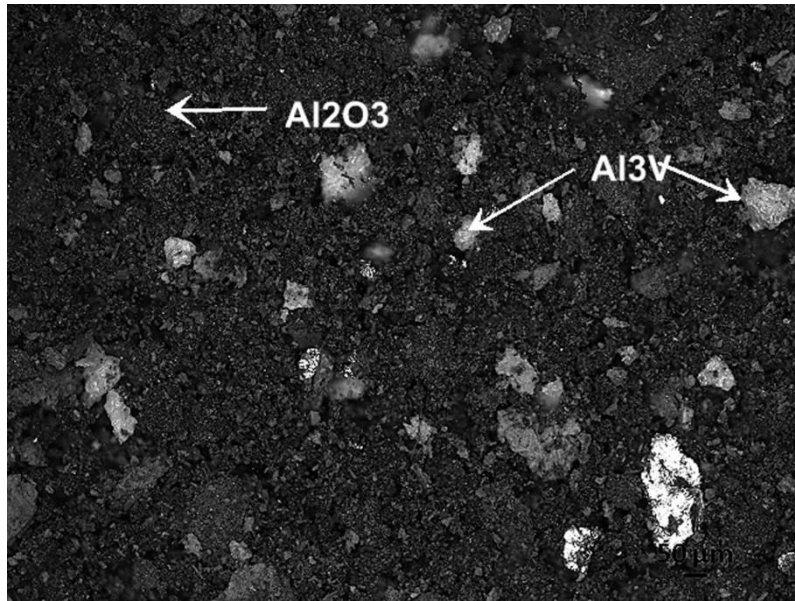


Figure 4.7 SEM Image of Extracted Al₂O₃ Particles

In addition, scanning electron microscopy of extracted particles from cast in-situ composite was carried out to confirm the presence of Al₂O₃, Al₃V and other phases in the composite. The SEM image of extracted particles is presented in Figure 4.7.

4.2 Mechanical Properties

4.2.1 Microhardness and tensile strength

Table 4-1 shows the Mechanical properties of cast pure aluminum and in situ Al-Al₂O₃ composites. The variation in Microhardness of in-situ composites over pure aluminum is shown in Figure 4.8, it is marked from this figure that Microhardness increases with V₂O₅ particle addition to a certain extent and decreases afterward. The maximum Microhardness is observed with 5% V₂O₅ addition. Figure 4.9 indicates the variation of the tensile strength of the in-situ composite as compared to pure aluminum. This figure reveals that tensile strength increases up to a certain extent of V₂O₅ addition and decreases afterward. The trend is similar to that of Microhardness. The maximum tensile strength is observed with 5% V₂O₅ addition.

Table 4-1 Mechanical Properties of Al-Al₂O₃ Composite with Various Percentage of V₂O₅

Sample	Material	Microhardness (HV)	UTS (MPa)	Elongation (%)	Porosity Content (Vol. %)
A	Pure Al	25.4(1.01)	39.1(6.7)	3.25(0.4)	2.730
AV3	Al-3% V ₂ O ₅	58.2(1.45)	57.3(4.8)	5.73(0.7)	2.420
AV5	Al-5% V ₂ O ₅	62.3(1.82)	64.8(2.6)	7.12(1.3)	2.100
AV7	Al-7% V ₂ O ₅	58.7(2.03)	60.7(3.5)	6.44(0.8)	3.040

#A stands for Aluminum, V stands for V₂O₅ and the last digit represents the wt. % of oxide added.

Standard deviations are shown in parentheses.

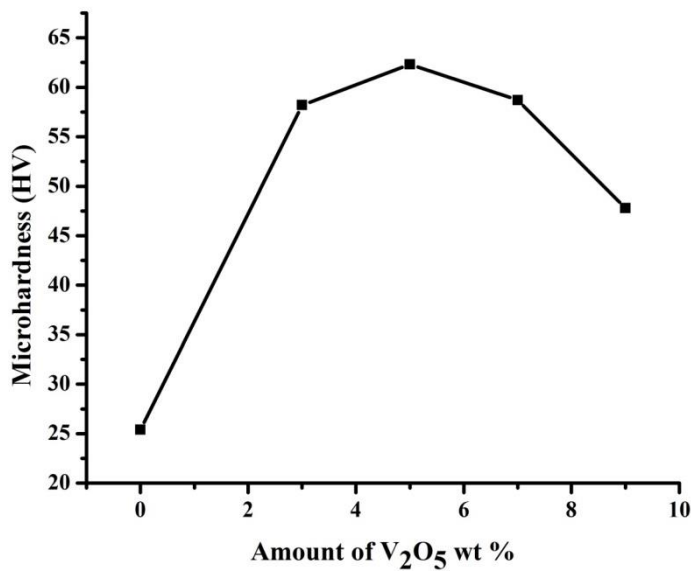


Figure 4.8 Variation of Microhardness with the amount of V₂O₅

The maximum tensile strength was observed in case of AV5 than all other composites and pure aluminum. Figure 4.9 shows that tensile strength

increases linearly with respect to particle addition up to 5% and it starts decreasing by further addition of V_2O_5 particles in the molten aluminum. The measured tensile strength values are taken by the averaging of three sample readings.

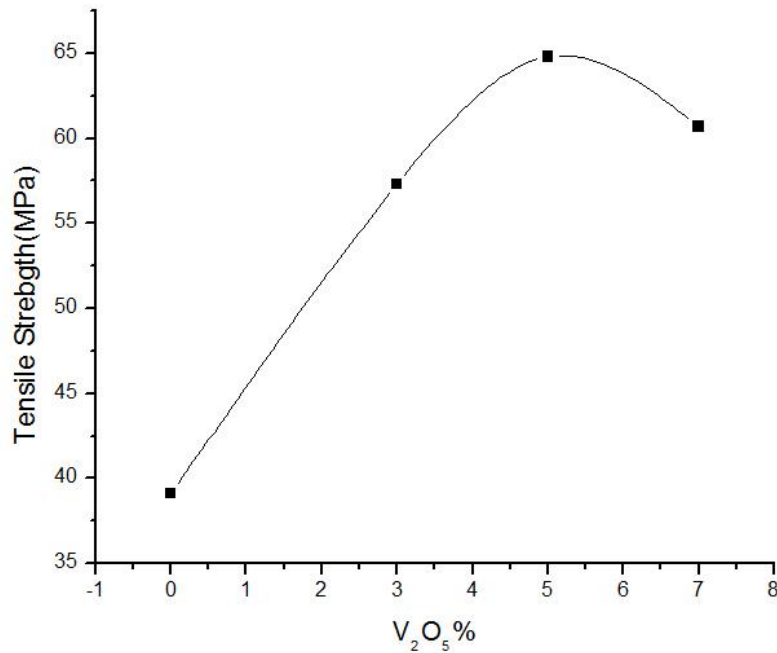


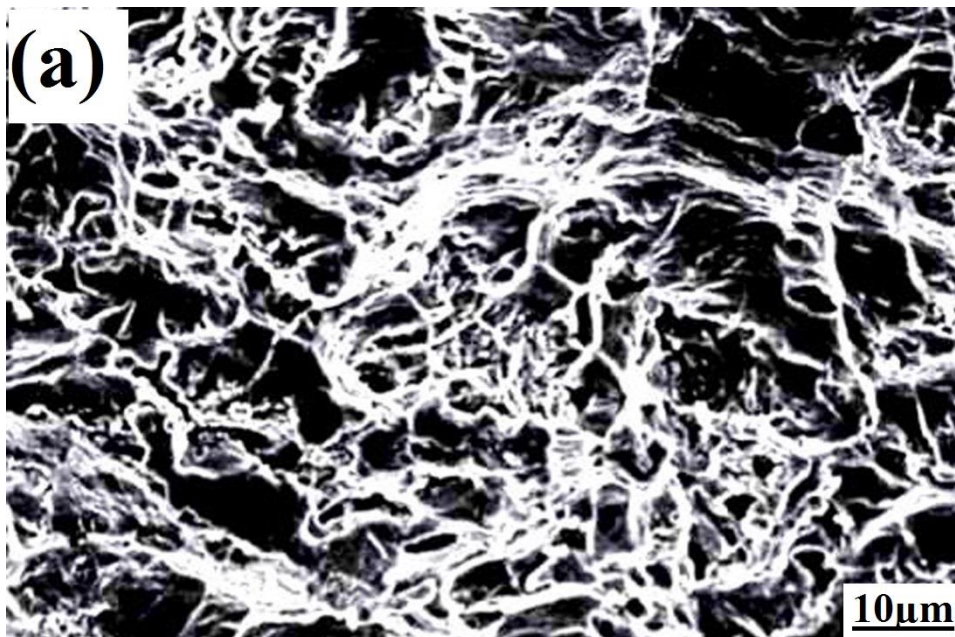
Figure 4.9 Tensile Strength Variation with the addition of V_2O_5

Ductility, as measured in percent elongation for pure aluminum and in-situ composite, trails the similar trend as detected in the case of tensile strength and Microhardness. The elongation increases by the addition of Al_2O_3 particles up to 5% addition of V_2O_5 particles and decreases afterward. In the case of porosity, we have found the highest porosity content in AV7 composite. In general, the porosity increases with the particle content, the values of porosity are mentioned in Table 4-1.

Figure 4.10 (a) and (b) show the tensile fractured surfaces of cast in-situ composites which were respectively with 5 & 7 % V_2O_5 addition. The fractured surfaces of both the composites exhibit a mix of dimple type ductile fracture and cleavage type shear fracture. These figures also show the presence of

porosity in cast composites. The presence of dimples and cleavage may be indicative to have moderate ductility in the composites whereas the presence of porosity is an indication of a decrease in microhardness.

The volume fraction of porosity present in the cast-in-situ composite is given in Table 4-1 as evident from the table that the porosity content increases and high volume fraction of porosity content is a probable reason for the decrease in Microhardness. However, despite having higher porosity content the composite with 7% V_2O_5 addition exhibit higher hardness than pure Al due to more volume fraction of hard Al_2O_3 particles in the matrix.



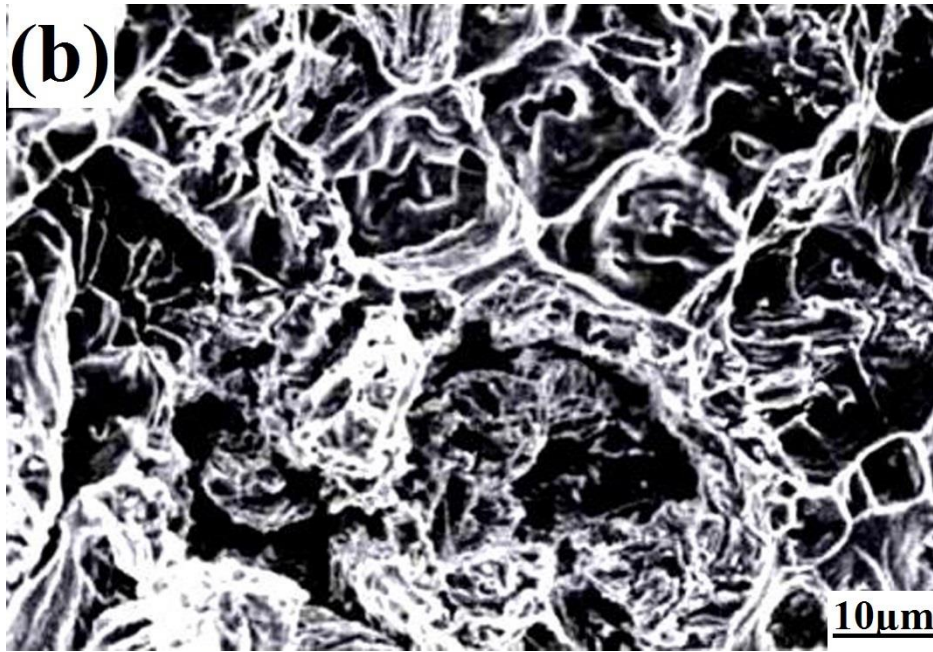


Figure 4.10 SEM images of tensile fractured surfaces of (a) AV5 (b) AV7

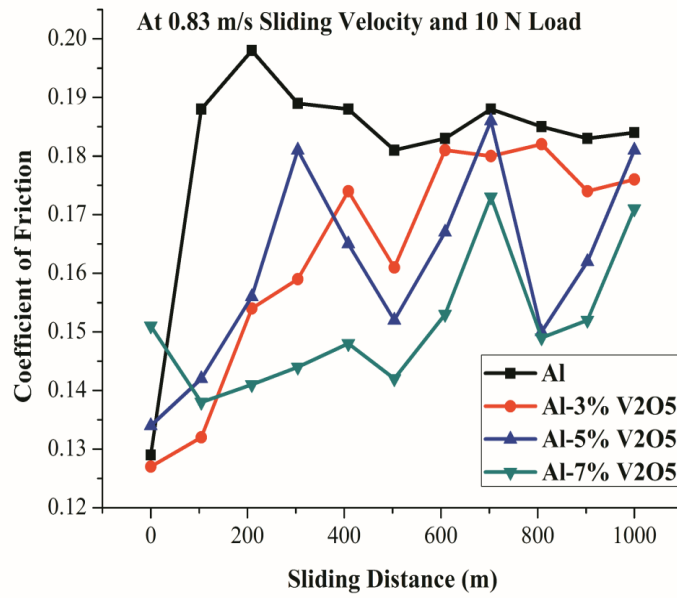
4.3 Tribological Behavior

The tribological properties of in-situ composites is investigated in terms of coefficient of friction and wear under dry sliding condition against the hardened steel. The main focus of the study was to find out the role of in-situ generated reinforcement particles in the tribological behavior of the composite. For the comparison purpose, the tribological behavior of commercial aluminum without any reinforcement was investigated under the same conditions.

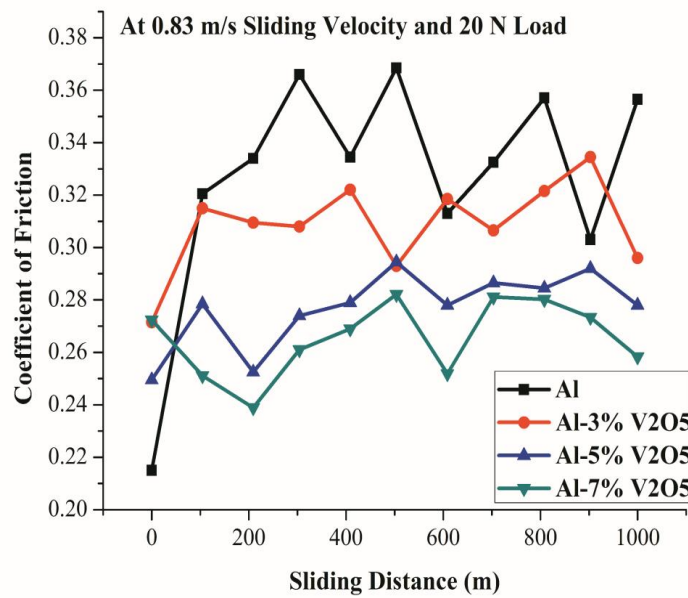
4.3.1 Coefficient of friction

Figure 4.11 shows the variation in the coefficient of friction with sliding distance at different loads i.e. 10 N, 20 N & 30 N and at a constant sliding velocity of 0.83m/s. Generally, the coefficient of friction increases with increasing load. The figure reveals that pure aluminum exhibits a maximum coefficient of friction. After addition of V_2O_5 particles, a significant decrease in the coefficient of friction is observed. However, the coefficient of friction

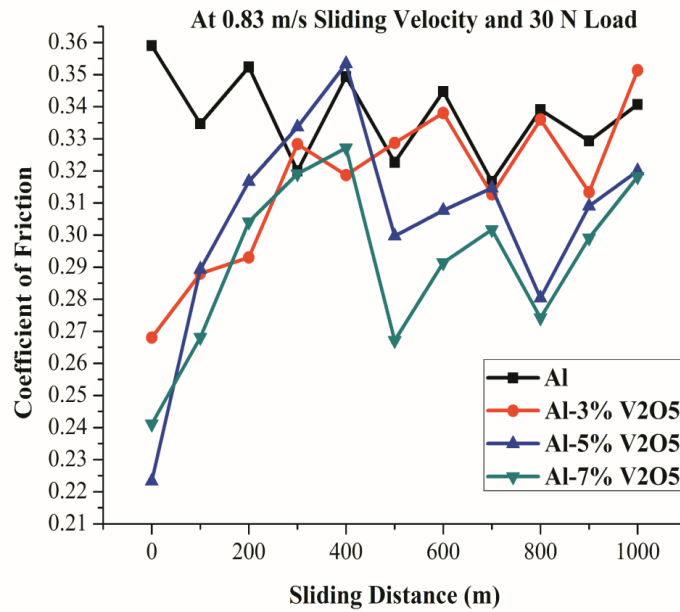
varies in a zigzag manner with sliding velocity for cast pure aluminum and in-situ composite at all testing loads.



(a)



(b)



(c)

Figure 4.11 Coefficient of friction as a function of sliding distance at (a) 10 N (b) 20 N & (c) 30 N Load

Figure 4.12 displays the comparative plot of the frictional coefficient with the load. As stated before, the coefficient of friction increases linearly with load but variation is very small at higher loads. Pure aluminum shows the maximum coefficient of friction whereas in situ composites with 7% V₂O₅ particles show the minimum coefficient of friction. A decrease of about 10% is observed with 3 wt.% and 5 wt.% V₂O₅ particle addition and about 17.5 % is observed with 7% V₂O₅ particle addition overcast pure aluminum at lower load of 10 N. At higher loads of 20 & 30N a significant decrease of about 5.5 %, 19.4 %, & 16.6 % is observed with the addition of 3 wt. %, 5 wt. % and 7 wt. % respectively.

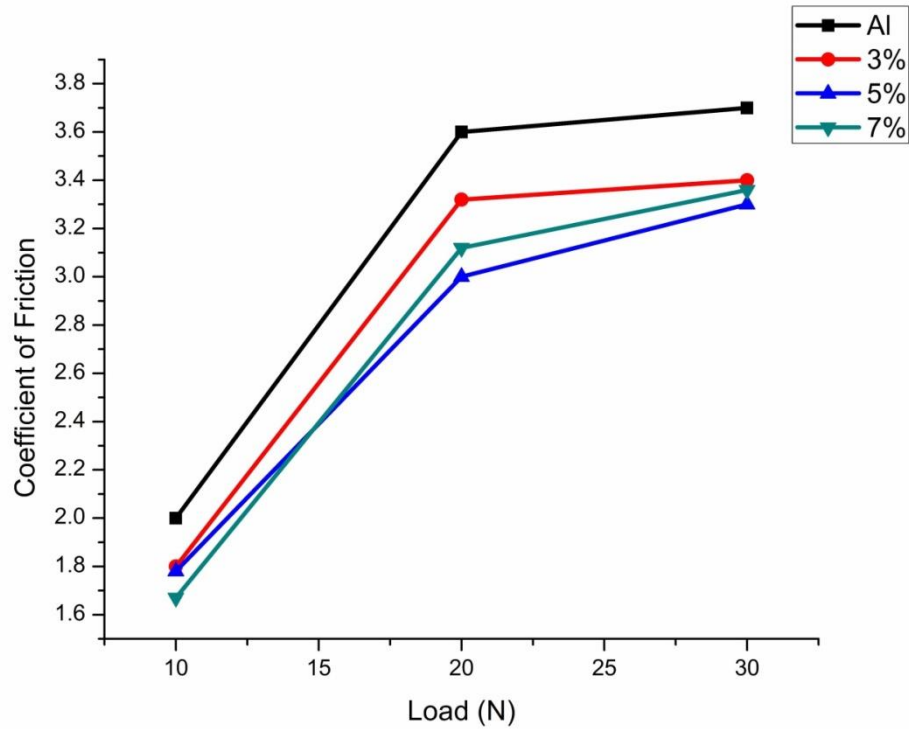


Figure 4.12 Cumulative Coefficient of friction as a function of load

4.3.2 Volume loss

Figure 4.13, shows the variation in volume loss of a pin with the load. The reading is taken at a constant speed of 0.83m/s for 1000 m sliding distance (steady state regime). The volume loss was determined by the ratio of weight loss to the density of the pin. The decrease in volume loss is observed in the cast in situ composite as compared to pure aluminum. It is evident from the figure that volume loss of both as cast aluminum and the in-situ composites increases with increasing normal load which is in good agreement with Archard's law i.e. volume loss is proportional to load applied.

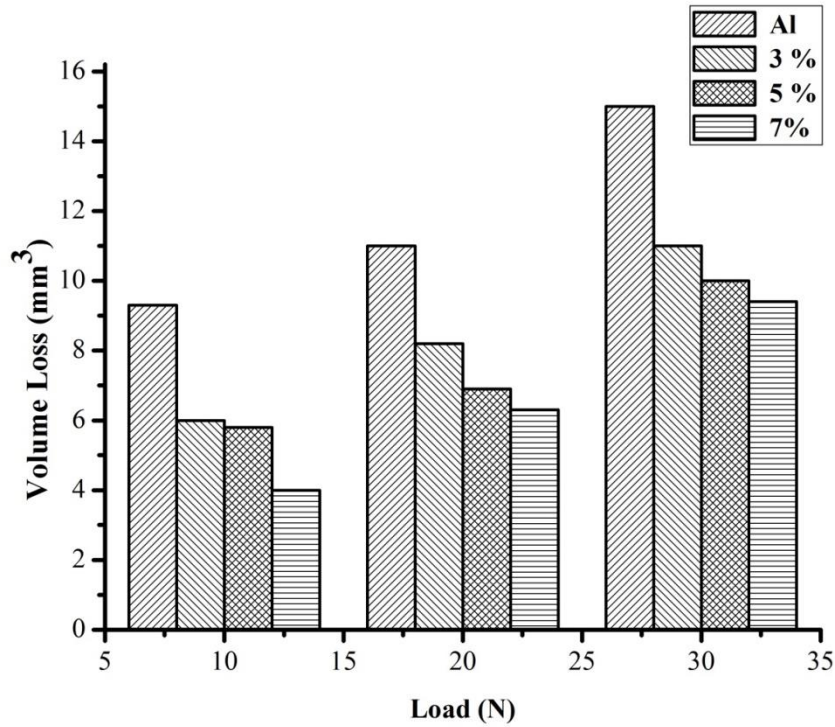


Figure 4.13 Volume loss vs Load of cast in-situ composites

At a higher load of 30N, a reduction in volume loss of about 20 %, 33.3 %, and 46 % is observed with the addition of 3%, 5% and 7% V_2O_5 particle addition respectively. Porosity, content in cast-in-situ composites is slightly higher than as cast pure aluminum. This reduction in volume loss in cast in-situ composites over pure aluminum can be attributed to the reinforcing effect of hard Al_2O_3 particles in an aluminum matrix.

4.3.3 Wear rate

The bulk wear is calculated by taking the difference of pin weight before and after the experiment. Specific wear rate that is also known as wear factor or wear coefficient and generally measured in (mm^3/Nm).

$$W_{sp} = V/ND \text{ mm}^3/N\text{-m}$$

V, represent the total wear volume,

N and D stands for normal load, and total sliding distance, respectively.

Figure 4.14 shows the specific wear rate of pure aluminum and cast in-situ composites as a function of the applied load.

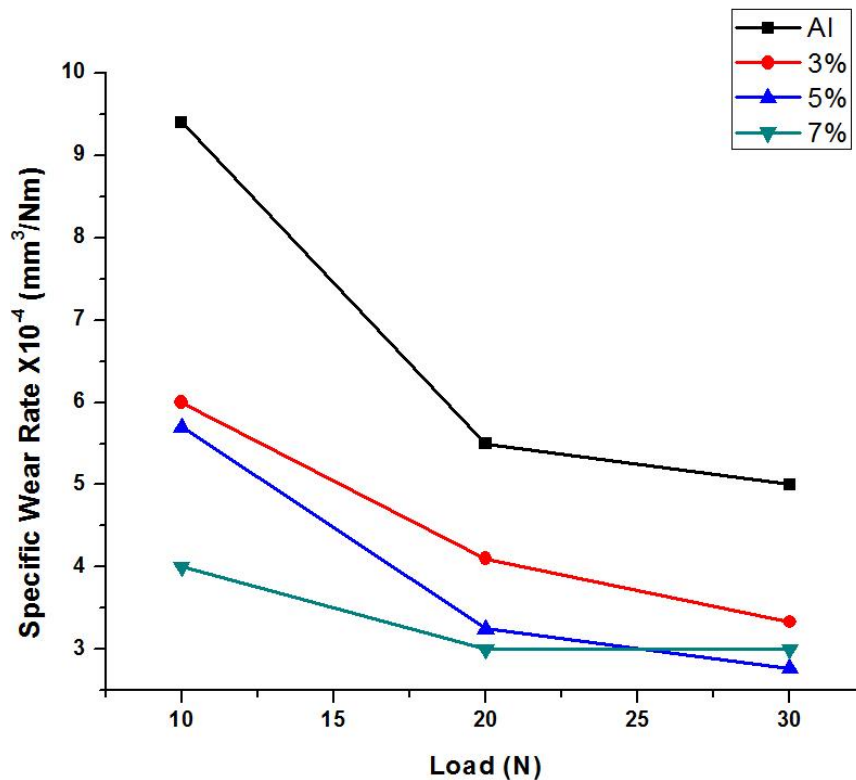


Figure 4.14 Specific wear Rate as a function of the applied load

The specific wear rate of cast in-situ composite was found lower as compared to cast pure aluminum. At 10N load, specific wear rate was $9.4 \times 10^{-4} \text{ mm}^3/\text{Nm}$ for cast pure aluminum and in case of 3%, 5%, and 7% it was $6.1 \times 10^{-4} \text{ mm}^3/\text{Nm}$, $5.7 \times 10^{-4} \text{ mm}^3/\text{Nm}$, and $4 \times 10^{-4} \text{ mm}^3/\text{Nm}$ respectively. There is a clear difference in the specific wear rate has been observed at this load. However, at 30N load small difference in wear rate has been observed. This decrease in wear rate by increasing the load indicates the improvement in wear resistance due to the addition of V_2O_5 particles. The enrichment in wear resistance is attributed to an increase in the strain hardening [145].

The dry sliding wear behaviour of the in-situ composites are strongly based on, uniform distribution, size and the morphology of hard phases [146]. The uniform dispersion of the phase improves the interfacial bonding between the phases and the alloy matrix, which in turn helps in retaining the intermetallic

within the matrix, especially when the material undergoes for the sever wear test [147], [148].

At 30 N loads, a slight increase in wear rate has been observed in case of the in-situ composite with 7% addition of V_2O_5 particles. In this case, porosity plays an important role and with more addition of V_2O_5 particles porosity increases as mentioned in Table 4-1. High porosity causes the delamination of the surface and therefore specific wear rate increases slightly at higher load as shown in Figure 4.14 [149], [150].

The improvement in wear behavior is observed by the addition of V_2O_5 particles, which increases the volume fraction of hard Al_2O_3 and Al_3V , in the composite. These hard phases act as a load-bearing element and decrease the specific wear rate [151], [152].

4.3.4 Worn surface morphology

The worn surfaces were examined in order to investigate the wear mechanism.

Figure 4.15 Show the worn surface of cast in-situ composites with 5% and 7% V_2O_5 particle addition at 20N and 30N load. From the micrographs, it is clear that the more damage occurs at higher load in case of 7% cast in-situ composite. The best result of the wear rate has been found in the case of 5% addition as compared to the 7% addition. At low load, small grooves were observed on the worn surface in the sliding direction due to the abrasion mechanism. But in case of higher load delamination occurs as the real area of contact increases and eventually the fracture stresses of reinforced particles increases. The presence of alumina & intermetallic compound in the cast in situ composite provides hardness but if the porosity increases interaction between the matrix and reinforcement decreases.

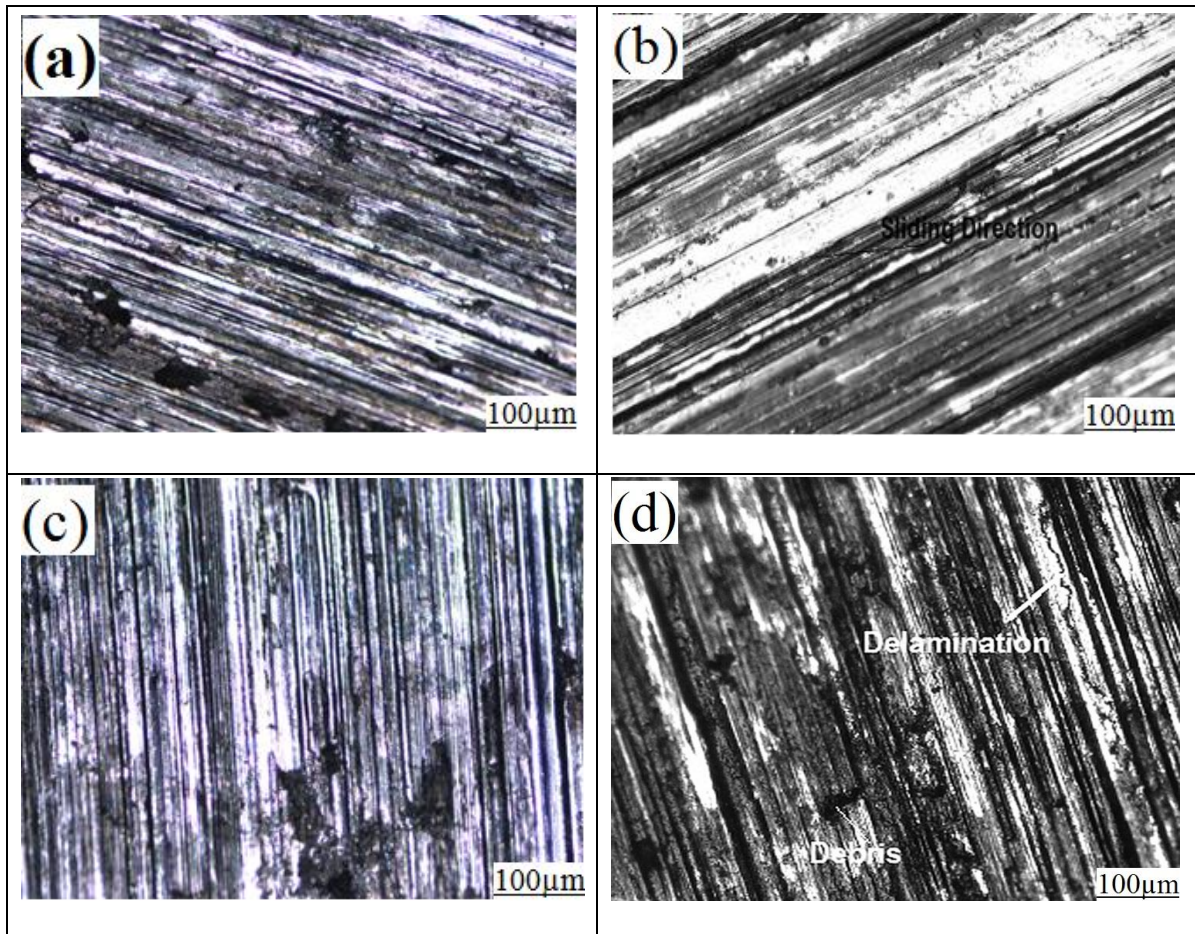


Figure 4.15 Micrographs of worn surface (a) & (b) AV% at 20N & 30 N load (c) & (d) AV& at 20N & 30N load respectively.

4.4 Discussion

For the comparison purpose, the XRD of commercially available aluminum has been used along with the in-situ composite samples. The phases identified by the x-ray diffraction technique are presented in Figure 4.1. The small peaks corresponding to the lower value of theta (θ) representing the fewer impurities present. A very small difference in the peaks has been observed between the composite and the pure aluminum, which is due to the mask of stronger peaks of aluminum on the weaker peaks of the minor phases present in the composite. Al_3V and Al_2O_3 were identified. Better peaks have been identified in case of AV5 as compared to the AV3 & AV7, this may be due to the nearly

complete reaction occurs in case of AV5. Reduction of Aluminum can be easily identified with a decrement of peaks with the increment of particle addition. Two phases have appeared apart from aluminum in XRD i.e. Al_3V and Al_2O_3 . According to Al-V phase equilibrium diagram Al_{21}V_2 , Al_{45}V_7 and Al_{23}V_7 are metastable over temperature 736°C & not observed in XRD [52].

The major increment in hardness is observed in case of AV3 & AV5. The increment in hardness is due to solid solution hardening, where V reduced from V_2O_5 and dissolved in molten metal. The solid solution hardening effect is attained by adding the alloying elements into the matrix, which results in the interaction between mobile dislocations and the solute atoms. The presence of solute atoms increases the initial yield stress and reduces the dynamic recovery rate of dislocations. According to Hall-petch, grain boundaries act as a barrier for dislocation slip thus the grain size refinement creates a high volumetric density of grain boundaries which impede the dislocation movement and propagation to adjacent grains, thereby consequently strengthening the material [153], [154]. Also, the uniform distribution of V_2O_5 particles act as an obstacle for the dislocation movement and forms the dislocation loops. According to Orowan mechanism, movement of dislocation is quite difficult in case of the loop rather than line [155], [156]. Dispersion of Al_2O_3 and intermetallic compound in the matrix also contributed to hardness increment.

The reason for hardness decrement is dendritic growth and release of latent heat. Agglomerations of large no. of particles in the crystal and at grain boundaries were also responsible for hardness decrement. AV7 has a low density as compared to the pure Al and indicates the presence of porosity, which is also a reason for low hardness.

Strengthening is possible due to the presence of Al_2O_3 and V particles in the matrix. It is well known that with increasing the particle content porosity also increases. The particles contribute to high strength with the condition that particles should have high modulus value. The high shear modulus does not allow the dislocations to cross it until the high stress is applied [157][158]. Generally strength at the interface also an important factor to consider. High

interface strength allows the particle to bear the load without breaking the bonds [159]. Sometimes lower tensile strength has reported even by adding the hard particles, which is attributed to lower strength at the interface. In the present investigation, both tensile strength and yield strength increase in spite of increasing the porosity. The value increases up to the 5% addition of oxide particles in the matrix. This may be fairly concluded that the particles were well bonded in the matrix. The decrease in the property by further addition is the interesting part and that could be due to the higher porosity content and the presence of the intermetallic compound.

Ductility plays an important role & affects the mechanical properties. Ductility increases till the 5% reinforcement, therefore tensile strength also increases. Higher reinforcement (more than 5 %) increases the porosity causing decrease in tensile strength of composites having 7% of reinforcement content. The decrease in UTS of the MMCs with increasing Al_2O_3 particle content may also be attributed to the rupture of the interface between Al_2O_3 and matrix during tensile loading. High UTS values exhibited by in-situ Al- Al_2O_3 composites may be due to fine Al_2O_3 particles & their uniform dispersion in the matrix [160]. On the other hand, the lower UTS values were obtained for Al- Al_2O_3 composites where particles were added directly. The large particles have more tendency of agglomeration as compared to smaller ones, therefore; agglomerated particles may have some flaws and easily crash under loading. This is why large particles reinforced composites show lower hardness as compare to small particles reinforced composites [161], [162].

A significant decrease in the coefficient of friction was observed with the addition of V_2O_5 particles. A decrease in Coefficient of friction is about 4.18%, 5.17% and 12.78 % in comparison to pure aluminum respectively for the composites containing 3 wt. %, 5 wt. % and 7 wt. % V_2O_5 particles. A significant decrease in the coefficient of friction can be attributed to the formation of the lubricating layer between contacting surfaces due to smaller particle size and proper dispersion of these particles [163].

it is well known that the dry sliding wear of in-situ composites decreases significantly by increasing the amount of reinforcing particles [164]. Some

researchers contradicted that the cast composites contain porosity due to increase in particle content, which tends to decline their behavior against wear. The porosity was found due to the poor wetting of the reinforced particles in Aluminum melt [111], [149].

With the addition of oxide particles, hardness increases and the real area of contact between the surfaces decreases. During the dry sliding test, the oxide debris is generated and this hard debris gets locked between the surfaces thereby promotes wear. At the same time, particles get compacted between the surfaces and form a protective transfer layer. This layer is responsible for the decrease in wear rate[140][98]. Specific wear rate tends to increase for higher particle content (7%) due to the presence of porosity in cast-in-situ composite. The real area of contact also increases with higher porosity and eventually increases the wear rate. Thus, the effect of porosity is not only softening the material but it also promotes the delamination and subsurface cracks.

The worn surface of material mainly depends on speed and applied load. At low load, a proportion of counterface material gets removed and is subjected to oxidation due to micromachining effect. This oxidized material (Fe_2O_3) act as a tribo layer between the two surfaces. Wear studies have reported that the wear rate temporarily reduces due to the tribo layer formation. This tribo layer acts as a solid lubricant between the mating surfaces. At high load, delamination occurs due to the removal of the tribo layer. At high load, high temperature near the surfaces reduces the shear strength in subsurface layers, which promotes the excessive material transfer.

The results of the present work suggest that it is feasible to improve the tensile properties while retaining percent elongation in the range of 3% to 4% by producing in-situ composites with the addition of V_2O_5 particles into molten aluminum. The addition of oxide particles could increase the mechanical & tribological properties up to some extent. The dry sliding wear resistance is improved by the addition of oxides. The coefficient of friction increases with the sliding distance as well as the load applied.

CHAPTER 5 RESULT & DISCUSSION Al-Si & V₂O₅

Other in situ composites were developed by the addition of V₂O₅ particles in Al-7Si matrix using stir casting method. Different amount of V₂O₅ particles were added to produce in-situ alumina particles by the reduction of vanadium oxide particles in the melt. This chapter covers the results obtained from the XRD analysis, microstructural characterization followed by evaluation of mechanical properties like hardness; tensile strength and tribological properties like wear behavior, the coefficient of friction. The results have been discussed thoroughly at the end of this chapter.

5.1 Al-7Si Characterization

5.1.1 Designation of the developed composite

Three different composites were developed by adding 1, 3 and 5% V₂O₅ and all the composites have been designated by sample name. A small amount of Mg was added to promote wettability. The designation given to the composite is on the basis of material composition as shown in Table 5-1.

Table 5-1 Designation of Al-Si alloy & its composite

Sample Designation	Material
AS	Aluminum-7%Silicon
ASV1	AS-1% V ₂ O ₅
ASV3	AS-3% V ₂ O ₅
ASV5	AS-5% V ₂ O ₅

Where AS represents the Aluminum-7% Silicon alloy, V followed by the number represents the wt. % of V₂O₅ added. Base alloy has been used for the comparative study.

5.1.2 XRD Analysis

The X-ray diffraction pattern of the developed in-situ composites is shown in Figure 5.1. The XRD of base alloy i.e. Al-7Si is also conducted along with the composites for the comparison purpose. The phases identified by the x-ray diffraction technique are presented in Figure 5.1

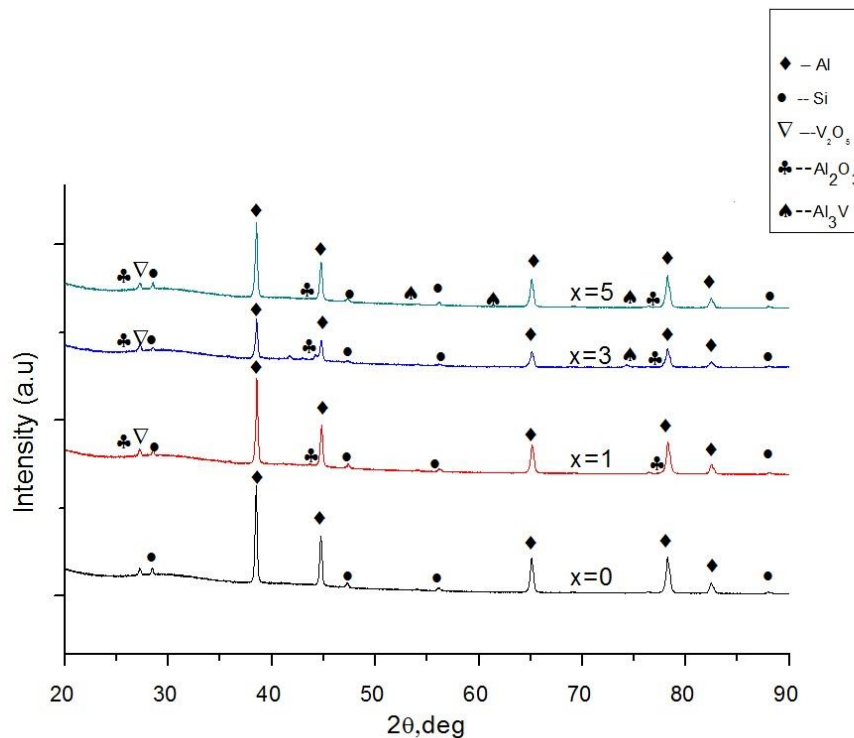


Figure 5.1 XRD analysis of Al-7Si composites

A very small variation in the peaks has been observed, which may be due to the small addition of particles. Another reason for the small difference in the peaks could be the masking of the strong peaks of Al on the weaker peaks of other phases identified as Al₃V and Al₂O₃ in the composite. Stronger peaks of Al₃V and Al₂O₃ are present in case of Al-1% V₂O₅ as compared to Al-3% V₂O₅ and Al-5% V₂O₅ composites. This may be due to occurrence of nearly complete reaction between Al-Si alloy and V₂O₅ particles for Al-1% V₂O₅ composites. Reduction of aluminum can be easily identified by a decrement of aluminum peaks with the increment of particle addition.

5.1.3 Microstructural characterization

Micrographs of the base Al-Si alloy with various percentage of V_2O_5 are shown in Figure 5.2. Figure 5.2(a) represents the microstructure of as-cast base Al-Si alloy. The microstructure of unmodified Al-Si alloy shows the coarse α -Al dendritic crystals. The crystals are surrounded by primary silicon particles. These eutectic silicon particles show the needle-like morphology & distributed within the interdendritic region throughout the microstructure.

Figure 5.2(b) indicates the grain refinement of aluminum alloy due to 1% V_2O_5 particles addition. The average SDAS value for base Al-Si alloy is $67\mu\text{m}$ whereas with the addition of 1% V_2O_5 particles, it decreases to $40\text{-}45\mu\text{m}$. Increasing the particle addition leads to further refinement as revealed from the microstructure of the composite with 3% V_2O_5 particles shown in Figure 5.2(c). However, further increase in particle addition results in coarsening of grains as revealed by the microstructure of the composite with 5 % V_2O_5 particles shown in Figure 5.2(d).



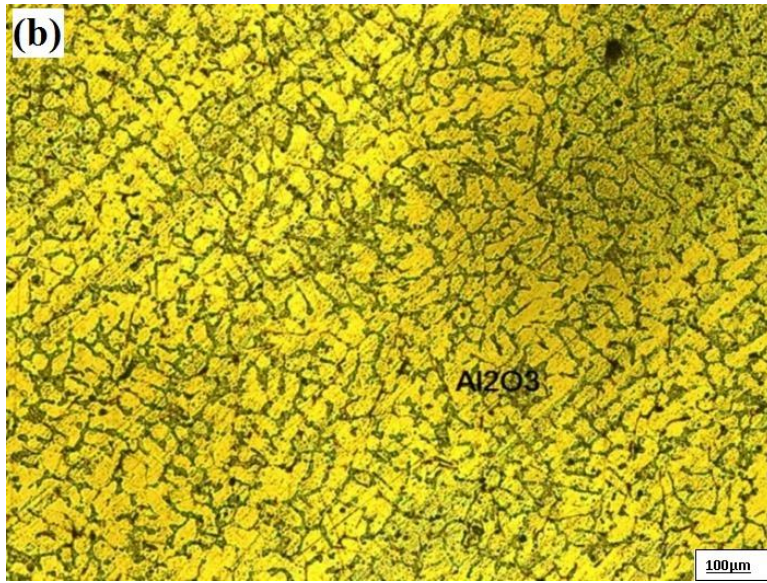


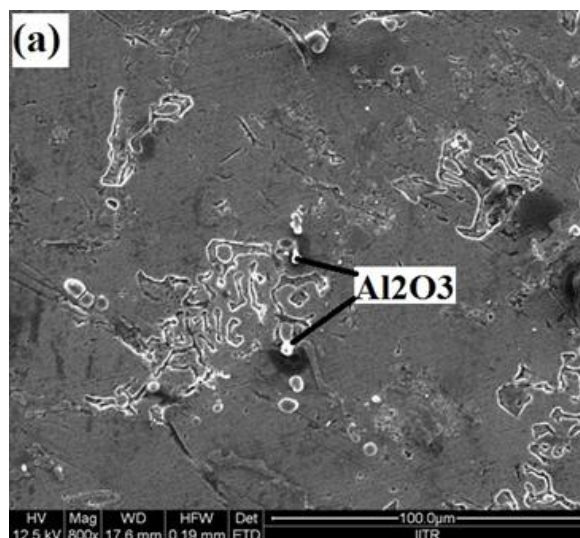


Figure 5.2 Microstructure of AS alloy & its composites (a) Al-Si (b) ASV1 (c) ASV3 (d) ASV5

Similar phases have been identified in all the microstructures. The chemistry of compounds/phases formed due to in-situ reaction is complex but mainly leads to the formation of Al_2O_3 and minor Al-V intermetallic compounds.

5.1.4 SEM Analysis

The Figure 5.3 (a), (b) & (c) shows the SEM images of Al-7Si with 1, 3 & 5 % addition of V_2O_5 respectively. From the images, it is clear that alumina content increases with increasing content of V_2O_5 particles.



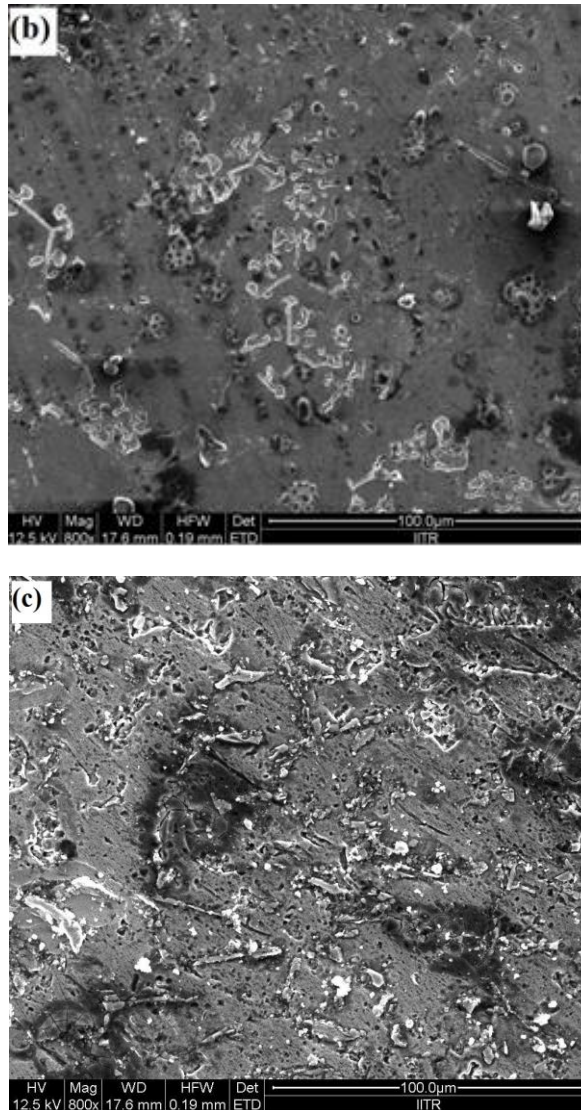
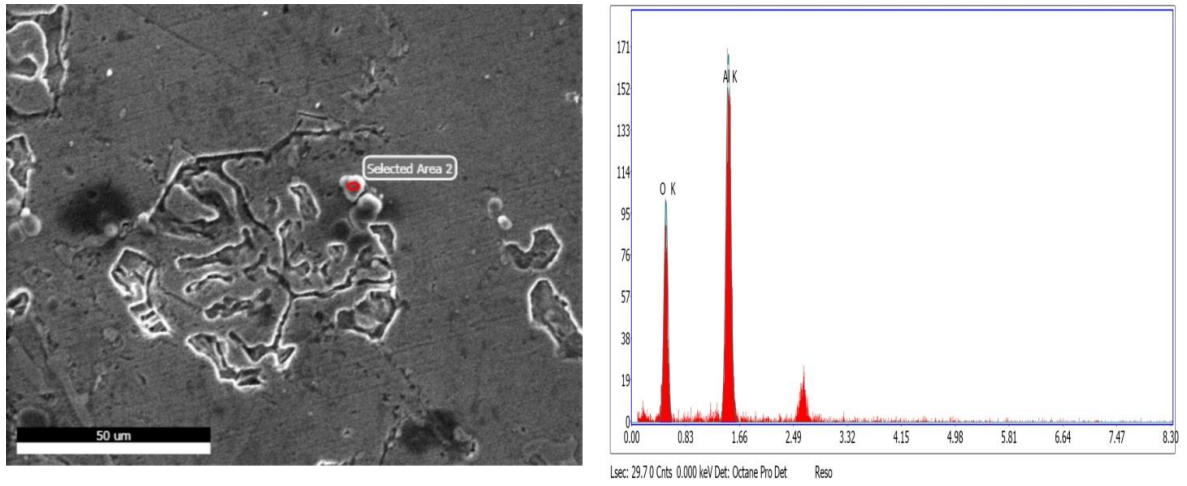


Figure 5.3 SEM images of (a) ASV1 (b) ASV3 (c) ASV5

The EDAX analysis shown in Figure 5.4 confirms the formation of nearly stoichiometric Al_2O_3 in the composite. The volume fraction of alumina has been estimated with the help of image J software by using threshold method and given in Table 5-1.



Element	Weight %	Atomic %	Net Int.
O K	45.76	58.73	51.68
Al K	54.24	41.27	104.04

Figure 5.4 EDAX of Al-7Si Composite

5.2 Mechanical Properties

5.2.1 Microhardness and Tensile Testing

Table 5-2 lists the mechanical properties of Al-Si alloy & its cast in-situ composites. Vickers Microhardness has been measured at a load of 100gf. The average of ten such readings has been stated for the results.

In the case of 1 % addition of oxide particles, there is an improvement of about 20% in hardness. The trend of hardness variation with respect to the amount of V_2O_5 addition is shown in Figure 5.5. The graph shows the highest value of hardness for ASV1 composite and it starts decreasing with the further addition of V_2O_5 particles but still higher than base alloy for all the composites. In addition to the presence of hard alumina particles, the size of eutectic Si particles and the refinement of α -Al may be responsible for the improvement in the properties.

Table 5-2 Mechanical properties of AS and its composites

S.No	Alloy/Composite*	Microhardness (HV)	UTS(MPa)	Elongation (%)
1	AS	51.7(2.3)	137	8
2	ASV1	64.1(1.8)	184	6
3	ASV3	59.7(1.5)	181	5
4	ASV5	56.3(1.2)	174	4

* Represents the wt. % of oxide added.

Standard deviations are in parentheses.

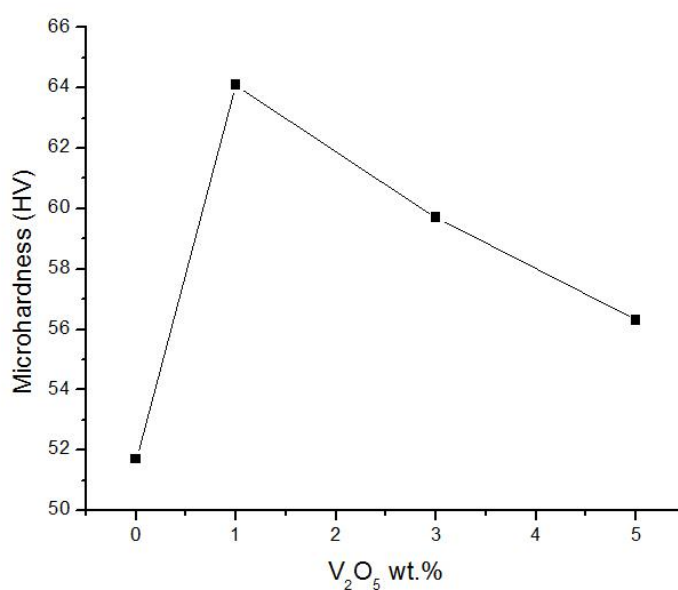


Figure 5.5 Hardness variation with the addition of V₂O₅ addition

The variation in Ultimate tensile strength with V₂O₅ particle content is shown in Figure 5.6. The variation pattern of ultimate tensile strength is similar to that of microhardness. The figure shows that tensile strength increases with particle addition up to 1% and start decreasing by further addition of V₂O₅ particles in the molten matrix; however, the strength values for all the cast composites are higher than that of base aluminum-silicon alloy. The

improvement in strength represents the synergic effects of reinforcement and the matrix. An increase of 35% increment in ultimate tensile strength has been achieved as compared to as cast Al-Si base alloy.

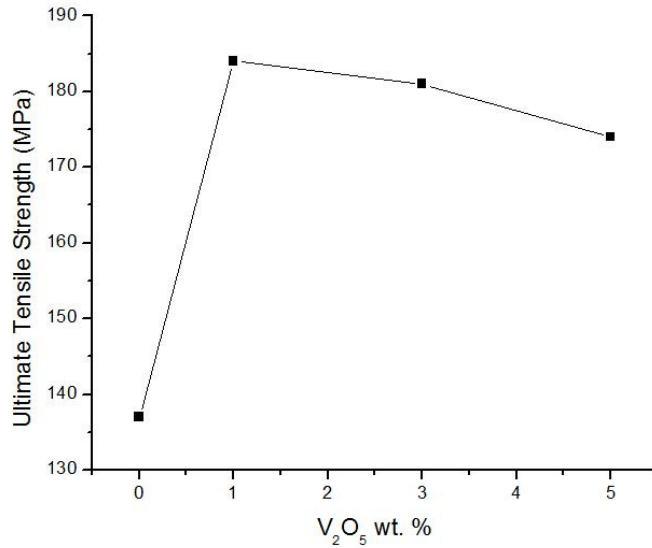


Figure 5.6 Tensile strength variation with the V₂O₅ addition

5.3 Heat treatment

A short time heat treatment comprised of Solutionizing process trailed by aging at 170⁰C for 2 h was found adequate to homogenize the structure and to form hardening precipitates[165]. Heat treatment of cast in-situ composites and base Al-Si alloy has been carried out to evaluate the effect of heat treatment on mechanical properties. The heat treatment diagram is shown in Figure 5.7 and the parameters used are given in Table 5-3.

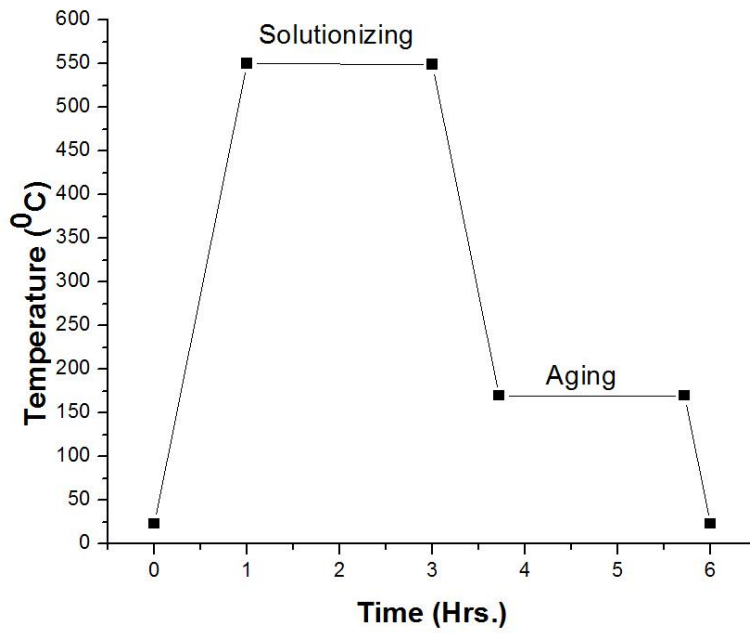


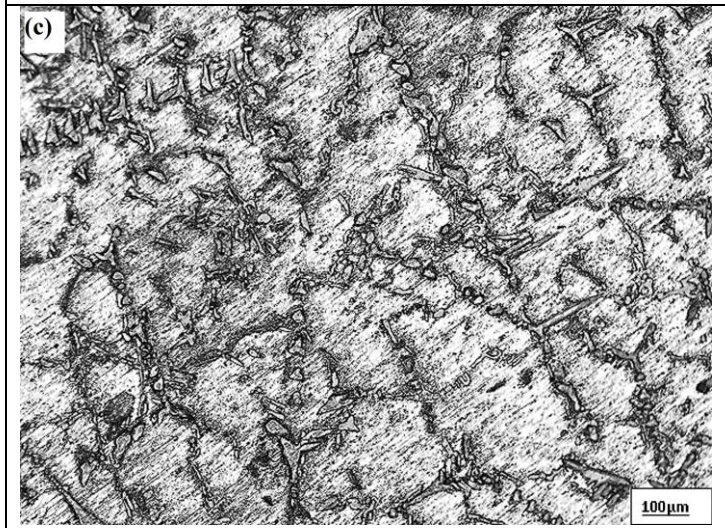
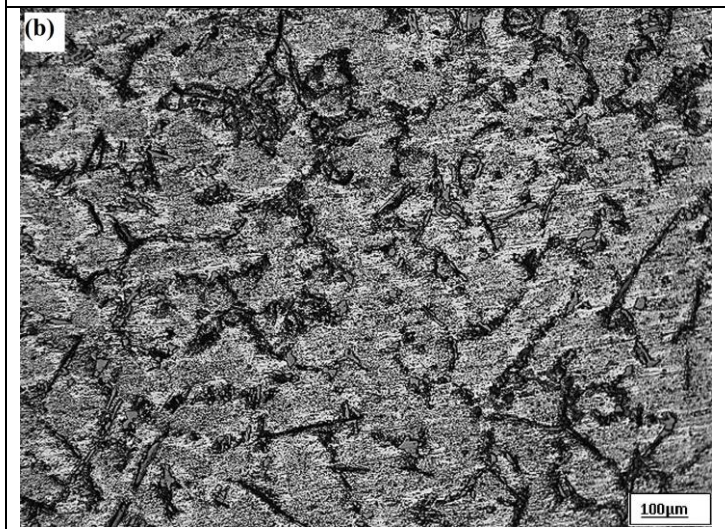
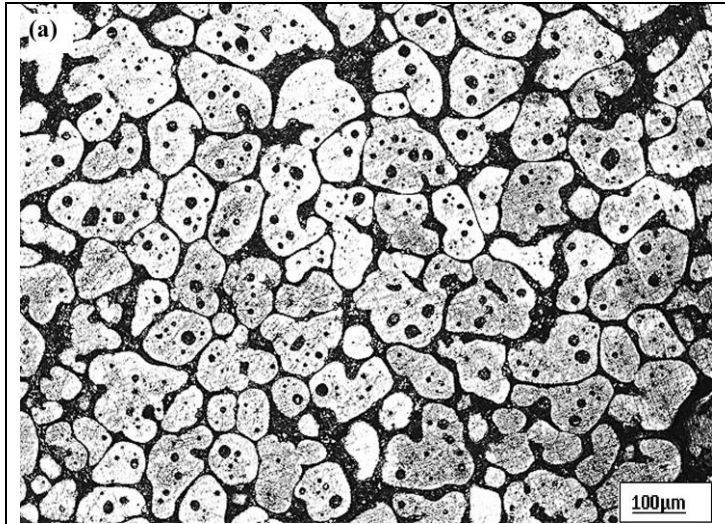
Figure 5.7 Heat Treatment Diagram

Table 5-3 Heat treatment Parameters

Treatment	Temperature (°C)	Holding Time (h)
Solution	549±5	2
Aging	170	2

5.3.1 Effect of heat treatment on microstructure

The optical micrographs of heat treated Al-Si alloy based composites (1, 3 & 5% V₂O₅) are shown in Figure 5.8 (a), (b), (c) respectively. From Figure 5.8 it is observed that the spheroidization of Si particles diminishes and the particle become needle shape by the heat treatment.



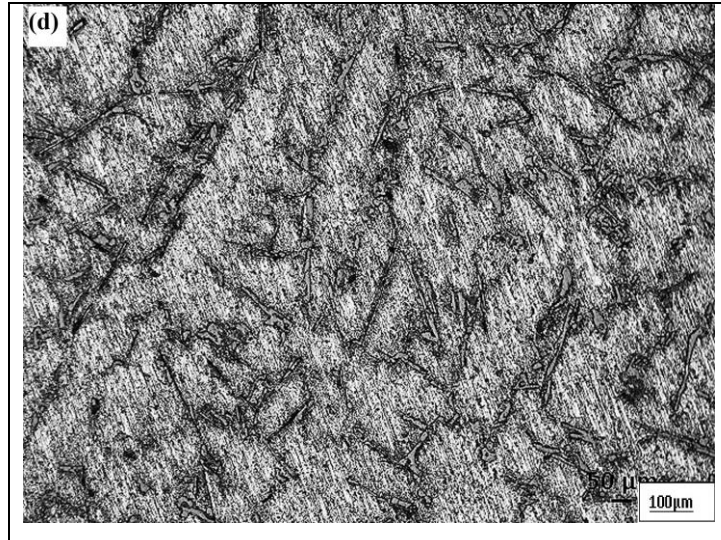


Figure 5.8 Optical micrographs of Al-Si base alloy and its composites after heat treatment (a) Al-Si (b) ASV1 (c) ASV3 (d) ASV5

These micrographs reveal a homogenize structure after the heat treatment and the redistribution of alloying elements may also occur due to heat treatment. The average particle size has increased while aspect ratio has decreased due to thermal modifications irrespective of vanadium pentoxide addition. In the case of 1% V_2O_5 addition, the oxide particles are settled along the grain boundaries without affecting the eutectic Si. While comparing the micrographs of cast composites, better modification of Si particles has been observed with optimum particle size for 3% V_2O_5 addition. It is clear from the micrographs that size of Si needles & α -Al dendrite decreases with the increment of V_2O_5 . The partial refinement of dendrites due to heat treatment also takes place as shown in Figure 5.8 (c). This partial refinement may be attributed to the addition of V_2O_5 particles, which aids in heterogeneous nucleation at the time of solidification.

5.4 Comparison of Mechanical Properties of as cast & heat treated composites

5.4.1 Effect of heat treatment on the hardness

A significant improvement in hardness has been observed after heat treatment as compared to as-cast condition. The hardness value of as cast and heat-treated base alloy and composites are given in Table 5-4. The comparison of hardness value for base Al-Si and its composites in as-cast condition and after heat treatment is shown in Figure 5.9.

Table 5-4 Mechanical properties of Al-Si and its composites before and after heat treatment

S.No	Alloy/Composite*	Micro hardness (HV)		UTS (MPa)		Elongation (%)	
		As Cast	Heat Treated	As Cast	Heat Treated	As Cast	Heat Treated
1	Al-Si	51.7(2.3)	126(2.1)	137	237	8	9
2	ASV1	64.1(1.8)	134(1.9)	184	252	6	8
3	ASV3	59.7(1.5)	121(3.9)	181	265	5	8
4	ASV5	56.3(1.2)	96(2.7)	174	231	4	6

* Represents the wt. % of oxide added.

Standard deviations are in parentheses.

Al-7si alloy with 1% addition of V_2O_5 shows maximum hardness in both conditions as compared to other composites. It has been reported by many researchers that due to aging process Mg_2Si (secondary phase) is formed within the structure. The formation of secondary phase is responsible for the precipitation hardening, which in turn improves the mechanical properties of these alloys [166], [167]. The value of hardness starts reducing with increasing the addition of oxide particles beyond 1% in as-cast condition and beyond 3% in the heat-treated condition. This could be attributed to the depletion of

hardening precipitates of Mg_2Si phase. The reaction of molten alloy with oxide particles at high temperature may cause Mg loss within the melt leading to depletion of Mg_2Si precipitates. Addition of fewer amounts of oxide particles promotes precipitation of Mg_2Si , hardening effect occurs because of hardening precipitates, and the presence of alumina particles formed due to the in-situ reaction. With higher addition of 5 % V_2O_5 particles, depletion of age hardening Mg_2Si precipitates takes place and therefore hardening effect occurs only due to the presence of aluminum oxide particles.

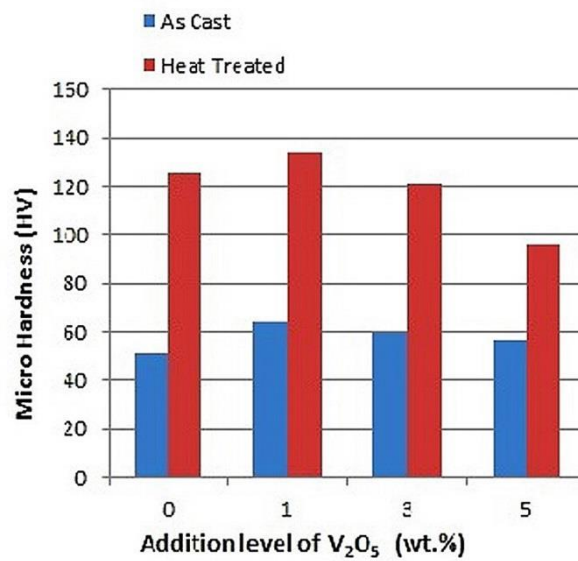


Figure 5.9 Hardness of AS alloy as cast & its heat-treated composites

5.4.2 Effect of heat treatment on Tensile Properties

The comparison of ultimate tensile strength before and after heat treatment is shown in Figure 5.10. A significant improvement in tensile strength has been observed after heat treatment as compared to as-cast condition. The increment in tensile strength does not follow the linear relationship with the V_2O_5 addition. The reason is the same as discussed in the earlier section. A similar trend has been observed by other researchers also [39]. Although the ultimate tensile strength of base alloy and the all the composites increases after the heat treatment, the maximum ultimate tensile strength after the heat treatment is observed for composite with 3% addition of V_2O_5 particles as the ultimate

tensile strength reaches to 265 MPa. Strength of heat-treated composites with 1% and 3% addition of V_2O_5 particles is found to be higher than that of the heat-treated base alloy. Whereas, the strength of heat-treated composite with 5% addition of V_2O_5 particles is lower than that of the heat-treated base alloy.

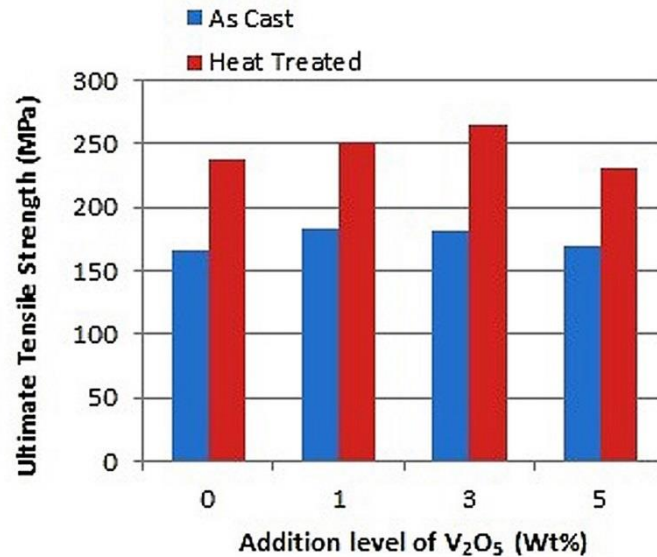


Figure 5.10 Comparison of UTS of Al-Si alloy as cast & its heat-treated composites

Improvement in tensile strength of base alloy after heat treatment indicates the involvement of some strengthening mechanism. For Al-Si base alloy with a minor concentration of other alloying elements, the probable strengthening mechanisms may be solid solution hardening during homogenization followed by rapid cooling and precipitation hardening during the aging process. During homogenization, the alloying elements like Mg and Si get dissolved in the solution and are trapped there due to rapid cooling. It has been reported that during solutionizing, two steps occur simultaneously; formation of Al solution saturated with Si and Mg, and spheroidization of Si particles. During aging, Si, Mg_2Si and other phases are precipitated out according to the sequence in Al-Mg-Si alloys with excess Si [105]. The needle-shaped Mg_2Si precipitates are observed uniformly distributed in Al dendrites as well as in the eutectic region as exhibited in the microstructure. Considerable enhancement in tensile strength after heat treatment may be accredited to the strengthening of the

matrix as discussed above and improvement in interfacial bonding between the matrix and the reinforcement. A relatively low value of ultimate tensile strength of the composite with 5% addition of V_2O_5 particles after heat treatment may be attributed to the high volume fraction of porosity and agglomeration of reinforcement particles during the ageing process. On the other hand, de-bonding of larger Si particles to smaller one affects the ductility. With more addition of oxide particles ductility starts decreasing and the formation of complex intermetallic starts. This increases the brittleness in the composite and decreases the tensile strength [168], [169].

5.5 Comparison of result with literature

The properties of as-cast Al- Al_2O_3 composites fabricated under present investigation are compared with those of the composites fabricated by S.A. Sajjadi & H.R. Ezatpour. In their research, they have taken A356 as a matrix & Al_2O_3 as reinforcement. Two different types of composites were made by adding Al_2O_3 in Nano & Micro size. Two different methods of fabrication; stir casting & compo casting have been used for both types of composites. The results obtained by them for the composites micro size Al_2O_3 and fabricated by stir casting are considered for comparison. Table 5-5. Lists the results of present work and the results reported by H.R.Ezatpour [170].

Table 5-5 Comparison of Al-Al₂O₃ composite properties

S. No	Sample/Composite		Vol %		Hardness (BHN)		UTS (MPa)	
	Reported	Present work	Reported	Present work	Reported	Present work	Reported	Present work
1	A356	AS	0	0	54	51.7(2.3)	134	137(3)
2	A356-1% Al ₂ O ₃	ASV1	0.82	0.72	63	64.1(1.8)	140	184(4)
3	A356-3% Al ₂ O ₃	ASV3	2.34	2.1	65	59.7(1.5)	147	181(2)
4	Al-5% Al ₂ O ₃	ASV5	3.29	3.4	75	57.3(1.2)	154	174(3)

**In reported columns the approximate values are taken from Graph published in the paper (S.A.Sajjadi 2011 & 2012)[75], [161]

#AS stands for Al-7Si, V stands for V₂O₅ and the last digit represents the wt. % of oxide added.

Standard deviations are shown in parentheses.

In the reported work, Al₂O₃ particles were added externally in the matrix and the vol% were calculated by an image analyzer. In present work, the volume percentage was calculated by the image J software & interception method.it can be seen from the Table 5-5 that hardness and strength values increase continuously with particle volume percent in the reported study whereas, these increase up to 0.70 volume percent and decreases afterward in the present study. Hardness values of the present study are lower than those of reported study but strength values of the present study are higher than those of reported study. Lower hardness values in the present study may be attributed to the comparatively low volume percentage of particles. The volume percent of reinforcing particles in the composite decreases with increasing stirring speed [161]. Stirring speed used in the present study was 700 rpm, which is very much higher than the stirring speed of 300 rpm used in the reported study.

Higher strength values in the present study may be attributed to uniform dispersion of fine Al_2O_3 particles of 126nm average size generated through Insitu reaction at 700 rpm stirring speed as compared to relatively non-uniform distribution of externally added coarse Al_2O_3 particles of 20-micron average size at 300 rpm stirring speed. This comparison leads to the conclusion that Insitu approach of adding reinforcement results in better mechanical properties than ex situ approach of adding the reinforcement externally.

5.5.1 Effect of Volume fraction of reinforcement on porosity

Figure 5.11 shows the variation of porosity with the nano- Al_2O_3 content in the composites. This figure reveals that porosity content increases with the increasing volume fraction of the reinforcement. It is already reported that as the volume fraction of reinforcement increases porosity in the composite also increases due to an increase in contact surface area. In the present study also, pure aluminum and Al-Si alloy based composites are developed with a substantial volume fraction of porosity, which increases, with the volume fraction of the reinforcement. This is due to the effect of low wettability, agglomeration at high content of reinforcement and pore nucleation at the matrix/ Al_2O_3 interfaces. Moreover, decreasing of liquid metal flow associated with the particle clusters leads to the formation of porosity. There may be a possibility that preheating could not remove completely any volatile material present in V_2O_5 particles [161], [171].

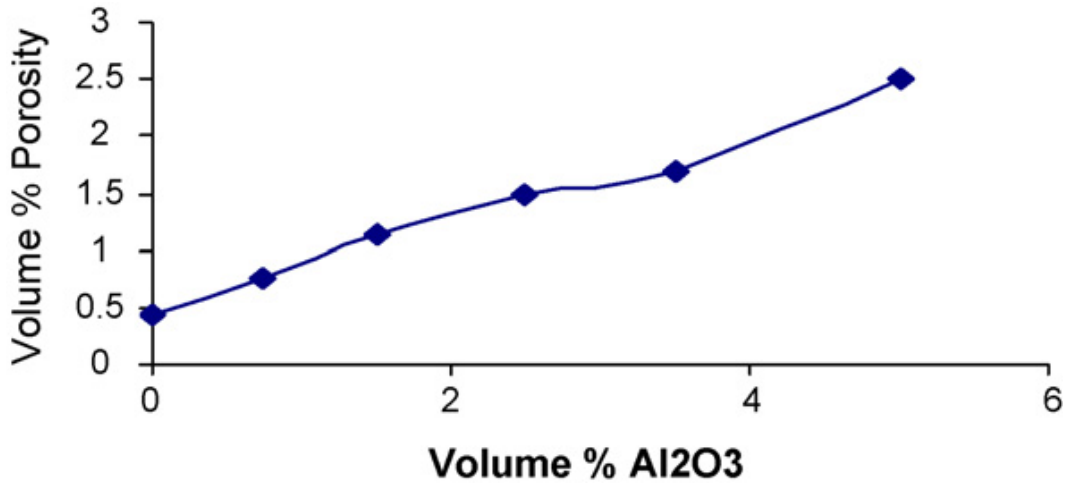


Figure 5.11 Variation of porosity with vol. % of the Al₂O₃ content

5.5.2 Effect on Tensile strength

A model has been proposed to examine the strengthening effects of particles on the tensile properties [156], [157], [172].

$$\Delta\sigma = \Delta\sigma_{load} + \Delta\sigma_{Hall-Petch} + \sqrt{[(\Delta\sigma_{Orowan})^2 + (\Delta\sigma_{CTE})^2]}$$

Where $\Delta\sigma_{load}$ is the transfer of load from the soft matrix to the hard ceramic particles,

$\Delta\sigma_{Hall-Petch}$ is the involvement of grain refinement to strength;

$\Delta\sigma_{Orowan}$ is the dislocation's interaction with the particles and

$\Delta\sigma_{CTE}$ is change in the value of the Coefficient of thermal expansion between the matrix and Al₂O₃ reinforcement.

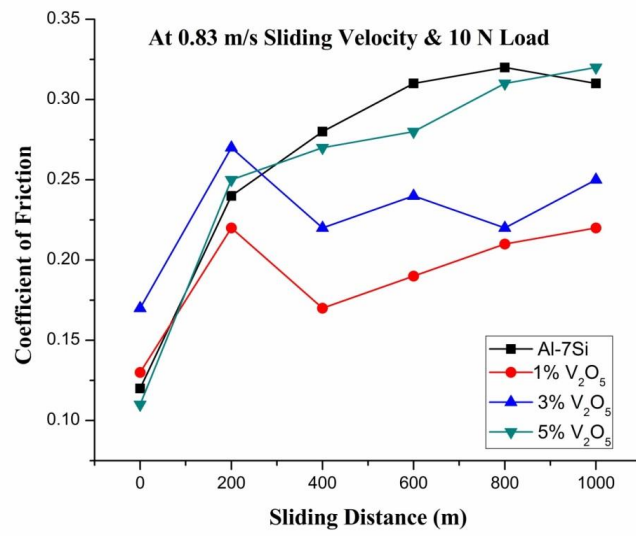
In the present study, the tensile strength of the Al-Al₂O₃ composites increases initially up to a certain volume fraction of alumina due to the increase in load stress and the rate of work hardening of the particles. Tensile strength of the composites decreases with further increase in the volume fraction of alumina particle addition due to the agglomeration of Al₂O₃ particles, which leads to more defects and porosity. The results are consistent with the trends reported by other investigators [75], [161], [173], [174].

In the present work, the particles formed during in-situ reaction are of nano size. High stirring speed employed during fabrication of the composites eliminates clustering/agglomeration of the particles and enables uniform distribution in the matrix for the low volume fraction of the reinforcement. Strength of A356 based composite decreases beyond 1.5 vol. % Al_2O_3 particles due to high porosity and agglomeration. The volume of the interface area increases with Al_2O_3 content, which leads to high porosity and lowers flow stress in the composite. In addition, dislocations start inducing around alumina particles due to different CTE values of matrix and Al_2O_3 . It leads to de-bonding of the interface and results in a decrease in ultimate tensile strength. [175].

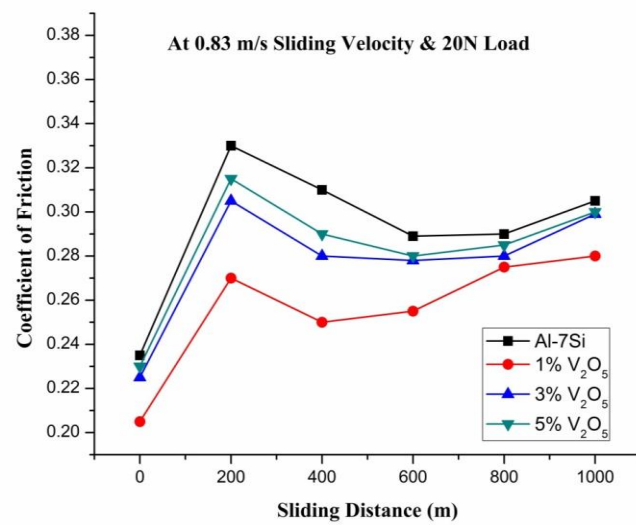
5.6 Tribological Behavior

5.6.1 Coefficient of friction

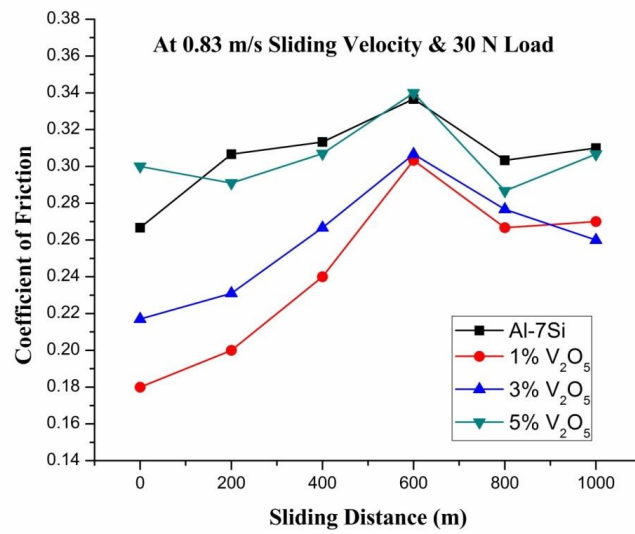
An experimental study has been carried out to estimate the effect of weight fraction of V_2O_5 Particles and normal load, on the wear rate of Al-Si- Al_2O_3 in-situ composites. The coefficient of friction is measured for different composites at different sliding distances(200, 400, 600, 800 & 1000m) at a different loads (10, 20, and 30 N) under constant sliding velocity of 0.83m/s. Figure 5.12 shows the variation of coefficient of friction with sliding distance at different loads for all the composites.



(a)



(b)



(c)

Figure 5.12 Coefficient of Friction with sliding distance (a) 10N load (b) 20N load (c) 30N load

It is revealed from the Figure 5.12 (a), (b) & (c) that at low load, the coefficient of friction increase continuously with sliding distance with one or two exceptions. At intermediate loads, the maximum coefficient of friction is observed at a small sliding distance (200m) and decreases afterwards with some exceptions. At higher loads, the coefficient of friction increases continuously up to a sliding distance of 600m and decreases afterwards. Among all the in-situ composites and the matrix alloy, Al-7Si base alloy exhibits the highest coefficient of friction whereas Al-7Si-1% V₂O₅ in-situ composite displays the lowest coefficient of friction.

Generally, the friction coefficient has a tendency to increase with increasing load. Addition of V₂O₅ particles leads to the formation of hard alumina particles, which helps to reduce the coefficient of friction. Significant variation in the coefficient of friction is observed with the sliding distance but in most of the cases, it decreases with increase in load for large sliding distances [176]–[178].

Figure 5.13 shows the variation of coefficient of friction with load under constant sliding velocity and constant sliding distance for base Al-7Si alloy and different Al-Si-Al₂O₃ in-situ composites. The figure reveals that the coefficient of friction increases continuously with load for all the materials which conforms to Archard's law of wear [179], [180]. The base alloy matrix exhibits the highest coefficient of friction and in-situ composite having 1% V₂O₅ exhibits the lowest coefficient of friction at all loads.

The reduction in the coefficient of friction at 1000m for 10N load is about 21.3 % for 1 wt. % V₂O₅ composite, 13.7 % for 3 wt. % V₂O₅ composite and 3% for 5 wt. % V₂O₅ composite over the coefficient of friction of base Al-Si alloy. Similar trend of reduction in the coefficient of friction are obtained at 20 & 30 N load.

The Significant decrease in the coefficient of friction can be attributed to the decrease in the contacting area of two mating surfaces due to the presence of uniformly distributed fine Al₂O₃ particles in Al-Si matrix. With increases in weight percentage of V₂O₅ particles, more alumina particles are generated which agglomerate to form clusters of the particles. This clustering of agglomerated particles affects the size and dispersion of alumina particles in the matrix that eventually leads to an increase in the coefficient of friction [181].

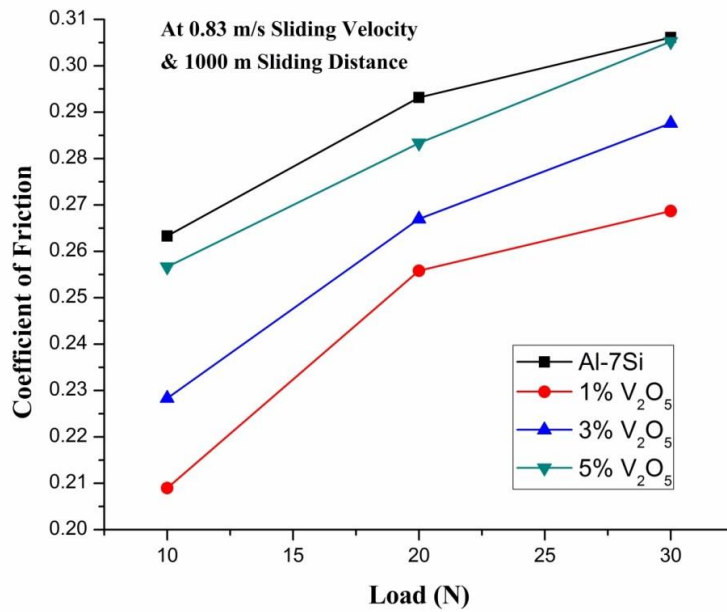


Figure 5.13 Variation of Coefficient of friction with load

5.6.2 Volume loss

Figure 5.14 shows the variation of pin volume loss of base Al-Si alloy and different composites with load for 1000m sliding distance (steady state regime). This figure reveals that volume loss increases with increase in load for base Al-Si alloy and all Insitu composites.

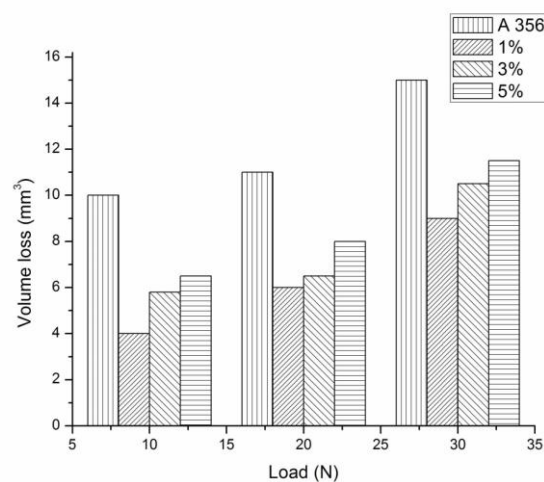


Figure 5.14 Variation of volume loss with load at a 1000m sliding distance

Volume loss with the addition of V_2O_5 particles decreases in comparison to pure Al-Si alloy. Volume loss also increases with increase in V_2O_5 addition, as the in-situ composite with 1% V_2O_5 particles addition exhibits lower volume loss as compared to other in-situ composites having more wt. % of V_2O_5 . The reduction in volume loss in in-situ composite over the Al-Si alloy can be attributed to the effect of reinforcing hard Al_2O_3 particles in the aluminum alloy matrix. Less addition of V_2O_5 leads to the uniform dispersion of the optimum quantity of fine coherent Al_2O_3 particles in the matrix. Higher addition leads to the agglomeration of Al_2O_3 particles causing incoherency with the matrix. These incoherent particles may detach easily during wear testing. The average reduction in volume loss is determined to be 47.3 %, 36.3 % and 27.5 % for composites with 1%, 3% and 5% V_2O_5 addition respectively as compare to base Al-Si alloy.

5.6.3 Wear

Figure 5.15 & Figure 5.16 clearly describes the wear response of Al-Si and its cast composites under dry sliding conditions. Bulk wear increases with load for the base Al-Si alloy and all the composites. Wear also increases with increase in weight percent of V_2O_5 additions. It is well known that the dry sliding wear of in-situ composites decreases enormously by increasing the amount of reinforcing particles. Hard particles act as a load bearer and in case of in-situ, it produces the pure interfaces which in turn enhance interfacial bonding strength [182]. However, some researchers propounded that the porosity content of cast composites increases with increase in particle content which in turn decline their behavior against wear. Porosity generation in composites can be attributed to dismal wetting of reinforced particles in molten aluminum alloy [183].

A higher percentage of V_2O_5 particles shoots up the hardness with the addition of alumina particles. These particles form a compress protective layer at low loading condition and this layer corresponds to dwindling wear rate [143]. However, at high loads, the generation of fresh oxide debris during the dry

sliding test led to locking of previously generated debris, which eventually resulted in surge wear. With more addition of V_2O_5 particles e.g. 5 % addition, specific wear rate tends to increase. Again, porosity in the cast in situ composite is responsible for this increase. As the real area of contact increases with higher porosity which eventually increases the wear rate [184]. Hence, porosity not only leads to softening of material but it also encourages the delamination and subsurface cracks.

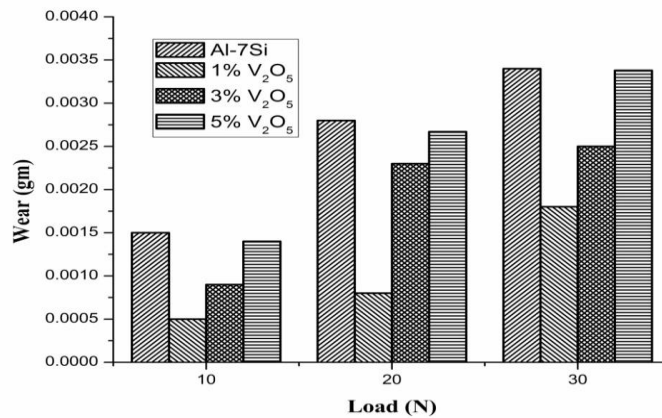


Figure 5.15 Variation of wear with load for Al-Si based composites

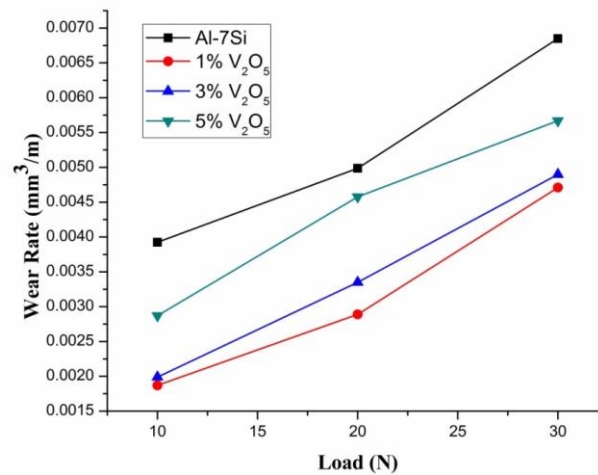


Figure 5.16 Wear rate of the different composite at different loads

Increase in applied load results in the worn-out surface of the material. On account of micromachining effect at low loads, a part of counterface material

gets separated and subjects to oxidation. This oxidized material (Fe_2O_3) spreads as a tribo layer between the mating surfaces. Wear studies has established that this temporary reduction in wear rate can easily be attributed to the formation of this tribo layer, which acts as a solid lubricant between the mating surfaces. Application of high loads, dismantle this tribo layer, which in turn results in the delamination. High load gives rise to the generation of high temperature at near surfaces and reduces the shear strength in subsurface layers of the materials, which promotes excessive material transfer. Similar kind of transfer layers has been perceived by various investigators specifically in case of aluminum-based composites [185]–[187].

5.6.4 Worn surfaces

The most favorable results of wear rate have been found with the condition of 1% addition of V_2O_5 particles as contrary to 3% & 5% V_2O_5 addition. Because of the abrasion mechanism, tiny grooves are formed in the sliding direction at low loads. At higher loads, delamination occurs with an increase in the real area of contact and finally results in an increase in fracture stresses of the reinforced particles as shown in Figure 5.17.

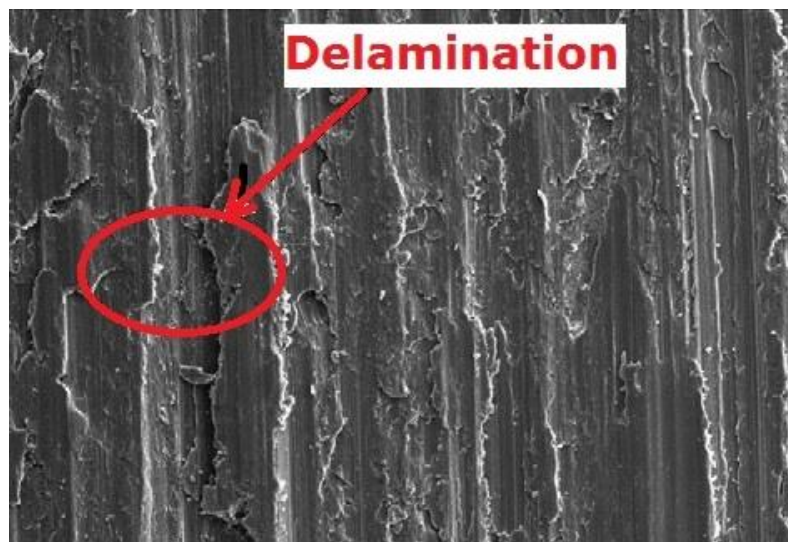


Figure 5.17 SEM image of the composite with 5% V_2O_5

It can be inferred that the presence of alumina particles & intermetallic compound in the cast in situ composites props up the hardness together with

the increasing porosity, which in turn reduces the interaction between the matrix and reinforcement.

5.7 Effect of reinforcement

It is evident from **Error! Reference source not found.** that addition of V_2O_5 particles ameliorates the hardness of composite, which resulted in lower wear rate as compared to base matrix alloy. The severe adhesive wear mainly depends on the hardness of the material [181]. Further evidence & support from the practical work suggested that, scuff & seizure, the onset of adhesive process stunting when the hardness of mating parts increased [24].

Figure 5.15 clearly depicts the influence of increasing the weight percentage of V_2O_5 particles on the wear rate of Al-Si- Al_2O_3 in-situ composites. The observed decrease in wear rate of the composites as compared to base Al-Si alloy may be attributed to increase in hardness with the addition of V_2O_5 particles as reduction of V_2O_5 particles during in-situ reaction results in the generation of hard alumina particles in the matrix.

The micrographs shown in Figure 5.2 clearly reveals the presence of a pure and clean interface between Al-7Si matrix and Al_2O_3 particles leading to the better load-bearing capacity of the composite which in turn brings down the rate of wear with the addition of V_2O_5 particles. Presence of dislocations around the Al_2O_3 particles due to the difference in coefficient of linear thermal expansion between matrix and reinforcement also increases the resistance to wear.

Although, the wear rate of all composites is found to be lower than that of the base Al-Si alloy. The wear rate of composites increases with increasing the weight percent of V_2O_5 particles. As mentioned earlier, the Insitu reaction of V_2O_5 with molten aluminum results in the formation of alumina and the rate of this reaction depends on the quantity of V_2O_5 particles. Thus, an increase in weight percentage of V_2O_5 particle results in the formation of more alumina particles or in other words, more interfacial area between the matrix and the reinforcement. High temperature generated during dry sliding condition leads

to interfacial debonding due to the large difference in CTE of matrix and reinforced alumina particles. This interfacial debonding effect together with increased porosity overtake the positive effect of the dislocation presence around the alumina particles and contributes to increasing wear rate through debonding and subsequent delamination of agglomerated alumina particles.

5.8 Effect of parameters on wear

There are various parameters, which affect the dry sliding wear of the composites. High sliding velocity & high load lead to comparatively more heat generation between the mating surfaces. The heat generation results in mellowing down of surfaces, which in turn increases the penetration of counter surface into the pin (composite) surface. Different thermal expansion of Al_2O_3 particle and the matrix is vital in wearing down of the composites. This incongruity in terms of thermal expansion causes the development of stresses at the interface. As the sliding velocity increases, the heat generation also surges to a high value, leads to an increase in interfacial stress. When this interface stress surpasses the interface bond strength, cracks may develop in the matrix region or particle may leave its place to create a cavity.

Si present in the matrix alloy has a substantial impact on the interfacial bond strength. The presence of Al_2O_3 particles, secondary hard phases, and intermetallic phases restricts the metal flow during the dry sliding wear as these hard particles /phases decrease the area of contact between the mating surfaces and decrease material removal during dry sliding wear [188], [189]. Figure 5.17. portrays the eroded surface of the composite under study at sliding velocity of 0.83m/s. Though much damage has not been inflicted upon the subsurface at this sliding velocity but at a higher sliding velocity, the subsurface may receive comparatively more damage.

5.9 Discussion

Addition of V_2O_5 particles produces evident changes in the microstructure. Alumina particles formed due to in-situ reaction between molten aluminum

alloy and V_2O_5 particles as indicated in the micrographs. Vanadium released from V_2O_5 particles after in-situ reaction helps in grain refinement as vanadium is a good grain refiner for aluminum [190]. The grain refinement is due to the presence of Al_3V phase created by the reduction reaction between aluminum and released vanadium. Al_3V phase impedes the recrystallization, nucleation, and growth of the grains, as a result, the grain size of the composite matrix was found smaller as compared to the base alloy. With 1%, the addition of V_2O_5 particles, few alumina particles get settled along the grain boundaries and a decrease in dendritic arm spacing was observed.

The grain size was found to increase with the increase in V_2O_5 addition as observed in the micrographs of the specimen produced with 3% & 5% addition of V_2O_5 particles. The observed behavior is in good agreement with other researchers who had reported that Vanadium acts as a grain refiner at a very minute level [191]. However, the alumina particles formed after in-situ reaction segregate at the eutectic grain boundaries causing a change in Si particles morphology as segregation of these particles at the grain boundaries restricts the further refinement of the Si particles and their redistribution. Segregated Nano size alumina particles formed after in-situ reaction start forming clusters in interdendritic regions thus causing a change in morphology of α -Al dendrites from columnar to cellular. This kind of behavior generally observed in grain refined Al-7Si alloy and can be attributed to peritectic hulk theory [192]. The comparison of the microstructure confirms that eutectic Si can be modified up to a substantial extent by the addition of V_2O_5 particles.

A significant improvement in hardness has been observed as given in Table 5-2. The improvement in hardness is mainly due to the presence of hard phase alumina particles acting as obstacles to the motion of dislocations [193]. The highest hardness was found for ASV1 sample as compared to other composites. Another reason for hardness increment is a better interface between the matrix and the alumina particles [194].

Hardness of the in-situ composites increases up to 2.6 Vol % of Al_2O_3 particles formed by the reduction of vanadium pentoxide. In the present work,

high hardness values are obtained as compared to other researchers. It may be attributed to the presence of hard alumina particles together with intermetallic Al_3V phase formed during the reduction of vanadium pentoxide & identified in the XRD of the composites shown in Figure 5.1. In Al-V binary phase diagram, four intermetallics are characterized. Out of these four intermetallic Al_3V has more tendency of formation. According to Miedema's model Al_3V has a highest negative enthalpy of formation as given in Table 5-6 [195] and According to Bragg-Williams theory, the ordering energy is higher for the intermetallic having less vanadium [196].

Table 5-6 Formation Enthalpy of intermetallic in Al-V system (V less than 25 at.%).

Al_{21}V_2	-15.6
Al_{45}V_7	-31.5
Al_{23}V_4	-41.9
Al_3V	-115.3

The development of the composite by nanoparticles addition shows the significant improvement in the tensile flow stress. The highest tensile strength of 184 MPa was obtained with 1.5 vol. % of Al_2O_3 nanoparticles. The ductility of composites continuously decreases with increasing Al_2O_3 nanoparticles for as-cast in-situ composites and heat-treated composites. Maximum percentage elongation was observed with 1.5 Vol % Al_2O_3 particles.

According to Hall-Petch theory, the strength of the composites increases due to the grain refinement as strength is inversely proportional to the square root of the grain size. Also, the in-situ generated particles act as a barrier and try to restrict the motion of dislocation within the matrix. The uniform distribution of alumina particles and low porosity are other important factors contributing to the strength, which is evident from micrographs and SEM images.

Tensile strength decreases beyond 1.5 vol. % alumina particles in the composites. Increase in alumina content due to the addition of V_2O_5 particles causes a significant increase in porosity level as given in Table 4-1, which finally affects the strength of the composite. Addition of more V_2O_5 particles tends to increase the volume percent of Al_2O_3 particles that leads to the formation of alumina particle clusters at the interdendritic regions surrounded by the eutectic silicon as marked from the micrographs shown in Figure 5.3. The similar results have been reported earlier by many researchers.

The presence of Al_2O_3 particles in the composites have a great influence on their wear properties. α - Al_2O_3 particles show good cohesive interfacial bonding with matrix and have the ability to take high external loads [181].

CHAPTER 6 CONCLUSION

In-situ Al- Al₂O₃ metal matrix composites were developed using pure aluminum & Al-7Si alloy as matrices and V₂O₅ particles as a source of Al₂O₃ particle reinforcement. Al₂O₃ particles were generated in the molten matrices by the reduction of V₂O₅. The effect of Al₂O₃ reinforcement on mechanical properties and on microstructure was evaluated and analyzed. The wear behavior of aluminum, aluminum alloy and cast in situ composites containing different wt. % of oxide particles under dry sliding condition has been investigated. The conclusions drawn from the present study are summarized as follows:

1. In-situ Al-Al₂O₃ and Al-Si-Al₂O₃ composites with different volume percent of Al₂O₃ particles are successfully fabricated by stir casting using V₂O₅ particles. Al₂O₃ particles are generated by the reaction between aluminium/aluminium silicon alloy and V₂O₅ particles. Volume fraction of Al₂O₃ particles is varied by varying the amount of V₂O₅ particles because rate of reaction for generation of Al₂O₃ particles depends upon the amount of V₂O₅ particles added to the molten aluminium/aluminium silicon alloy.
2. The microstructure of Al- Al₂O₃ composites consists of fine Al₂O₃ particles and Al₃V phase distributed along the grain boundaries and within the grains of α -aluminum. Dispersion of Al₂O₃ particles is relatively more uniform in the composites with low volume fraction of reinforcement particles. Increasing the volume fraction leads to agglomeration and clustering of Al₂O₃ particles in the matrix as revealed by optical and scanning electron microscopy.

3. In addition to Al_2O_3 and Al_3V , the microstructure of $\text{AlSi- Al}_2\text{O}_3$ composites shows the presence of Si phase. These phases are dispersed more uniformly in the matrix for low volume fraction of reinforcement particles. With increase in volume fraction, agglomeration and clustering of reinforcement occurs.
4. XRD analysis of the samples of different $\text{Al- Al}_2\text{O}_3$ composites confirms the presence of Al_2O_3 , Al_3V and $\alpha\text{-Al}$ in these composites. XRD analysis of different $\text{Al-Si- Al}_2\text{O}_3$ composites confirms the presence of an additional Si phase besides the phases present in $\text{Al- Al}_2\text{O}_3$ composites. EDX analysis of the composites further confirms the formation of almost stoichiometric Al_2O_3 particles during in-situ reaction between molten pure Al/Al alloy and V_2O_5 particles.
5. Apart from being a source of Al_2O_3 generation, addition of V_2O_5 particles helps in grain refinement of the matrices as the released vanadium from reduction of V_2O_5 particles combines with aluminium to form Al_3V phase, which impedes the recrystallization, nucleation and grain growth. This is evident from the fact that grain size of the composite matrices are found smaller than the base alloy.
6. The microstructure of Al-7Si alloy matrix shows $\alpha\text{-Al}$ dendrites with eutectic Si particles. Addition of oxide particles changes the morphology of eutectic Si particles from columnar to cellular. Oxide particle addition also imparts grain refinement as the SDAS value decreases after addition of only 1% V_2O_5 particles.
7. Microhardness of the pure Al/Al-Si alloy increases with the addition of Al_2O_3 particles as the microhardness of all the composites is found to be higher than their respective base material. However, hardness of the composites increases to a certain extent of V_2O_5 particles addition and decreases afterwards. Less addition of V_2O_5 particles helps in generating optimum quantity of uniformly dispersed fine Al_2O_3 particles with coherent interfacial bonding between reinforcement and matrix in the porosity free composite. More addition of V_2O_5 particles leads to generation of more Al_2O_3 particles, which agglomerates to

cause nonuniform dispersion, incoherent interfacial bonding and porosity generation during solidification.

8. The tensile strength of pure Al/Al-Si alloy increases with the addition of V_2O_5 particles as the strength of all the composites is found to be higher than their respective base material. The improvement in the strength of the composite is due to the presence of hard Al_2O_3 particles in pure Al based composites and presence of hard Mg_2Si phase together with Al_2O_3 particles in Al-Si based composites. These hard phases acts as obstacles to the movement of dislocations during deformation, which leads to increase in the strength of these composites. Moreover, grain refinement imparted by released vanadium also contribute to strength improvement according to Hall-Petch relation.
9. The tensile strength of as cast in-situ Al composites increases up to 5% V_2O_5 addition and decreases afterwards, whereas tensile strength of as cast and heat-treated Al-Si composite increases up to 3% of V_2O_5 addition and decreases on further addition. Decrease in tensile strength of pure Al based composites after 5 % V_2O_5 addition and of Al-Si based composites after 3% V_2O_5 addition is associated with agglomeration of Al_2O_3 particles and increasing porosity content. More addition of V_2O_5 particles tends to generate more Al_2O_3 particles, which subsequently agglomerate in the melt, and finally leads to high porosity content during solidification of composites.
10. Ductility of pure Al based composites increases with increasing V_2O_5 addition as percentage elongation of all Al based composites is found to be higher than the pure Al. However, percentage elongation of pure Al based composites increases up to 5 wt.% addition of V_2O_5 particles and decreases with further addition of V_2O_5 particles. Ductility of Al-Si alloy based as cast composites and heat treated composites decreases with increasing V_2O_5 addition as percentage elongation of all Al-Si based as cast and heat treated composites is found to be lower than the base Al-Si alloy. Volume fraction of Al_2O_3 reinforcement in the composite is directly related to amount of V_2O_5

added to molten metal since more V_2O_5 , addition generates more Al_2O_3 particles in the melt. Al_2O_3 being a brittle phase, increasing its volume fraction results in the decrease of percentage elongation of the composites. Formation of intermetallic Al_3V phase in all composites, brittle Si phase in as cast and Mg_2Si phase in heat treated Al-Si based composites also affects the ductility.

11. Using Al-Si alloy as matrix in place of pure Al alloy have insignificant effect on microhardness and percentage elongation of the composites since as cast composites of both the matrices with same V_2O_5 addition exhibit very slight difference in microhardness and percentage elongation. However, there is very significant improvement in tensile strength of Al-Si based composites over that of pure Al based composites. This improvement in tensile strength may be attributed to the strength of base Al-Si alloy.
12. Mechanical properties of as cast Al-Si based composites are improved to a great extent after the heat treatment as microhardness increases many folds and tensile strength increases by 35-70% for different composites. Heat treatment also imparts a significant improvement in percentage elongation. The improvement in mechanical properties may be due to dissolution of detrimental phases in aluminum during homogenization followed by rapid cooling and formation of fine and coherent precipitates of strengthening phases in the solid solution during ageing. Thus, both solid solution stretching and precipitation hardening are responsible for the observed improvement in mechanical properties.
13. Coefficient of friction of Al-based in-situ composites is found to be less than that of pure aluminum. It varies randomly with sliding distance but increases with increasing load and decreases with the increasing volume fraction of Al_2O_3 particles for all values of sliding distance. Wear volume follows the same trend as the coefficient of friction but specific wear rate follows opposite trend with load. Coefficient of friction is a function of normal applied load so

naturally will increase with load. With the incorporation of hard Al_2O_3 particles, hardness increases and real area of contact between the surface decreases, which reduces the coefficient of friction and wear volume. At low loads, a portion of counter face surface is removed due to micromachining effect and contribute to wear volume. At higher loads, high temperature generated near the surfaces reduces the shear strength of subsurface material, which promotes the excessive material removal. The increase in wear volume with load is substantial but being inversely proportional to the load, the specific wear decreases with increasing load.

14. Coefficient of friction of Al-Si based in-situ composites is found to be less than that of Al-Si alloy. It varies randomly with sliding distance but increases with increasing load and increasing volume fraction of Al_2O_3 particles for all values of sliding distance. Wear volume and wear rate follow the same trend as the coefficient of friction. Coefficient of friction is a function of normal applied load so naturally will increase with load. Incorporation of more Al_2O_3 particles leads to more porosity, which increases the real area of contact hence, coefficient of friction, wear volume and wear rate increases. At low loads, a portion of counter face surface is removed due to micromachining effect and contribute to wear volume and wear rate. At higher loads, high temperature generated near the surfaces reduces the shear strength of subsurface material, which promotes the excessive wear.

6.1 Future Scope

- 1) The work can be extended to study the effect of reaction time on size and distribution of the particles in the matrix.
- 2) It can be extended to other Al-alloys like Al-Mg-Si, Al-Cu, and Al-Zn alloys etc.
- 3) In addition to in-situ some other particles can be added externally using stir casting and in the form of fibers.

6.2 Publications obtained from this work

6.2.1 Peer reviewed journal

1. **Singla, A.**, Garg, R., & Saxena, M. (2015). Microstructure and wear behavior of Al-Al₂O₃ in situ composites fabricated by the reaction of V₂O₅ particles in pure aluminum. *Green Processing and Synthesis*, 4(6), 487-497.
2. **Singla, A.**, Garg, R., & Saxena, M. (2016). Effect of Heat Treatment on Microstructure and Tensile Properties of A356/V₂O₅ Insitu Composites. *International Journal of Manufacturing, Materials, and Mechanical Engineering (IJMMME)*, 6(3), 1-10.
3. **Singla, A.**, Garg, R., & Saxena, M. (2017, February). Wear Properties of A356/Al₂O₃ Metal Matrix Composites Produced by Insitu Squeeze Casting Techniques. In *International Conference on Nano for Energy and Water* (pp. 213-217). Springer, Cham.
4. **Singla, A.**, Garg, R., & Saxena, M. (2018). Tribological behavior of cast in-situ Al-Al₂O₃ composite developed by stir casting using V₂O₅ particles. *Journal of the Chinese society of Mechanical Engineers* Communicated and under review since 7/8/18.

REFERENCES

- [1] T. W. CLYNE, "An Introductory Overview of MMC Systems, Types, and Developments," *Compr. Compos. Mater.*, pp. 1–26, 2000.
- [2] A. K. Dhingra, "Metals replacement by composites," *JOM J. Miner. Met. Mater. Soc.*, vol. 38, no. 3, p. 17, 1986.
- [3] A. K. Dhingra and I. J. Toth, *Advances in Composite Materials*, vol. 39, no. 11. Applied Science, 1987.
- [4] D. Mangalgiri, P, "Composite materials for aerospace applications," *Bull. Mater. Sci.*, vol. 22, no. 3, pp. 657–664, 1999.
- [5] G. Fisher, "Composites- Engineering the ultimate material," *Am. Ceram. Soc. Bull.*, vol. 63, pp. 360–364, 1984.
- [6] A. W. Urquhart, "Novel reinforced ceramics and metals: a review of Lanxide's composite technologies," *Mater. Sci. Eng. A*, vol. 144, no. 1–2, pp. 75–82, 1991.
- [7] B. C. Pai, B. C. Pal, R. M. Pillai, and K. G. Satyanarayana, "Light Metal Matrix Composites - Present Status and Future Strategies," no. Mmc, pp. 26–40, 1998.
- [8] A. Kelly, "The nature of composite materials," *Sci. Am.*, vol. 217, no. 3, pp. 161–176, 1967.
- [9] A. Berghezan, "Nucleus, 8 (5)," *Nucl. A Ed. 1, rhe, Chalgrin, Paris*, vol. 16, 1966.
- [10] J. Van Suchtelen, "Product properties: a new application of composite materials.," *Philips Res. Rep 27.1*, vol. 27, no. 1, pp. 28–37, 1972.

- [11] R. M. Aikin, "The mechanical properties of in-situ composites," *Jom*, vol. 49, no. 8, pp. 35–39, Aug. 1997.
- [12] A. A. Hamid, P. K. Ghosh, S. C. Jain, and S. Ray, "The influence of porosity and particles content on dry sliding wear of cast in situ Al(Ti)-Al₂O₃(TiO₂) composite," *Wear*, vol. 265, no. 1–2, pp. 14–26, 2008.
- [13] Y. Gao, D. G. Zhu, L. Cheng, H. L. Sun, and Q. Wang, "In Situ Fabrication of Particles Reinforced Al-Si-Al₂O₃ Composites by Hot Isostatic Pressing.," *Adv. Mater. Res. Vol pp Trans Tech Publ.*, vol. 284 SRC-, pp. 38–42, 2011.
- [14] Z. Jing, Y. Huashun, C. Hongmei, and M. Guanghui, "Al-Si / Al₂O₃ in situ composite prepared by displacement reaction of CuO / Al system," *Res. Dev.*, vol. 7, no. February, pp. 19–23, 2010.
- [15] J. Xu and W. Liu, "Wear characteristic of in situ synthetic TiB₂ particulate-reinforced Al matrix composite formed by laser cladding," *Wear*, vol. 260, no. 4–5, pp. 486–492, 2006.
- [16] "J.A. Al-Jarrah.. Ph University of Roorkee, India, pp.,," 1998.
- [17] A. Banerji, M. K. Surappa, and P. K. Rohatgi, "Cast aluminum alloys containing dispersions of zircon particles," *Metall. Trans. B*, vol. 14, no. 2, pp. 273–283, 1983.
- [18] K. Sivaprasad, S. P. K. Babu, S. Natarajan, R. Narayanasamy, B. A. Kumar, and G. Dinesh, "Study on abrasive and erosive wear behaviour of Al 6063/TiB₂in situ composites," *Mater. Sci. Eng. A*, vol. 498, no. 1–2, pp. 495–500, 2008.
- [19] A. Mandal, M. Chakraborty, and B. S. Murty, "Effect of TiB₂particles on sliding wear behaviour of Al-4Cu alloy," *Wear*, vol. 262, no. 1–2, pp. 160–166, 2007.
- [20] S. Kumar, M. Chakraborty, V. Subramanya Sarma, and B. S. Murty, "Tensile and wear behaviour of in situ Al-7Si/TiB₂particulate

- composites,” *Wear*, vol. 265, no. 1–2, pp. 134–142, 2008.
- [21] A. Pauschitz, M. Roy, and F. Franek, “2008.Mechanisms of sliding wear of metals and alloys at elevated temperatures.pdf,” *Tribol. Int.*, vol. 41, no. 7 SRC-GoogleScholar FG-0, pp. 584–602, 2008.
- [22] H. Torabian, J. P. Pathak, and S. N. Tiwari, “Wear characteristics of Al-Si alloys,” *Wear*, vol. 172, no. 1 SRC-GoogleScholar FG-0, pp. 49–58, 1994.
- [23] J. E. Gruzleski and B. M. Closset, “Liquid treatment to Al-Si alloys,” *AFS, Illinois*, pp. 1–254, 1990.
- [24] S. S. S. Kumari, R. M. Pillai, and B. C. Pai, “Effect of iron in Al-7Si-0.3 Mg alloy,” *Indian Foundry J.*, vol. 48, no. 1, pp. 27–31, 2002.
- [25] S. C. Tjong and Z. Y. Ma, “Microstructural and mechanical characteristics of in situ metal matrix composites,” *Mater. Sci. Eng. R Reports*, vol. 29, no. 3, pp. 49–113, 2000.
- [26] A. R. Sarkisyan, S. K. Dolukhanyan, and I. P. Borovinskaya, “Self-propagating high-temperature synthesis of transition metal silicides,” *Powder Metall. Met. Ceram.*, vol. 17, no. 6 SRC-GoogleScholar FG-0, pp. 424–427, 1978.
- [27] K. A. Philpot, Z. A. Munir, and J. B. Holt, “An investigation of the synthesis of nickel aluminides through gasless combustion,” *J. Mater. Sci.*, vol. 22, no. 1, pp. 159–169, 1987.
- [28] V. A. Ravi and T. S. Srivatsan, “Processing and fabrication of advanced materials for high temperature applications-II,” 1993.
- [29] S. D. Dunmead, D. W. Readey, C. E. Semler, and J. B. Hol, “Kinetics of Combustion Synthesis in the Ti-C and Ti-C-Ni Systems,” *J. Am. Ceram. Soc.*, vol. 72, no. 12, pp. 2318–2324, 1989.
- [30] “J.B. Holt, Rep. UCRL- Lawrence Livemore National Laboratory, ..” vol. 53258 SRC, 1982.

- [31] K. Hirao, Y. Miyamoto, and M. Koizumi, "Combustion reaction characteristics in the nitridation of silicon.," *Adv. Ceram. Mater.*, vol. 2, no. 4 SRC-GoogleScholar FG-0, 1987.
- [32] A. N. Tabachenko, T. A. Panteleeva, and V. I. Itin, "Interaction of titanium and carbon burning in the presence of a solution-melt.," *Combust. Explos. Shock Waves*, vol. 20, no. 4 SRC-GoogleScholar FG-0, pp. 387–391, 1984.
- [33] L. Pressure and L. Metal, "Fabrication of metal matrix composites by metal.pdf," *Metallurgical*, vol. 23, no. 9 SRC-GoogleScholar FG-0, pp. 2387–2392, 1993.
- [34] Y. R. M. A.K. Kuruvilla, K.S. Prasad, V.V. Bhanuprasad, "Microstructure-property correlation in Al/TiB₂ (XD) composites," *Scr. Metall. Mater.*, vol. 24, no. c, pp. 873–878, 1990.
- [35] P. C. Maity, S. C. Panigrahi, and P. N. Chakraborty, "Preparation of aluminium-alumina in-situ particle composite by addition of titania to aluminium melt," *Scr. Metall. Mater.*, vol. 28, no. 5, pp. 549–552, 1993.
- [36] H. Nakata, T. Choh, and N. Kanetake, "Fabrication and mechanical properties of in situ formed carbide particulate reinforced aluminium composite," *J. Mater. Sci.*, vol. 30, no. 7, pp. 1719–1727, 1995.
- [37] J. Kellie and J. Wood, "Reaction processing in the metals industry," *Mater. Process.*, vol. 3, no. 1 SRC-GoogleScholar FG-0, pp. 10–12, 1995.
- [38] P. Davies, J. L. F. Kellie, and J. V. Wood, "Development of Cast Aluminium Metal Matrix Composites," *Key Eng. Mater.*, vol. 77–78, pp. 357–362, 1992.
- [39] J. V. Wood, P. Davies, and J. L. F. Kellie, "Properties of reactively cast aluminium–TiB₂ alloys," *Mater. Sci. Technol.*, vol. 9, no. 10, pp. 833–840, 1993.

- [40] L. Lu, M. O. Lai, and F. L. Chen, "Al-4 wt% Cu composite reinforced with in-situ TiB₂ particles," *Acta Mater.*, vol. 45, no. 10, pp. 4297–4309, 1997.
- [41] Y. Chen and D. D. L. Chung, "In situ Al-TiB composite obtained by stir casting," *J. Mater. Sci.*, vol. 31, no. 2, pp. 311–315, Jan. 1996.
- [42] Z. Y. Chen, Y. Y. Chen, G. Y. An, Q. Shu, D. Li, and Y. Y. Liu, "Microstructure and properties of In situ Al/TiB₂ composite fabricated by in-melt reaction method," *Metall. Mater. Trans. A*, vol. 31, no. 8, pp. 1959–1964, Aug. 2000.
- [43] M. K. Aghajanian, N. H. Macmillan, C. R. Kennedy, S. J. Luszcz, and R. Roy, "Properties and microstructures of Lanxide | Al₂O₃-Al ceramic composite materials," *J. Mater. Sci.*, vol. 24, no. 2 SRC-GoogleScholar FG-0, pp. 658–670, 1989.
- [44] O. Salas, H. Ni, V. Jayaram, K. C. Vlach, C. G. Levi, and R. Mehrabian, "Nucleation and growth of Al₂O₃/metal composites by oxidation of aluminum alloys," *J. Mater. Res.*, vol. 6, no. 9, pp. 1964–1981, 1991.
- [45] V. S. R. Murthy and B. S. Rao, "Microstructural development in the directed melt-oxidized (DIMOX) Al-Mg-Si alloys," *J. Mater. Sci.*, vol. 30, no. 12, pp. 3091–3097, 1995.
- [46] H. Fukunaga, X. Wang, and Y. Aramaki, "Preparation of intermetallic compound matrix composites by reaction squeeze casting," *J. Mater. Sci. Lett.*, vol. 10, no. 1, pp. 23–25, 1991.
- [47] "J. Pan, Ph.D. of Technology, .," 1994.
- [48] J. Pan *et al.*, "Microstructural study of the interface reaction between titania whiskers and aluminum," *Compos. Sci. Technol.*, vol. 57, no. 3, pp. 319–325, 1997.
- [49] D. Z. Wang, Z. R. Liu, C. K. Yao, and M. Yao, "A novel technique for

- fabricating in situ Al₂O₃/Ti_xAl_y composites,” *J. Mater. Sci. Lett.*, vol. 12, no. 18, pp. 1420–1421, 1993.
- [50] H. X. Peng, D. Z. Wang, L. Geng, C. K. Yao, and J. F. Mao, “Evaluation of the microstructure of in-situ reaction processed Al₃Ti-Al₂O₃-Al composite,” *Scr. Mater.*, vol. 37, no. 2, pp. 199–204, 1997.
- [51] V. A. Chianeh, H. R. M. Hosseini, and M. Nofar, “Micro structural features and mechanical properties of Al-Al₃Ti composite fabricated by in-situ powder metallurgy route,” *J. Alloys Compd.*, vol. 473, no. 1, pp. 127–132, 2009.
- [52] N. Yazdian, F. Karimzadeh, and M. H. Enayati, “In-situ fabrication of Al₃V/Al₂O₃ nanocomposite through mechanochemical synthesis and evaluation of its mechanism,” *Adv. Powder Technol.*, vol. 24, no. 1, pp. 106–112, Jan. 2013.
- [53] A. K. Lee, L. E. Sanchez-Caldera, S. T. Oktay, and N. P. Suh, “Liquid-metal mixing process tailors MMC microstructures,” *Adv. Mater. Process.*, vol. 142, no. 2, pp. 31–34, 1992.
- [54] J. Hashim, L. Looney, and M. S. J. Hashmi, “Metal matrix composites: production by the stir casting method,” *J. Mater. Process. Technol.*, vol. 92–93, pp. 1–7, 1999.
- [55] S. Ghanaraja, C. M. Ramanuja, C. J. G. gowda, and K. S. Abhinandhan, “Fabrication and Mechanical Properties of Al (Mg)-TiO₂Based In-Situ Composites,” *Mater. Today Proc.*, vol. 2, no. 4–5, pp. 1282–1290, 2015.
- [56] P. C. Maity and P. N. Chakraborty, “Preparation of Al-MgAl₂₀, -- MgO in situ particle-composites by addition of MnO₂ particles to molten Al-2 wt % Mg alloys,” *Science (80-.)*, vol. 20, no. July, pp. 93–97, 1994.
- [57] N. Yoshikawa, Y. Watanabe, Z. M. Veloza, A. Kikuchi, and S. Taniguchi, “Microstructure-Process-Property Realationship in

- Al/Al₂O₃ Composites Fabricated by Reaction between SiO₂ and Molten Al,” *Key Eng. Mater.*, vol. 161–163, pp. 311–314, 1999.
- [58] T. Fan, D. Zhang, G. Yang, T. Shibayanagi, and M. Naka, “Fabrication of in situ Al₂O₃/Al composite via remelting,” *J. Mater. Process. Technol.*, vol. 142, no. 2, pp. 556–561, 2003.
- [59] P. C. Maity, P. N. Chakraborty, and S. C. Panigrahi, “Al-Al₂O₃ in situ particle composites by reaction of CuO particles in molten pure Al,” *Mater. Lett.*, vol. 30, no. 2–3, pp. 147–151, 1997.
- [60] P. Yu, C. J. Deng, N. G. Ma, and D. H. L. Ng, “A new method of producing uniformly distributed alumina particles in Al-based metal matrix composite,” *Mater. Lett.*, vol. 58, no. 5, pp. 679–682, Feb. 2004.
- [61] Y. F. Li, C. D. Qin, and D. H. L. Ng, “Morphology and growth mechanism of alumina whiskers in aluminum-based metal matrix composites,” *J. Mater. Res.*, vol. 14, no. 7, pp. 2997–3000, 1999.
- [62] M. K. Surappa, “Aluminium matrix composites: Challenges and opportunities,” *Sadhana*, vol. 28, no. 1–2, pp. 319–334, 2003.
- [63] S. Ray, “Casting of Metal Matrix Composites,” *Key Eng. Mater.*, vol. 104–107, pp. 417–446, 1995.
- [64] N. El-Kaddah and K. E. Chang, “On the dispersion of SiCAl slurries in rotating flows,” *Mater. Sci. Eng. A*, vol. 144, no. 1–2, pp. 221–227, Oct. 1991.
- [65] J. Hashim, L. Looney, and M. S. J. Hashmi, “Particle distribution in cast metal matrix composites - Part I,” *J. Mater. Process. Technol.*, vol. 123, no. 2, pp. 251–257, 2002.
- [66] P. K. Ghosh and S. Ray, “A model study on the particle dispersion on fluid-particle interaction in slurry of liquid alloy and ceramic particle,” *Trans. Japan Inst. Met.*, vol. 29, no. 6, pp. 502–508, 1988.
- [67] P. K. Ghosh and S. Ray, “Particle Dispersion and Fluid-Particle

- Interaction in a Slurry of Liquid Al-Mg Alloy and Al₂O₃ Particles,” *Trans. Japan Inst. Met.*, vol. 29, no. 6, pp. 509–519, 1988.
- [68] J. C. Middleton, “Gas–liquid dispersion and mixing,” *Mix. Process Ind.*, pp. 322–363, 1992.
- [69] J. a. Al-Jarrah, S. Ray, and P. K. Ghosh, “Solidification processing of Al-Al₂O₃ composite using turbine stirrer,” *Metall. Mater. Trans. A*, vol. 29, no. June, pp. 1711–1718, Jun. 1998.
- [70] D. J. Lloyd, “The Solidification Microstructure of Particulate Reinforced Aluminium / SiC Composites,” *Compos. Sci. Technol.*, vol. 35, no. 2 SRC-GoogleScholar FG-0, pp. 159–179, 1989.
- [71] J. Hashim, L. Looney, and M. S. J. Hashmi, “Particle distribution in cast metal matrix composites - Part II,” *J. Mater. Process. Technol.*, vol. 123, no. 2, pp. 258–263, 2002.
- [72] P. K. Ghosh and S. Ray, “Fabrication and Properties of Compocast Aluminium-Alumina Particulate Composite,” *Indian J. Technol.*, vol. 26, no. 2, pp. 83–94, 1988.
- [73] D. J. Lloyd, “Particle reinforced aluminium and magnesium matrix composites,” *Int. Mater. Rev.*, vol. 39, no. 1, pp. 1–23, 1994.
- [74] “MIWA, K., & OHASHI, T. . Preparation of fine SiC particle reinforced Al alloy composites by compocasting process.,” *Achiev. Compos. Japan United States*, pp. 355-362 SRC-GoogleScholar FG-0, 1990.
- [75] S. A. Sajjadi, M. Torabi Parizi, H. R. Ezatpour, and A. Sedghi, “Fabrication of A356 composite reinforced with micro and nano Al₂O₃ particles by a developed compocasting method and study of its properties,” *J. Alloys Compd.*, vol. 511, no. 1, pp. 226–231, Jan. 2012.
- [76] A. Mortensen and I. Jin, “Solidification processing of metal matrix composites,” *Int. Mater. Rev.*, vol. 37, no. 1, pp. 101–128, 1992.

- [77] M. K. Surappa and P. K. Rohatgi, "Technical note.," *Met. Technol.*, vol. 5, no. 1 SRC-GoogleScholar FG-0, pp. 358–361, 1978.
- [78] M. K. Surappa and P. K. Rohatgi, "Melting, degassing, and casting characteristics of Al-11.8Si alloys containing dispersion of copper-coated graphite particles," *Met. Technol.*, vol. 7, no. 1, pp. 378–383, 1980.
- [79] M. K. Surappa and P. K. Rohatgi, "Production of al-graphite particle composites using copper coated graphite particles," *Met. Technol.*, pp. 338–360, 1978.
- [80] A. A. Hamid, P. K. Ghosh, S. C. Jain, and S. Ray, "Influence of particle content and porosity on the wear behaviour of cast in situ Al(Mn)-Al₂O₃(MnO₂) composite," *Wear*, vol. 260, no. 4–5, pp. 368–378, 2006.
- [81] L. V Ramanathan and P. C. R. Nunes, "Effect of Liquid Metal Processing Parameters of Microstructure and Properties of Alumina Base Mmc.," *Met. Matrix Compos. Microstruct. Prop. Proc 12 th Riso Int Symp Mater. Sci. Roskilde Vol No 6*, vol. 2 SRC-G, 1991.
- [82] T. B. Cameron, W. W. Swanson, J. M. Tartaglia, T. B. Cox, and D. C. Washington, "U.S. Patent No.," 713111 *US Pat. Trademark Off.*, vol. 4 SRC-G, 1987.
- [83] D. J. Lloyd, A. D. McLeod, P. L. Morris, I. U. S. Jin, and D. C. Washington, "Patent No.," 028392 *US Pat. Trademark Off.*, vol. 5 SRC-G, 1991.
- [84] S. Pardeep, C. Gulshan, and S. Neeraj, "Production of AMC by Stir Casting – An Overview," *Int. J. Contemp. Pract.*, vol. 2, no. 1, pp. 23–46, 2013.
- [85] D. C. Halverson and R. L. Landingham, "Infiltration processing of boron carbide-, boron-, and boride-reactive metal cermets," 1988.

- [86] P. K. Rohatgi, S. Ray, and Y. Liu, "Tribological properties of metal matrix-graphite particle composites," *Int. Mater. Rev.*, vol. 37, no. 1, pp. 129–152, 1992.
- [87] S. R. Westwood, H. D. Psaras, D. C. Washington, and R. N. Is, "A.R.C. Winzer, in: P.A. Langford (Eds.), *Advanced Material Press*, p. 225.," vol. 1987 SRC.
- [88] K. L. Tee, L. Lu, and M. O. Lai, "Improvement in mechanical properties of in-situ Al-TiB₂ composite by incorporation of carbon," *Mater. Sci. Eng. a-Structural Mater. Prop. Microstruct. Process.*, vol. 339, no. 1–2, pp. 227–231, 2003.
- [89] N. C. Beck Tan, R. M. Aikin, and R. M. Briber, "Fracture toughness of discontinuously reinforced Al-4Cu-1.5Mg/TiB₂ composites," *Metall. Mater. Trans. A*, vol. 25, no. 11, pp. 2461–2467, Nov. 1994.
- [90] O. Liuzhang, L. Chengping, S. Xiandong, Z. Meiqin, and Z. Min, "Fabrication and microstructure of in situ Al₂O₃ decomposed from Al₂(SO₄)₃-reinforced aluminum matrix composites," *Mater. Lett.*, vol. 57, pp. 1712–1715, 2003.
- [91] Z. Y. Ma *et al.*, "In-situ formed Al₂O₃ and TiB₂ particulates mixture-reinforced aluminum composite," *Scr. Metall. Mater.*, vol. 31, no. 5, pp. 635–639, Sep. 1994.
- [92] Z. Y. Ma and S. C. Tjong, "In Situ ceramic particle-reinforced aluminum matrix composites fabricated by reaction pressing in the TiO₂ (Ti)-Al-B (B₂O₃) systems," *Metall. Mater. Trans. A*, vol. 28, no. 9, pp. 1931–1942, 1997.
- [93] K. L. Tee, L. Lu, and M. O. Lai, "In situ processing of Al-TiB₂ composite by the stir-casting technique," *J. Mater. Process. Technol.*, vol. 89–90, pp. 513–519, 1999.
- [94] K. Niranjana and P. R. Lakshminarayanan, "Optimization of process parameters for in situ casting of Al/TiB₂ composites through response

- surface methodology,” *Trans. Nonferrous Met. Soc. China (English Ed.)*, vol. 23, no. 5, pp. 1269–1274, May 2013.
- [95] S. Kumar, V. Subramaniya Sarma, and B. S. Murty, “Functionally graded Al alloy matrix in-situ composites,” *Metall. Mater. Trans. A Phys. Metall. Mater. Sci.*, vol. 41, no. 1, pp. 242–254, Oct. 2010.
- [96] T. G. Durai, K. Das, and S. Das, “Synthesis and characterization of Al matrix composites reinforced by in situ alumina particulates,” *Mater. Sci. Eng. A*, vol. 445–446, pp. 100–105, 2007.
- [97] B. Yang *et al.*, “In situ Al₂O₃ particle-reinforced Al and Cu matrix composites synthesized by displacement reactions,” *J. Alloys Compd.*, vol. 494, no. 1–2, pp. 261–265, Apr. 2010.
- [98] A. A. Hamid, S. C. Jain, P. K. Ghosh, and S. Ray, “Characterization and Tribological Behavior of Cast In-Situ Al (Mg , Mo) -Al₂O₃ (MoO₃) Composite,” *Metall. Mater. Trans. B*, vol. 37, no. August, pp. 519–529, 2006.
- [99] G. H. Zahid *et al.*, “In situ processing and aging behaviour of an aluminium/Al₂O₃ composite,” *Mater. Des.*, vol. 32, no. 3, pp. 1630–1635, Mar. 2011.
- [100] I. El-Mahallawi, H. Abdelkader, L. Yousef, A. Amer, J. Mayer, and A. Schwedt, “Influence of Al₂O₃ nano-dispersions on microstructure features and mechanical properties of cast and T6 heat-treated Al Si hypoeutectic Alloys,” *Mater. Sci. Eng. A*, vol. 556, pp. 76–87, 2012.
- [101] M. J. Abden, J. D. Afroze, M. A. Gafur, and F.-U.-Z. Chowdhury, “Influence of Al₂O₃ addition on microstructure and mechanical properties of 3YSZ-Al₂O₃ composites,” *Mater. Test.*, vol. 57, no. 6, pp. 499–505, Jun. 2015.
- [102] T. Wang, Y. Zheng, Z. Chen, Y. Zhao, and H. Kang, “Effects of Sr on the microstructure and mechanical properties of in situ TiB₂ reinforced A356 composite,” *Mater. Des.*, vol. 64, no. February, pp. 185–193,

2014.

- [103] W. Zhang, D. Chai, G. Ran, and J. Zhou, “Study on microstructure and tensile properties of in situ fiber reinforced aluminum matrix composites,” *Mater. Sci. Eng. A*, vol. 476, no. 1–2, pp. 157–161, 2008.
- [104] R. L. Deuis, C. Subramanian, and J. M. Yellup, “Dry sliding wear of aluminium composites - A review,” *Compos. Sci. Technol.*, vol. 57, no. 4, pp. 415–435, 1997.
- [105] J. Clarke and A. D. Sarkar, “Wear characteristics of as-cast binary aluminium-silicon alloys,” *Wear*, vol. 54, no. 1, pp. 7–16, 1979.
- [106] D. K. Dwivedi, A. Sharma, and T. V. Rajan, “Friction and wear behaviour of cast hypereutectic Al-Si alloy (LM28) at low sliding velocities,” *Trans. Indian Inst. Met.*, vol. 54, no. 6, pp. 247–254, 2001.
- [107] A. Patel, A. Bhabhor, and V. Patel, ““ Effect of grain refinement and modification on the dry sliding wear behaviour of eutectic Al – Si alloys using gravity die casting ,”” *Tribol. Int.*, vol. 2, no. 3, pp. 2897–2902, 2012.
- [108] M. Zhu, Z. Jian, G. Yang, and Y. Zhou, “Effects of T6 heat treatment on the microstructure, tensile properties, and fracture behavior of the modified A356 alloys,” *Mater. Des.*, vol. 36, pp. 243–249, 2012.
- [109] A. Osorio, W.R., Garcia, L.R.& Garcia, “Effect of eutectic modification and T4 heat treatment on mechanical properties and corrosion resistance of an Al-9 wt%Si casting alloy,” *Mater. Chem. Phys.*, vol. 106, no. 2–3, pp. 343–349, 2007.
- [110] Z. Zhang and J. Zhu, “Effectiveness of short-term aeration in treating swine finishing manure to reduce odour generation potential,” *Agric. Ecosyst. Environ.*, vol. 105, no. 1–2, pp. 115–125, 2005.
- [111] P. N. Suh, “The delamination theory of wear,” *Wear*, vol. 25, no. 1, pp. 111–124, 1973.

- [112] H. Sin, N. Saka, and N. P. Suh, "Abrasive wear mechanisms and the grit size effect," *Wear*, vol. 55, no. 1, pp. 163–190, 1979.
- [113] M. A. Moore and R. Douthwaite, "Plastic deformation below worn surface," *Metall. Trans. A*, vol. 7, no. December, pp. 1833–1839, 1976.
- [114] E. Rabinowicz, L. A. Dunn, and P. G. Russell, "A study of abrasive wear under three-body conditions," *Wear*, vol. 4, no. 5, pp. 345–355, 1961.
- [115] R. L. Deuis, C. Subramanian, and J. M. Yellup, "Abrasive wear of aluminium composites—a review," *Wear*, vol. 201, no. 1–2, pp. 132–144, 1996.
- [116] I. M. Hutchings, "Wear by particulates," *Chem. Eng. Sci.*, vol. 42, no. 4, pp. 869–878, 1987.
- [117] A. G. Wang and I. M. Hutchings, "Wear of alumina metal matrix composites by abrasion," *Mater. Sci. Technol.*, vol. 5, no. January, pp. 71–76, 1989.
- [118] P. L. Ko, "Metallic wear - A review, with special reference to vibration-induced wear in power plant components," *Trib*, vol. 20, no. 2, pp. 66–78, 1987.
- [119] X. S. Jiang, N. J. Wang, and D. G. Zhu, "Friction and wear properties of in-situ synthesized Al₂O₃ reinforced aluminum composites," *Trans. Nonferrous Met. Soc. China (English Ed.)*, vol. 24, no. 7, pp. 2352–2358, 2014.
- [120] N. P. Suh, S. Jahanmir, E. P. Abrahamson, and A. P. L. Turner, "Further Investigation of the Delamination Theory of Wear," *J. Lubr. Technol.*, vol. 96, no. 4, p. 631, 1974.
- [121] F. Alshmiri, H. V. Atkinson, S. V. Hainsworth, C. Haidon, and S. D. A. Lawes, "Dry sliding wear of aluminium-high silicon hypereutectic alloys," *Wear*, vol. 313, no. 1–2, pp. 106–116, 2014.

- [122] L. N. Thanh and M. Suéry, "Influence of oxide coating on chemical stability of SiC particles in liquid aluminium," *Scr. Metall. Mater.*, vol. 25, no. 12, pp. 2781–2786, 1991.
- [123] B. S. Murty, S. K. Thakur, and B. K. Dhindaw, "On the infiltration behavior of Al, Al-Li, and Mg melts through SiC p bed," *Metall. Mater. Trans. A*, vol. 31, no. 1, pp. 319–325, 2000.
- [124] T. P. D. Rajan, K. Narayan Prabhu, R. M. Pillai, and B. C. Pai, "Solidification and casting/mould interfacial heat transfer characteristics of aluminum matrix composites," *Compos. Sci. Technol.*, vol. 67, no. 1, pp. 70–78, 2007.
- [125] L. M. Tham and L. Cheng, "Effect of limited matrix – reinforcement interfacial reaction on enhancing the mechanical properties of aluminium – silicon carbide composites," *Acta Mater.*, vol. 49, no. 16 SRC-GoogleScholar FG-0, pp. 3243–3253, 2001.
- [126] B. N. P. Bai and S. K. Biswas, "Characterization of dry sliding wear of AlSi alloys," *Wear*, vol. 120, no. 1, pp. 61–74, 1987.
- [127] A. T. Alpas and J. Zhang, "Effect of microstructure and counterface material on the sliding wear resistance of particulate reinforced aluminum matrix composites," *Met. Mater. Trans. A*, vol. 25, no. 5 SRC-GoogleScholar FG-0, pp. 969–983, 1994.
- [128] A. Sato and R. Mehrabian, "Aluminum Matrix Composites: Fabrication and Properties," *Alum. matrix Compos. fand Prop.*, vol. 7, no. 3, pp. 443–451, 1976.
- [129] R. Jamaati and M. R. Toroghinejad, "Manufacturing of high-strength aluminum/alumina composite by accumulative roll bonding," *Mater. Sci. Eng. A*, vol. 527, no. 16–17, pp. 4146–4151, 2010.
- [130] M. Roy, B. Venkataraman, V. V Bhanuprasad, Y. R. Mahajan, and G. Sundararajan, "The Effect of Particulate Reinforcement on the Sliding Wear Behavior of Aluminum Matrix Composites," *Metall. Trans. A*,

vol. 23A, no. October, pp. 2833–2847, 1992.

- [131] A. M. Hassan, A. Alrashdan, M. T. Hayajneh, and A. T. Mayyas, “Wear behavior of Al-Mg-Cu-based composites containing SiC particles,” *Tribol. Int.*, vol. 42, no. 8, pp. 1230–1238, 2009.
- [132] L. Guobin, S. Jibing, G. Quanmei, D. Hemin, L. Jianwei, and Z. Zhenyan, “Wear of Al-Mg-Cu composite reinforced by in situ formation of ceramics,” *J. Mater. Process. Technol.*, vol. 170, no. 1–2, pp. 416–420, 2005.
- [133] H. Kaftelen, H. Henein, and A. Part, “nlü, N., Göller, G., Öveçoğlu, M. L., & Comparative processing-structure–property studies of Al-Cu matrix composites reinforced with TiC particulates.,” *Compos. Appl. Sci. Manuf.*, vol. 42, no. 7 SRC-GoogleScholar FG-0, pp. 812–824, 2011.
- [134] X. F. Wu, G. G. Zhang, and F. F. Wu, “Microstructure and dry sliding wear behavior of cast Al-Mg₂Si in-situ metal matrix composite modified by Nd,” *Rare Met.*, vol. 32, no. 3, pp. 284–289, Apr. 2013.
- [135] A. Kumar, P. K. Jha, and M. M. Mahapatra, “Abrasive wear behavior of in situ tic reinforced with Al-4.5%Cu matrix,” *J. Mater. Eng. Perform.*, vol. 23, no. 3, pp. 743–752, 2014.
- [136] X. C. Tong, “Fabrication of in situ TiC reinforced aluminum matrix composites. Part I: Microstructural characterization,” *J. Mater. Sci.*, vol. 33, no. 22, pp. 5365–5374, 1998.
- [137] K. Niranjan and P. R. Lakshminarayanan, “Dry sliding wear behaviour of in situ Al-TiB₂composites,” *Mater. Des.*, vol. 47, pp. 167–173, 2013.
- [138] C. A. Caracostas, W. A. Chiou, M. E. Fine, and H. S. Cheng, “Tribological Properties of Aluminum Alloy Matrix TiB₂ Composite Prepared by In Situ Processing,” *Metall. Mater. Trans. A*, vol. 28, no. February, pp. 491–502, 1997.

- [139] A. A. Hamid, S. C. Jain, P. K. Ghosh, and S. Ray, "Processing, microstructure, and mechanical properties of cast in-Situ Al(Mg,Mn)-Al₂O₃(MnO₂) composite," *Metall. Mater. Trans. A*, vol. 36, no. 8, pp. 2211–2223, 2005.
- [140] A. W. Tesfay, S. K. Nath, and S. Ray, "Effect of transfer layer on dry sliding wear behaviour of cast Al-based composites synthesized by addition of TiO₂ and MoO₃," *Wear*, vol. 266, no. 11–12, pp. 1082–1090, 2009.
- [141] S. L. Pramod, A. K. Prasada Rao, B. S. Murty, and S. R. Bakshi, "Effect of Sc addition on the microstructure and wear properties of A356 alloy and A356-TiB₂ in situ composite," *Mater. Des.*, vol. 78, pp. 85–94, 2015.
- [142] A. Mandal, B. S. Murty, and M. Chakraborty, "Sliding wear behaviour of T6 treated A356-TiB₂ in-situ composites," *Wear*, vol. 266, no. 7–8, pp. 865–872, 2009.
- [143] X. JIANG, N. WANG, and D. ZHU, "Friction and wear properties of in-situ synthesized Al₂O₃ reinforced aluminum composites," *Trans. Nonferrous Met. Soc. China*, vol. 24, no. 7, pp. 2352–2358, Jul. 2014.
- [144] A. A. Hamid, S. C. Jain, P. K. Ghosh, and S. Ray, "Processing, microstructure, and mechanical properties of cast in-Situ Al(Mg,Mn)-Al₂O₃(MnO₂) composite," *Metall. Mater. Trans. A*, vol. 36, no. 8, pp. 2211–2223, Aug. 2005.
- [145] T. Yasmin, A. A. Khalid, and M. M. Haque, "Tribological (wear) properties of aluminum–silicon eutectic base alloy under dry sliding condition," *J. Mater. Process. Technol.*, vol. 153, pp. 833–838, 2004.
- [146] Y. Wang, W. M. Rainforth, H. Jones, and M. Lieblich, "Dry wear behaviour and its relation to microstructure of novel 6092 aluminium alloy–Ni₃Al powder metallurgy composite," *Wear*, vol. 251, no. 1–12, pp. 1421–1432, Oct. 2001.

- [147] K. V. Ojha, A. Tomar, D. Singh, and G. C. Kaushal, "Shape, microstructure and wear of spray formed hypoeutectic Al–Si alloys," *Mater. Sci. Eng. A*, vol. 487, no. 1–2, pp. 591–596, Jul. 2008.
- [148] A. S. Anasyida, A. R. Daud, and M. J. Ghazali, "Dry sliding wear behaviour of Al–12Si–4Mg alloy with cerium addition," *Mater. Des.*, vol. 31, no. 1, pp. 365–374, Jan. 2010.
- [149] N. P. Suh, "An overview of the delamination theory of wear," *Wear*, vol. 44, no. 1, pp. 1–16, 1977.
- [150] A. Simchi and H. Danninger, "Effects of porosity on delamination wear behaviour of sintered plain iron," *Powder Metall.*, vol. 47, no. 1, pp. 73–80, Jan. 2004.
- [151] A. K. Dey, P. Poddar, K. K. Singh, and K. L. Sahoo, "Mechanical and wear properties of rheocast and conventional gravity die cast A356 alloy," *Mater. Sci. Eng. A*, vol. 435–436, pp. 521–529, Nov. 2006.
- [152] Y. Birol and F. Birol, "Wear properties of high-pressure die cast and thixoformed aluminium alloys for connecting rod applications in compressors," *Wear*, vol. 265, no. 5–6, pp. 590–597, Aug. 2008.
- [153] E. J. Lavernia, B. Q. Han, and J. M. Schoenung, "Cryomilled nanostructured materials: Processing and properties," *Mater. Sci. Eng. A*, vol. 493, no. 1–2, pp. 207–214, Oct. 2008.
- [154] D. B. Witkin and E. J. Lavernia, "Synthesis and mechanical behavior of nanostructured materials via cryomilling," *Prog. Mater. Sci.*, vol. 51, no. 1, pp. 1–60, Jan. 2006.
- [155] R. Subramanian, C. G. McKamey, J. H. Schneibel, L. R. Buck, and P. A. Menchhofer, "Iron aluminide–Al₂O₃ composites by in situ displacement reactions: processing and mechanical properties," *Mater. Sci. Eng. A*, vol. 254, no. 1–2, pp. 119–128, Oct. 1998.
- [156] Z. Zhang and D. L. Chen, "Consideration of Orowan strengthening

- effect in particulate-reinforced metal matrix nanocomposites: A model for predicting their yield strength,” *Scr. Mater.*, vol. 54, no. 7, pp. 1321–1326, Apr. 2006.
- [157] Z. Zhang and D. L. Chen, “Contribution of Orowan strengthening effect in particulate-reinforced metal matrix nanocomposites,” *Mater. Sci. Eng. A*, vol. 483–484, pp. 148–152, Jun. 2008.
- [158] S. I. Cha, K. T. Kim, S. N. Arshad, C. B. Mo, and S. H. Hong, “Extraordinary Strengthening Effect of Carbon Nanotubes in Metal-Matrix Nanocomposites Processed by Molecular-Level Mixing,” *Adv. Mater.*, vol. 17, no. 11, pp. 1377–1381, Jun. 2005.
- [159] M. Alizadeh, “Strengthening mechanisms in particulate Al/B4C composites produced by repeated roll bonding process,” *J. Alloys Compd.*, vol. 509, no. 5, pp. 2243–2247, Feb. 2011.
- [160] H. Wang, G. Li, Y. Zhao, and G. Chen, “In situ fabrication and microstructure of Al₂O₃ particles reinforced aluminum matrix composites,” *Mater. Sci. Eng. A*, vol. 527, no. 12, pp. 2881–2885, 2010.
- [161] S. A. Sajjadi, H. R. Ezatpour, and H. Beygi, “Microstructure and mechanical properties of Al-Al₂O₃ micro and nano composites fabricated by stir casting,” *Mater. Sci. Eng. A*, vol. 528, no. 29–30, pp. 8765–8771, Nov. 2011.
- [162] S. M. Zebarjad and S. A. Sajjadi, “Microstructure evaluation of Al-Al₂O₃ composite produced by mechanical alloying method,” *Mater. Des.*, vol. 27, no. 8, pp. 684–688, Jan. 2006.
- [163] C. Rynio, H. Hattendorf, J. Klöwer, and G. Eggeler, “The evolution of tribolayers during high temperature sliding wear,” *Wear*, vol. 315, no. 1, pp. 1–10, 2014.
- [164] N. Saka, J. J. Pamies-Teixeira, and N. P. Suh, “Wear of two-phase metals,” *Wear*, vol. 44, no. 1, pp. 77–86, 1977.

- [165] J. H. Peng, X. L. Tang, J. T. He, and D. Y. Xu, "Effect of heat treatment on microstructure and tensile properties of A356 alloys," *Trans. Nonferrous Met. Soc. China (English Ed.)*, vol. 21, no. 9, pp. 1950–1956, 2011.
- [166] G. Ran, J. E. Zhou, and Q. G. Wang, "Precipitates and tensile fracture mechanism in a sand cast A356 aluminum alloy," *J. Mater. Process. Technol.*, vol. 207, no. 1–3, pp. 46–52, Oct. 2008.
- [167] G. A. Edwards, K. Stiller, G. L. Dunlop, and M. J. Couper, "The precipitation sequence in Al–Mg–Si alloys," *Acta Mater.*, vol. 46, no. 11, pp. 3893–3904, Jul. 1998.
- [168] H. Liao and G. Sun, "Mutual poisoning effect between Sr and B in Al–Si casting alloys," *Scr. Mater.*, vol. 48, no. 8, pp. 1035–1039, Apr. 2003.
- [169] H. Liao, Y. Sun, and G. Sun, "Correlation between mechanical properties and amount of dendritic α -Al phase in as-cast near-eutectic Al–11.6% Si alloys modified with strontium," *Mater. Sci. Eng. A*, vol. 335, no. 1–2, pp. 62–66, Sep. 2002.
- [170] S. A. Sajjadi, H. R. Ezatpour, and M. Torabi Parizi, "Comparison of microstructure and mechanical properties of A356 aluminum alloy/Al₂O₃ composites fabricated by stir and compo-casting processes," *Mater. Des.*, vol. 34, pp. 106–111, Feb. 2012.
- [171] H. R. Ezatpour, M. Torabi-Parizi, and S. A. Sajjadi, "Microstructure and mechanical properties of extruded Al/Al₂O₃ composites fabricated by stir-casting process," *Trans. Nonferrous Met. Soc. China (English Ed.)*, vol. 23, no. 5, pp. 1262–1268, 2013.
- [172] R. Mahmudi and W. J. Poole, "Enhanced properties of Mg-based nano-composites reinforced with Al₂O₃ nano-particles Superplastic forming of Aluminum and Magnesium alloys View project Extrusion of Aluminum Alloys View project," *Mater. Sci. Eng. A*, vol. 519, pp. 198–

203, 2009.

- [173] A. Vencel, I. Bobic, S. Arostegui, B. Bobic, A. Marinković, and M. Babić, “Structural, mechanical and tribological properties of A356 aluminium alloy reinforced with Al₂O₃, SiC and SiC + graphite particles,” *J. Alloys Compd.*, vol. 506, no. 2, pp. 631–639, Sep. 2010.
- [174] A. Mazahery, H. Abdizadeh, and H. R. Baharvandi, “Development of high-performance A356/nano-Al₂O₃ composites,” *Mater. Sci. Eng. A*, vol. 518, no. 1–2, pp. 61–64, Aug. 2009.
- [175] M. Karbalaei Akbari, H. R. Baharvandi, and O. Mirzaee, “Nano-sized aluminum oxide reinforced commercial casting A356 alloy matrix: Evaluation of hardness, wear resistance and compressive strength focusing on particle distribution in aluminum matrix,” *Compos. Part B Eng.*, vol. 52, pp. 262–268, Sep. 2013.
- [176] I. Sulima and B. Mikulowski, “Influence of silicon on the wetting-bond strength-structure relationship in the AlSi11/Al₂O₃ joints,” *Metall. Mater. Trans. A*, vol. 37, no. 11, pp. 3275–3281, Nov. 2006.
- [177] D. K. Dwivedi, “Adhesive wear behaviour of cast aluminium–silicon alloys: Overview,” *Mater. Des.*, vol. 31, no. 5, pp. 2517–2531, 2010.
- [178] Z. XIU, G. CHEN, X. WANG, G. WU, Y. LIU, and W. YANG, “Microstructure and performance of Al-Si alloy with high Si content by high temperature diffusion treatment,” *Trans. Nonferrous Met. Soc. China*, vol. 20, no. 11, pp. 2134–2138, Nov. 2010.
- [179] J. F. Archard, “Contact and Rubbing of Flat Surfaces,” *J. Appl. Phys.*, vol. 24, no. 8, pp. 981–988, Aug. 1953.
- [180] D. H. Buckley and K. Miyoshi, “Friction and wear of ceramics,” *Wear*, vol. 100, no. 1, pp. 333–353, 1984.
- [181] Y. Iwai, T. Honda, T. Miyajima, Y. Iwasaki, M. . Surappa, and J. . Xu, “Dry sliding wear behavior of Al₂O₃ fiber reinforced aluminum

- composites,” *Compos. Sci. Technol.*, vol. 60, no. 9, pp. 1781–1789, Jul. 2000.
- [182] I. Dinaharan and N. Murugan, “Dry sliding wear behavior of AA6061/ZrB₂ in-situ composite,” *Trans. Nonferrous Met. Soc. China (English Ed.)*, vol. 22, no. 4, pp. 810–818, 2012.
- [183] P. K. Ghosh and S. Ray, “Effect of porosity and alumina content on the high temperature mechanical properties of compocast aluminium alloy-alumina particulate composite,” *J. Mater. Sci.*, vol. 22, no. 11, pp. 4077–4086, Nov. 1987.
- [184] O. Yılmaz and S. Buytoz, “Abrasive wear of Al₂O₃-reinforced aluminium-based MMCs,” *Compos. Sci. Technol.*, vol. 61, no. 16, pp. 2381–2392, Dec. 2001.
- [185] A. M. Al-Qutub, I. M. Allam, and M. A. Abdul Samad, “Wear and friction of Al–Al₂O₃ composites at various sliding speeds,” *J. Mater. Sci.*, vol. 43, no. 17, pp. 5797–5803, Sep. 2008.
- [186] H. Zhu, C. Jar, J. Song, J. Zhao, J. Li, and Z. Xie, “High temperature dry sliding friction and wear behavior of aluminum matrix composites (Al₃Zr_α-Al₂O₃)/Al,” *Tribol. Int.*, vol. 48, pp. 78–86, 2012.
- [187] J. Yang, W. Gu, L. M. Pan, K. Song, X. Chen, and T. Qiu, “Friction and wear properties of in situ (TiB₂ + TiC)/Ti₃SiC₂ composites,” *Wear*, vol. 271, no. 11–12, pp. 2940–2946, Sep. 2011.
- [188] C. S. Ramesh and A. Ahamed, “Friction and wear behaviour of cast Al 6063 based in situ metal matrix composites,” *Wear*, vol. 271, no. 9–10, pp. 1928–1939, Jul. 2011.
- [189] B. Yang *et al.*, “In situ Al₂O₃ particle-reinforced Al and Cu matrix composites synthesized by displacement reactions,” *J. Alloys Compd.*, vol. 494, no. 1–2, pp. 261–265, Apr. 2010.
- [190] A. Johanson, “Effect of Vanadium on Grain Refinement of

Aluminium,” no. June, 2013.

- [191] A. A. Mahasneh and S. M. A. Al-Qawabah, “Effect of vanadium addition at a rate of 0.1% on the mechanical characteristics, microstructure, and microhardness of Al-Cu casted alloys,” *Mod. Appl. Sci.*, vol. 5, no. 2, pp. 92–102, Apr. 2011.
- [192] A. K. Prasada Rao, “Influence of vanadium on the microstructure of A319 alloy,” *Trans. Indian Inst. Met.*, vol. 64, no. 4–5, pp. 447–451, 2011.
- [193] M. K. Surappa and P. K. Rohatgi, “Preparation and properties of cast aluminium-ceramic particle composites,” *J. Mater. Sci.*, vol. 16, no. 4, pp. 983–993, 1981.
- [194] S. A. Sajjadi, M. Torabi Parizi, H. R. Ezatpour, and A. Sedghi, “Fabrication of A356 composite reinforced with micro and nano Al₂O₃ particles by a developed compocasting method and study of its properties,” *J. Alloys Compd.*, vol. 511, no. 1, pp. 226–231, 2012.
- [195] A. R. Miedema, P. F. de Châtel, and F. R. de Boer, “Cohesion in alloys — fundamentals of a semi-empirical model,” *Phys. B+C*, vol. 100, no. 1, pp. 1–28, Apr. 1980.
- [196] F. H. (Sam)Froes, C. Suryanarayana, K. Russell, and C.-G. Li, “Synthesis of intermetallics by mechanical alloying,” *Mater. Sci. Eng. A*, vol. 192–193, pp. 612–623, Feb. 1995.